The Canadian Journal of Chemical Engineering

formerly

CANADIAN JOURNAL OF TECHNOLOGY

CONTENTS

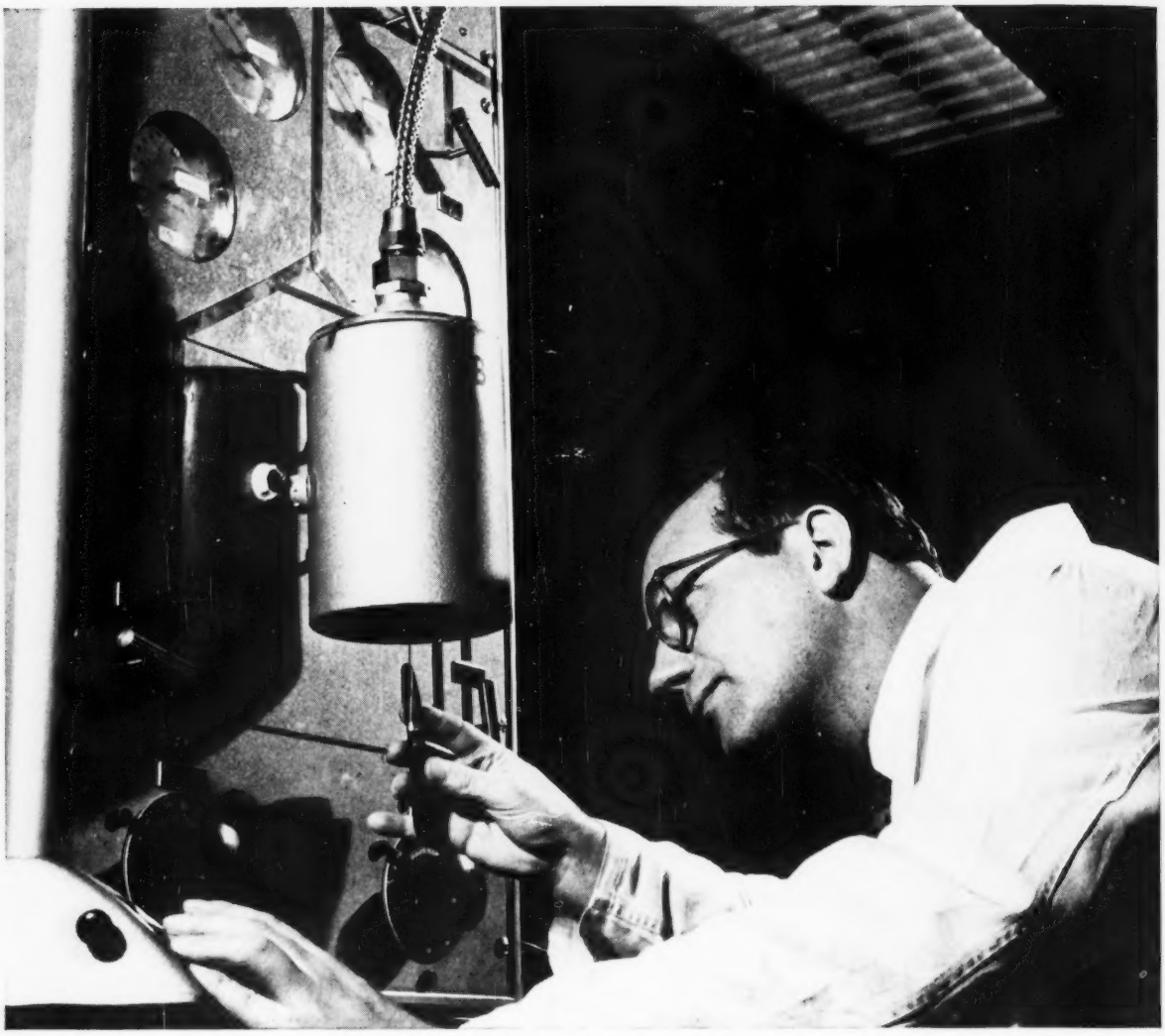

Photograph taken at C-I-L Central Research Laboratory, McMasterville, Que.

Plastics Detective

This photograph shows the High Shear Viscometer, designed and built at our Central Research Laboratory, used to investigate factors involved in complex flow behaviour of molten thermo-plastics during commercial processing.

Information on this newly developed pressure-driven capillary Viscometer has been made available to industry by C-I-L, and many industrial laboratories in the United States, England, India and Australia have built identical machines.

Such C-I-L research contributes to higher standards of performance in the plastics industry, to new and better plastics products and—through better technical service—to greater success in the application of these new materials to modern living.

C-I-L **CANADIAN INDUSTRIES LIMITED**

Serving Canadians Through Chemistry

Agricultural Chemicals • Ammunition • Coated Fabrics — Industrial Chemicals • Commercial Explosives • Paints • Plastics • Textile Fibres

The Canadian Journal of Chemical Engineering

formerly

Canadian Journal of Technology

VOLUME 37 **FEBRUARY, 1959** **NUMBER 1**

Authorized as second class mail, Post Office Department, Ottawa. Printed in Canada

Manuscripts for publication should be submitted to the Publishing Editor: D. W. Emmerson, *The Canadian Journal of Chemical Engineering*, 18 Rideau Street, Ottawa 2, Ont. (Instructions to authors are on inside back cover).

Editorial, Production and Circulation Offices: 18 Rideau Street, Ottawa 2, Ont.

Advertising Office: C. N. McCuaig, manager of advertising sales, *The Canadian Journal of Chemical Engineering*, Room 601, 217 Bay Street, Toronto, Ont. Telephone—EMpire 3-3871.

Plates and Advertising Copy: Send to *The Canadian Journal of Chemical Engineering*, 18 Rideau Street, Ottawa 2, Ont.

Subscription Rates: In Canada—$3.00 per year and 75c per single copy; U.S. and U.K.—$4.00; Foreign—$4.50.

Change of Address: Advise Circulation Department in advance of change of address, providing old as well as new address. Enclose address label if possible.

The Canadian Journal of Chemical Engineering is published by The Chemical Institute of Canada every two months.

Unless it is specifically stated to the contrary, the Institute assumes no responsibility for the statements and opinions expressed in *The Canadian Journal of Chemical Engineering*. Views expressed in the editorials do not necessarily represent the official position of the Institute.

Liquid-Solid Separation Factors in Hydrometallurgical Leach Circuit Design[1]

R. C. EMMETT[2] *and D. A. DAHLSTROM*[3]

Practically all hydrometallurgical processes involve leaching of solids to dissolve valuable constituents. This usually is followed by a liquid-solids separation before producing the final product. The liquid-solids separation step requires careful investigation because:

1. **Soluble values must be recovered to a very high degree for economic purposes.**
2. **Final liquor volume must be minimized to reduce capital and operating costs of later steps.**
3. **Usually large amounts of gangue solids are associated with the digested pulp requiring care in minimizing wash volumes.**
4. **The colloidal solids are strongly dispersed by retention times and pH conditions in leaching. This necessitates flocculation investigations to achieve desired results.**
5. **Operation must be dependable under severe conditions of pH, abrasion, fast settling solids, temperature, etc. Equipment must have flexibility to allow efficient operation under even abnormal fluctuations.**
6. **An appreciable percentage of initial investment is required for this portion of the plant.**

The two common liquid-solids separation methods —countercurrent decantation and filtration with cake washing, are discussed. Investigation and correlation procedures for prediction of full scale results and design requirements are stressed. Emphasis is given to the influence of particle size distribution, temperature, pH, flocculation, repulping, solids concentration, and filter cake permeability.

HYDROMETALLURGY involves dissolution of the metal from its ore, separation of the solution from insoluble impurities, and recovery of the particular metal or concentrate at a high degree of purity from this solution. One of the most critical steps in the process is the separation of the leached gangue from the valuable solution. With a few rare exceptions, such as the Resin in Pulp process for Uranium, it is necessary to completely remove the insoluble material from the liquid before the valuable component can be recovered. The requirements of this step are, principally, the maximum recovery of dissolved values, minimum dilution of the solution with wash water, and, of course, minimum overall cost, including both capital and operating expense.

Several methods are in common usage for this step, and among these are continuous countercurrent decantation with gravitational thickeners, filtering and washing on continuous vacuum filters, and filtration and washing on batch operated pressure filters. Because of the greater operating labor costs, batch filtration is being used less in recent years except in special applications involving hot saturated solutions containing relatively small amounts of solids, or for low tonnage operations. Therefore, this paper will be limited to a comparison of the application of continuous filtration or countercurrent decantation to the liquid-solids separation step.

The choice of the optimum separation system must be based on several factors, which include recovery, liquor volume, nature of the solids, and equipment cost. Soluble recovery is the main objective in hydrometallurgical operations. There are many applications in the chemical industry where the insoluble material is the valuable component, and the same purity is necessary; however, the principles involved are the same. Both continuous countercurrent decantation (known generally as C.C.D.) and filtration are equally capable of attaining the same recovery, which in most cases is specified as at least 99% of the dissolved values.

Typical flow sheets for soluble recovery and insoluble solid removal are illustrated in Figure 1. Filters will normally require two stages of filtration, consisting of filtering and washing the solids, then repulping the cake and repeating this process on the second stage filter. Countercurrent flow of the second stage filtrate may or may not be used as required by the conditions. While in some cases it is materially feasible to obtain the necessary washing on a single filter, possible loss of soluble values due to plugging of the spray nozzles, blinding of the filter media, and blow-back of filtrate during cake discharge can occur. Consequently one stage filtration normally does not give the degree of flexibility desired.

[1]*Manuscript received August 24, 1958.*
[2]*Research Engineer, The Eimco Corp., Palatine, Ill.*
[3]*Director of Research and Development, The Eimco Corp., Palatine, Ill.*
Based on a paper presented at the Joint A.I.Ch.E.-C.I.C. Chemical Engineering Conference, Montreal, Que., April 20-23, 1958.

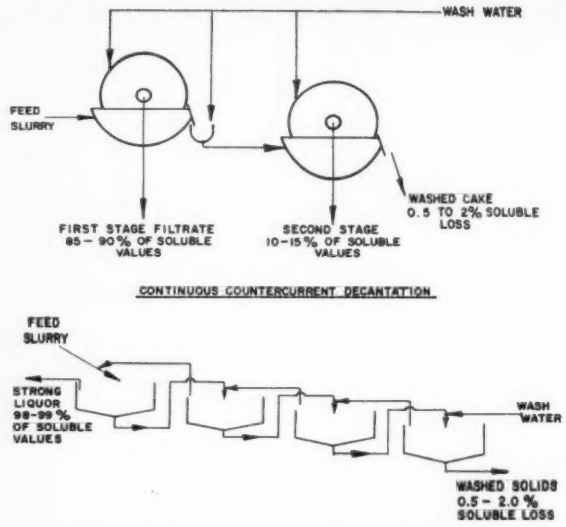

Figure 1—Two stage filtration and washing.

Using C.C.D., from three to six stages of thickeners are employed in most cases. The solid and liquid phases flow countercurrent to one another, with strong solution overflowing the first thickener to which the leached slurry is introduced and washed solids leaving in the underflow of the final thickener to which the fresh water is added. The major factors determining the soluble recovery are the feed and underflow dilution, the number of stages and the completeness of mixing between stages. This mixing is of critical importance and while it is assumed perfect in the calculations, it is frequently the main cause of loss in washing efficiency.

Calculation methods for washing effectiveness

Soluble recovery is always a critical function of the volume of fresh wash fluid per unit weight of insoluble solids in both systems. If a specific recovery is desired, then the remaining variables to be determined are the quantity of wash fluid, the number of stages, and the effectiveness of washing.

As mentioned, filtration is generally limited to two stages except in cases where a minimum volume of wash water must be used, and three stage, countercurrent operation is then employed. The minimum information necessary in order to determine the requirements of the step are (1) the feed solids concentration to both filter stages, (2) the filter cake moisture, and (3) the wash efficiency as applied to the recovery of dissolved values in the filter cake by means of cake washing. The recovery of solution by filtration alone is proportional to the weight ratio of liquor in the feed and in the cake in this form:

$$S = \frac{F - C}{F} \qquad (1)$$

where S = fraction of feed soluble values recovered in filtrate

F = lbs. liquor/lb. insoluble solids in feed

C = lbs. liquor/lb. insoluble solids in filter cake

The recovery by cake washing is not as readily determined as the effectiveness of washing is largely a function of the nature of the filter cake material and its permeability to wash. However, using an equation developed earlier expressing wash efficiency as a function of the wash volume and the properties of the system, and with the required amount of test work to determine the constants, it becomes possible to compute the recovery for any operating condition.[1] The equation is of the logarithmic decrement form, as follows:

$$\frac{R}{100} = \left(1 - \frac{E}{100}\right)^n \qquad (2)$$

where R = % of solubles remaining in the cake after washing on the basis of $R = 100$ if no washing were performed

n = wash ratio = volume of wash fluid/unit volume of liquor in cake prior to washing

E = wash efficiency, % = percent removal of soluble values by a 1.0 wash ratio.
(i.e., $E = 100 - R$ at $n = 1.0$)

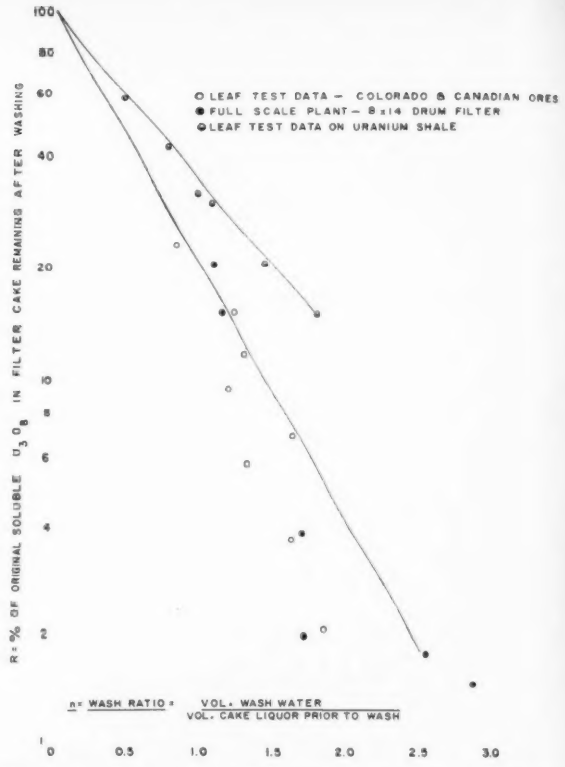

Figure 2—Removal of soluble values by cake washing vs. wash ratio - acid leached uranium ore.

The wash efficiency E term and the quantity of moisture in the cake are the major determinations that must be made in the test work. Figure 2 is a semi-log plot of the log of R as a function of the wash ratio n for different acid leached Uranium ores. One set of data compares laboratory leaf test results with full scale results wherein the latter are only slightly poorer than the former. This is not surprising as a perfectly even filter cake and distribution of the wash fluid across the entire area would not be expected on the full scale unit. Even so, deviations are not severe. The second set of data is for a Uranium shale which yielded a lower washing efficiency. From Equation (2) and the average straight

lines drawn in Figure 2, wash efficiency E is 80% for the first data and 65% for the second data. It will be noted that agreement with the straight lines drawn is very good for both cases except at low values of R. As the amount of solubles remaining in this area ranged from 0.001 to 0.005 wt. % to total dry solids, analytical precision would yield some scattering.

For most hydrometallurgical applications, E is equal to 75 to 85% although 70% is normally employed for design purposes to insure dependable scale-up. When slight adsorption of the soluble value occurs, due to certain properties of the solids, the value may drop to E = 60%. If the filter cake cracks before or during washing, the value of E will drop considerably, usually ranging from 35 to 55%. As a general rule, wash efficiency E will decrease as the wash rate through the filter cake increases. For example, with long fibers, as found in the paper industry, wash efficiency E values can be as low as 30% due to very high cake permeabilities and resultant channeling of the wash fluid.

After wash efficiency E and cake moisture contents are determined, it is possible to calculate the volume of wash needed for repulping and washing in order to effect the necessary recovery. Since the feed dilution and cake moisture are often properties of the system, and can be varied only within narrow limits, the water used for cake washing is the principal variable. In those cases where filtration is ideally suited for soluble recovery, the following examples illustrate soluble recovery and resultant solution volume by two stage filtration and washing without countercurrent flow.

Example 1

Feed solids: 50% or F = 1.0
Cake moisture 25% or C = 0.333
Liquor S. G.: 1.0
Recovery/stage by filtration:

$$S = \frac{1.0 - 0.333}{1.0} = 0.667$$

Solubles remaining/stage by washing, assuming wash efficiency E = 70%:
At a one displacement wash or n = 1.0

$$\frac{R}{100} = \left(1 - \frac{70}{100}\right)^{1.0} = 0.3$$

Total solubles lost to final washed cake =

$$(1 - S_1)\left(\frac{R_1}{100}\right)(1 - S_2)\left(\frac{R_2}{100}\right)$$

$$(.333)\quad (.3)\quad (.333)\quad (.3) = 0.01 \text{ or } 1\%$$

Combined filtrate volumes = 2 [(F − C) + nC] = 2 or 2 tons of fluid/ton of insoluble solids
Total soluble recovery: 99%

Example 2

Feed solids: 60% or F = 0.667
Cake moisture: 25% or C = 0.333
Recovery/stage by filtration:

$$S = \frac{0.667 - 0.333}{0.667} = 0.50$$

Solubles remaining/stage by washing, assuming E = 70% and n = 1.34;

$$\frac{R}{100} = \left(1 - \frac{70}{100}\right)^{1.34} = 0.20$$

Total solubles lost to final washed cake = (0.5) (.2) (.5) (.2) = 0.01 or 1%
Combined filtrate volumes = 2 [(F − C) + nC] = 1.56 tons of fluid/ton of insoluble solids
Total soluble recovery: 99%.

These two cases illustrate where filtration can be used to greatest advantage – low feed dilution and low cake moistures – assuming the physical properties are amenable to filtration. It should be pointed out that the wash efficiency equation should not be extrapolated beyond wash ratios of 2.5 to 3.0 without data at these values as at higher values capillary adsorption and other factors may cause a deviation in this relationship.

With continuous countercurrent decantation, the three principal variables are the feed dilution, the underflow dilution, and the number of stages, and frequently one of these is specified by process requirements. The practical maximum underflow dilution, like filter cake moisture, is determined mainly by the physical properties of the solids, and if sufficient detention time exists in the thickener, this value can be obtained.

The soluble recovery is readily found by mathematical calculation, and, as mentioned earlier, the only assumption is that complete mixing of underflow and overflow streams between stages does occur. For C.C.D. circuits where the only water added to the system is as wash to the final stage, and the overflow from the second stage thickener is used for leach liquor make-up, thus returning to the system in the feed stream to the first thickener, the following equation can be used to determine the soluble recovery:

$$S_1 = 1 - \left(\frac{D}{F - D}\right)^x \quad \ldots\ldots\ldots\ldots\ldots\ldots (3)$$

where S_1 = fraction of total solubles recovered in first stage thickener overflow
F = feed dilution to all stages except first
D = thickener underflow dilution lbs. liquor/lb. insoluble solids (assumed equal for all stages in Equation (3) as is F)
x = number of thickener stages

Other variations of the C.C.D. circuit must be calculated by material balance.

Another common flow sheet for C.C.D. employs no recirculation of second stage thickener overflow back to the leach circuit as in Figure 1. It is immediately obvious that, for the same values of F, D and x, this system will yield theoretically greater values for soluble recovery than the flow sheet represented by Equation (3). At the same time, concentration of soluble values per unit volume of liquor in stage one overflow decreases. Generally, this flow sheet is more common due to its simplicity, greater flexibility and higher soluble recovery. To calculate theoretical soluble recovery, material balances or graphical solutions can be employed. Due to the fact that the volume of overflow leaving the first thickener is generally greater than that from the other thickeners, a graphical presentation of soluble recovery as a function of underflow solids concentration with parameters of feed solids concentration and number of thickener stages is most convenient. Figure 3 is a typical plot of % soluble loss in the tailings or thickener underflow from the last stage as a function of underflow percent solids. Parameters of 25 wt.% solids in the feed to all stages but the first with five and six stages are indicated. In addition, parameters of 20% feed solids to all thickeners but the first stage for four, five and six stages are given. It is assumed that underflow solids concentrations are the same for all thickeners, the liquor specific gravity is materially unchanged throughout the circuit, and the leached slurry solids concentration is 33.3 wt. %. It should also be noted that feed solids concentration is measured after mixing of appropriate streams feeding each thickener. If any of the above

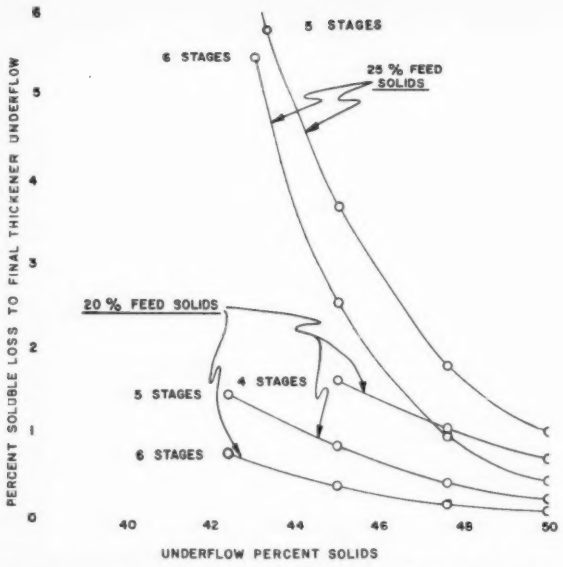

Figure 3—Theoretical soluble loss with C.C.D. vs. underflow solids concentration; parameters of feed % solids and number of thickener stages.

BASIS: Flow sheet as per Figure 1.
Leach slurry solids concentration 33.3%.
Thickener underflow concentrations are all equal.
Feed solids concentrations indicated are for all but first stage.

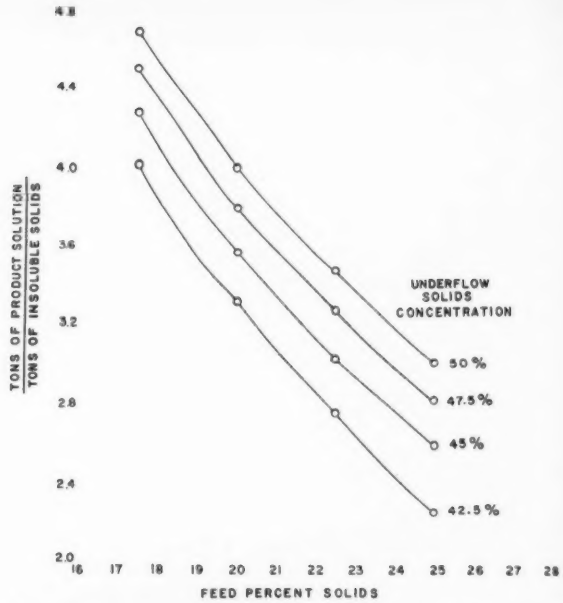

Figure 4—Overflow to insoluble solids ratio as a function of feed solids concentration; parameters of underflow concentration. BASIS: Same as Figure 3.

parameters are altered, a new graphical presentation is required. It is emphasized that theoretical soluble recovery for variations of any C.C.D. flow sheet can be calculated by material balances and presented as in Figure 3.

Along with soluble recovery calculations, volume of resultant product solution must also be determined. Figure 4 is a plot of tons of product solution per ton of insoluble solids as a function of feed solids concentration to all but the first thickener with parameters of underflow solids concentration of all stages. This figure is complimentary to Figure 3 and yields the necessary information required for an optimum economic balance. These calculations are also determined by material balance. It will be seen that in using a reasonable number of thickeners, the volume of liquor to be expected from a C.C.D. operation will be considerably more than with a filtration circuit. At the same time, soluble recovery and final solution volume is vitally influenced by underflow and feed solids concentration.

Testing procedures

Assuming representative samples are available for testing, then the laboratory scale of test work is often sufficient to indicate the proper approach, and thus narrow the pilot plant work down to the proposed system for the full scale plant. In some cases, the pilot plant work may be by-passed altogether, but in general this is not to be recommended, due mainly to the difficulty in obtaining a truly representative sample for small scale, batch-wise testing.

Testing for filtration is normally carried out with a 0.1 square foot filter leaf, attached with hose connections to a flask and vacuum pump. The test work consists of duplicating the steps in a continuous filtration cycle – cake formation, initial dewatering, cake washing, final dewatering, and cake discharge. The data necessary include the wet and dry filter cake weights, the volume of filtrate and wash water, and the filtering and washing times; drying and dewatering times are of use but generally of less importance. These data are used to scale up directly to the design conditions in terms of filtration rate, optimum cycle times, and ratio of filtering to washing time. Quite frequently the material will filter much more rapidly than it will wash, and hence the final scale up factor is determined by the limiting condition, which in this case would be the wash rate.

The effect of the physical characteristics of the slurry must be carefully considered. The temperature and degree of saturation of the solution are important, when the vacuum needed for filtration is close to the vapor pressure of the liquor. Flashing under vacuum of this solution can cause plugging in the filter piping and blinding of the media and must be avoided. Thus when solutions are near the boiling point, pressure filtration or C.C.D. methods will probably be more practical.

The particle size distribution is of course an important consideration. A typical readily filtered gangue from a leaching operation is illustrated by this screen analysis:

MESH SIZE	WEIGHT %
+ 50	0.3
− 50 +100	8.7
−100 +140	15.7
−140 +200	16.3
−200 +325	36.8
−325	22.2
Total	100.0

However, the same size distribution of another material, where the −325 fraction is composed of colloidal slimes, will have a totally different behavior, and may not be suitable to filtration at all. Flocculation can be used

to increase the filtration rate, but in some cases the wash rate is not improved proportionately and the end result is the same.

For most practical applications, the wash rate must be such that a 0.5 to 1.0 wash ratio can be passed through the cake in an interval equal to the filtering time. If the wash time for this volume is substantially longer, then it may be found that two stage filtration with washing is not the best method for soluble recovery. Three stage filtration or continuous countercurrent decantation might be more desirable. For slurries that are composed of mostly −200 mesh particles, C.C.D. will generally be the best method. In addition, the filtration rate may be too low, and hence the equipment cost excessive as compared to other methods. A detailed paper on the theory, testing and scale-up methods for filter cake washing will be found in the literature. (1)

Laboratory testing for thickening consists of running batch settling tests in 1 and 2 liter graduated cylinders, usually with some sort of slowly revolving stirring mechanism provided to help release trapped solution from the compacting solids. A settling test should last up to 24 hours or longer when it is desired to determine the ultimate density that can be reached. The initial free settling characteristics usually determine the thickener area, and this is found from the settling rate data over an interval comprising the first one or two hours of settling. Various methods are in use for determining the necessary settling area from the data taken in batch settling tests and the more common are the Coe-Clevenger method, which is described in most text books, and the more recent Kynch method, which is discussed in reference. (2) Generally, the latter method is better suited to flocculated pulps because it is limited in application to a sample of the same feed concentration as that anticipated in the full scale operation, thus eliminating the floc size variable. The Coe-Clevenger method is applicable to those slurries composed of fine size unflocculated particles, such as mineral concentrates, and fast settling pulps, and usually will give a more representative value for scale-up.

Temperature is an important variable in thickening, due to its effect on viscosity and therefore, particle settling rate. Hot slurries will, of course, cool from one thickening stage to the next, and a careful estimate of the degree of cooling will be necessary before conducting any tests.

Particle size distribution is also significant in thickening tests. All too frequently, upon dilution to the feed conditions, the coarse material will settle out rapidly in the bottom of the cylinder and the data taken in the test will be of questionable value. In these cases, pilot plant testing is frequently essential.

Flocculation as an aid to thickening has gained much popularity in recent years with the introduction of a number of synthetic polyelectrolytes which have the power to greatly accelerate sedimentation. Many slurries which might previously have been considered unsettleable are now found to be amenable to thickening.

Countercurrent bench scale tests are not generally performed, other than several settling tests at successively lower solution strength, which will determine if this factor has any effect on the settling rate. Also it is helpful to observe the mixing characteristics of the thickened slurry with fresh solution. Where the solids are composed mostly of flocculated slimes, large masses of this pulp may not be broken up upon mixing, and if this effect were to occur in the full scale application it would seriously reduce soluble recovery. Similarly, with coarse solids, porous particles can adsorb solute which is not readily dispersed into the dilution liquor. Some retention and mixing time would be necessary to bring about equilibrium conditions. The latter can best be determined by pilot plant investigations.

As mentioned before, pilot plant tests are useful in checking the design data. The equipment operation is essentially the same as in a full scale plant, with the exception of certain details which are due to the difference in dimensions of the units. In filtration testing, care must be taken to obtain uniform wash water distribution on the filter in order to simulate results on large filters. Pilot plant thickeners, unless they are of disproportionately deep design, will not operate at both the rate corresponding to the area requirement and the ultimate solids density which are determined from the laboratory tests, unless the material is extremely rapid settling. This will be evident from the fact that attainment of the ultimate density is dependent upon detention volume, which would not be available in the small, shallow thickeners frequently used in pilot plant work. These are usually operated at the maximum capacity as determined from the settling rate.

Full scale design considerations

Once a filter area has been established from the test work, several design factors must be considered. These include the effectiveness of cake discharge, the selection of a proper filter cloth to prevent blinding yet minimize the passage of solids into the filtrate, the placement of wash headers to obtain complete use of the wash water and in some cases prevent cracking from occurring, and the selection of a cake discharge method which eliminates blow back of liquor. The latter is a common problem where the filter cake is tight enough not to permit sufficient air to pass through and displace the liquor in the drainage deck and piping. One method of avoiding this is to use a string discharge, wherein no blow back is necessary. A second and more satisfactory method is to employ purge piping which permits air to be bled into the section of the drum just prior to discharge through a separate set of pipes, thus displacing any remaining liquid. The importance of this step cannot be overemphasized, as much of the benefit due to effective soluble recovery is lost by liquor blow-back.

Thickeners likewise require design considerations not always evident from test work. Significant among these is the possible need for mechanical repulping between stages in order to insure complete mixing. Another difficulty encountered occurs when a sand-slime mixture is fed to the thickener. All too frequently the sand will settle out immediately, overloading the rakes or plugging the underflow pump. Methods of avoiding this include the addition of sufficient flocculant, causing the slimes to retain the sands and prevent a separation, or simply to effect a sand-slime classification first, washing the sands on classifiers or filters with the slimes handled by C.C.D. methods. This is particularly advantageous where large thickeners are involved.

A third factor is the peculiar behavior of so-called thixotropic pulps. These tend to form "islands" which revolve with the rake arms and impair the action of the thickener. Methods of eliminating this include higher rake speeds, "picket" arms to break up the pulp mass, and the use of the "thixo" arm, in which the scraper blade is extended 1 to 3 feet below the supporting arm by means of vertical pipes. This keeps most of the structure above the compression zone, thereby preventing the island formation from occurring. The vertical pipes also serve to cut channels into the thickened solids

allowing freer passage for the fluid and thereby achieving a higher underflow solids concentration.

From the test work and design conditions just described, it might be possible to eliminate one of the methods from consideration. This is more often true of filtration, as some slurries by their very nature will not be filterable, and this will become evident early in the test work. When the slurry appears to be suited both to filtration and thickening for soluble recovery, then a careful analysis of all factors is called for.

Assuming equal recovery, then one must examine the data in the light of volume of liquor produced, the number of stages required, and finally the overall cost of either approach. The latter is difficult to arrive at because of the great number of variables. The following will illustrate the case in two mills, both of about the same tonnage, operating on nearly identical leached ores.

The C.C.D. plant consists of two lines of five 60 ft. thickeners of acid resistant construction. The filter plant includes 6 acid resistant filters of 575 sq. ft. area each, operating with a countercurrent wash system.

	C.C.D. CIRCUIT	FILTER CIRCUIT
Average recovery	98.5%	99.2%
Wash ratio, tons liquor/ton solids	1.85	1.5
Operating labor*	1 Operator	1 Operator, 1 Assistant
Flocculant cost dollars/ton, average	$0.20	$0.11
Power cost dollars/ton, at $.01/Kw.	$0.005	$0.018

* Duties may extend to other equipment.

Maintenance on the filters consists chiefly in string replacement (about $50.00/month/filter) and in filter cloth replacement, which may vary in frequency from once every two weeks to every three months. Filter valve wear plates and filter cake discharge and repulping mechanisms must be replaced from time to time, but rarely more often than once a year. Maintenance on thickeners is usually limited to replacement of the diaphragms on the slurry pumps. However, in this particular case the C.C.D. plant had more than normal maintenance difficulties due to the abrasive characteristics of the ore and the corrosiveness of the solution. Also, the excessive volume of liquor limited the production of the mill because of the capacity of the subsequent processing equipment.

A not so apparent difficulty is the effect of loss of one of the units due to maintenance. With C.C.D. this is represented by a loss of one stage with a reduction in recovery of about 1%. In the filter plant, as extra capacity is available by increasing the filter speed, which will not impair washing efficiency normally, no loss in overall soluble recovery should occur. If, however, the speed of the filter is not changed but the ratio of filtering time to washing time is increased by raising the level in the filter tank, a definite loss in efficiency will occur.

With reference to the operating characteristics pointed out in this example it might be said that a filter installation would have been preferable in this case, if filtration had proved satisfactory in the initial test work.

Comparison of advantages of continuous countercurrent decantation and filtration for soluble recovery

It is useful to compare the advantages of each of these systems in hydrometallurgical circuits.

Continuous countercurrent decantation:

1. Generally lower operating cost, provided excessive maintenance is not required due to mechanical failure.
2. Because of the large volumes employed, thickeners are less subject to upset due to process fluctuations.
3. Less down time due to maintenance work.

Multiple stage filtration:

1. Usually lower capital cost, particularly in climates where buildings are necessary.
2. Easier to restore normal operation after an upset from process fluctuation occurs.
3. Higher solution concentrations are produced because of the lower wash ratio necessary.
4. Less hold-up of valuable product in system. With thickeners this can represent a considerable cost attributable to inventory of product.
5. Lower floor space requirements. Particularly in rough terrain this can be of important significance.

In summary, it can be stated that in the selection of the best method for soluble recovery in hydrometallurgical circuits, extensive test work in the laboratory and pilot plant will be justified in view of the better plant operation which will be made possible by this work. Where both continuous countercurrent decantation and filtration appear equally feasible, an economic analysis based on the foregoing considerations will be very useful in choosing the better approach.

References

(1) Choudhury, A. P. R., and Dahlstrom, D. A., A.I.Ch.E. Journal, 3, 433-438 (1957).
(2) Talmadge, W. P., and Fitch, E. B., Ind. Eng. Chem., 47, 38 (1955).

★ ★ ★

ERRATUM

First Order Rate Processes and Axial Dispersion in Packed Bed Reactors by J. J. Carberry, from the October 1958 issue.

"On page 208, column 2, line 23: instead of 'equals $(L/D_p)_\epsilon$ or Lv/2E, the phrase should read–equals $(L/D_p\gamma)_\epsilon$ or Lv/2E. In other words the first term should be divided by γ'."

Horizontal Pipeline Flow of Mixtures of Oil and Water[1]

T. W. F. RUSSELL[2], *G. W. HODGSON*[3], *and G. W. GOVIER*[4]

The flow characteristics of the two-phase system —white mineral oil and water—were examined in a horizontal, smooth, one-inch pipe. Flow conditions were investigated over a range of input oil-water volume ratios from 0.1 to 10 at thirteen superficial water velocities ranging from 0.116 ft./sec. to 3.55 ft./sec. A theoretical analysis of the laminar flow of two immiscible liquids between wide parallel plates yielded a modified parallel plate friction factor based on the water properties and the superficial water velocity. It was evaluated for a number of input oil-water volume ratios and plotted against the superficial water velocity. The experimental pressure drop data that were obtained were correlated using a modified Fanning friction factor which was evaluated for the range of input ratios studied and correlated with the superfical water velocity. A flow pattern correlation was obtained for visually observed types of flow—bubble, stratified and mixed—and it was shown that these patterns occurred in laminar, transitional or turbulent conditions of flow. The theoretical analysis for flow between wide parallel plates was adapted to obtain hold-up relationships, and a plot of the hold-up ratio H_R (the input divided by the in situ oil-water volume ratio) versus the input oil-water ratio was constructed. This plot indicated that in the laminar region of flow the hold-up was not dependent on the superficial water velocity but was only a function of liquid viscosity and input ratio. Experimental results for flow in the pipe conformed with this prediction while indicating that in the turbulent region superficial water velocity was also a factor.

STUDIES concerned with the development of the Athabasca oil sands have from time to time revealed interesting problems in materials handling. Not the least of these is that associated with the handling of heavy crude oil in the presence of water.

Clark (1) observed that, under some conditions, the flow of the heavy Athabasca oil through a pipe was aided by the inclusion or injection of water into the flowing stream. It appeared that the inside of the pipe was wetted by the less viscous water, resulting in a "lubrication effect". Clark and Shapiro (2) noticed the same effect and patented a process for the injection of demulsifying agents with water into crude oil pipelines. The demulsifying agents were added to prevent destruction of the water film in the pipe. Other reports of water injection into crude oil pipelines substantiated the observations, but it appears that little detailed or quantitative study has been given to the flow mechanics of the oil-water system.

The present project was begun with a view to laying the foundations for a comprehensive study of the pipeline flow of oil-water mixtures. The flow of oil-water mixtures in porous media has been extensively studied (3), but the type of flow encountered is not analagous to that in a pipeline. The flow of solid-liquid mixtures has been quite widely studied and several useful correlations are available. Many of these correlations are based upon the rheological properties of the solid-liquid mixture and assume a uniform flowing material for all velocities, although special consideration has been given to systems in which distortions of the velocity profiles have resulted from the partial sedimentation of the suspended solids as reported by Bruce et al (4). Since the flow pattern in gas-liquid and in liquid-liquid systems is constantly changing, the "mixture property" approach is not too useful for these cases.

While little work on the pipeline flow of two immiscible liquids has been reported, a great deal of research has been carried out on the flow of gas-liquid mixtures, and this has a bearing on the liquid-liquid problem. The study of the flow of gas-liquid mixtures has been concerned mainly with the effect of certain variables on flow pattern, pressure drop and hold-up. The pertinent variables and those which to a greater or lesser extent have been examined in previous work are:

(1) Density of each phase,
(2) Viscosity of each phase,
(3) Flow rate of each phase, and
(4) Geometry of the system.

Since, for design purposes, it is often necessary to have pressure-drop data, much effort has been devoted to the development of a correlation between the variables mentioned and the experimental pressure-drop data.

An attempt to correlate two-phase flow in a manner similar to single-phase flow using a modified form of the Fanning equation has been made by some investigators. Uren et al (5) and Nowels (6), both working with gas-liquid systems in vertical pipes, suggested that the Fanning equation could be used by assuming "mixture properties" of density and viscosity and uniform mixture velocity. The difficulty in this method of correlation was the

[1]*Manuscript received October 24, 1958.*
[2]*Junior research engineer, Research Council of Alberta. Present address: Carbide Chemicals Company, Montreal, P.Q.*
[3]*Head, Petroleum Research, Research Council of Alberta, Edmonton, Alberta.*
[4]*Head, Department of Chemical and Petroleum Engineering, University of Alberta, Edmonton, Alberta.*
Contribution from the Research Council of Alberta and the Department of Chemical and Petroleum Engineering, University of Alberta. The work described here was done in partial fulfillment of the requirements for a Master of Science degree at the University of Alberta.

evaluation of the properties of the flowing mixture and the lack of attention to hold-up and flow pattern considerations. Lockhart and Martinelli [7], using an analysis of flow patterns made by Martinelli et al [8], have correlated pressure drop for horizontal flow by using two parameters ø and X. In their analysis, X is the ratio of (a) the pressure drop/unit length, assuming the liquid to be flowing alone to (b) the pressure drop/unit length, assuming the gas to be flowing alone; ø is the ratio of the pressure drop/unit length during two-phase flow to the pressure drop/unit length for either phase flowing alone. These two parameters were evaluated and interrelated for each of several flow patterns.

Jenkins [9] and Bergelin [10] found that while their data did fit the Lockhart and Martinelli "ø - X" correlations in general, there was a spread of ± 30%. Baker [11] obtained data for flow through pipes four to ten inches in diameter and found the Martinelli type correlation to be inadequate. White and Huntington [12] presented an empirical relation for the prediction of the pressure drop for the horizontal flow of gas-liquid mixtures from a knowledge of the flow rates, the physical properties and pipe diameter. This correlation is restricted to certain flow patterns, to low pressures and to liquids with viscosities less than 120 centipoise.

Chenoweth and Martin [13] attempted to correlate their data at higher pressures and in the turbulent region with Martinelli's and Lockhart's work, and found the predicted pressure drop to be 1.4 to 2.5 times the observed pressure drop.

Work done at the University of Alberta on the vertical flow of gas-liquid mixtures has been summarized and reported by Govier et al [14]; they applied a mechanical energy balance to the vertical system and expressed the total pressure drop in terms of a hydrostatic head component and an irreversibility component. Their correlations enable the prediction of flow pattern, hold-up and pressure-drop for air-water mixtures in a one-inch tube at an average temperature and pressure of 70°F. and 30 p.s.i.a. The pressure-drop correlation is in terms of a superficial friction factor, a superficial water velocity and the volume ratio of the two phases. This work has been extended by Short [15] and Sullivan [16] to cover a range of tube diameters and gas phase densities.

Govier et al [14] correlated their flow pattern description with pressure-drop observations. They describe the following types of flow patterns for vertical flow of gas-liquid mixtures:

(1) Bubble—bubbles of gas flowing in liquid;
(2) Slug—slugs of gas flowing in liquid;
(3) Froth—intensely mixed gas in liquid;
(4) Ripple—rippley wall layer of liquid with central core of gas;
(5) Film—smooth wall layer of liquid with central core of gas;
(6) Mist—droplets of liquid dispersed in gas

Both Martinelli [8] and White and Huntington [12] describe flow patterns for horizontal flow. While Martinelli did not present a detailed analysis, White and Huntington report flow patterns involving stratified, ripple, slug, and wave flow forms.

Although Moore and Wilde [17] were among the first investigators to recognize the presence of slippage leading to hold-up in two-phase flow, Govier et al [14] provide the best method for handling and defining hold-up. They define "hold-up ratio" as the ratio between the input and the in situ gas-liquid volume ratio, and relate it to the average velocities of the phases as follows:

$$H_R = \frac{V_G - V_L}{V_L} + 1$$

Theory

The pressure-drop relationships can be obtained for any single-phase Newtonian fluid flowing in a horizontal pipeline by using the Fanning equation $\Delta P = \frac{2f\,\Delta L V^2 \rho}{g_c D}$ and empirical relationships between f, the friction factor, $\frac{\epsilon}{D}$ the relative roughness, and $\frac{DV\rho}{\mu}$ the Reynolds number.

The flow of two liquid phases in a circular pipe is much more complicated, but an arbitrary friction factor can be described as $f_w = \frac{\Delta P g_c D}{2\,\Delta L V_w^2 \rho}$. In this case, f_w is some complicated function of the variables: D, V_w, V_o, ρ_w, ρ_o, μ_w, μ_o. In principle it would be possible to obtain theoretical equations relating these variables under laminar flow conditions. However, lack of knowledge of flow mechanism at the boundaries makes the problem too difficult to solve for stratified flow in a circular conduit. An analysis of two liquid phases flowing between wide parallel plates has been made by Russell and Charles [18] and although the geometry is different the general relationships might be expected to shed some light on the circular pipe problem.

Russell and Charles [18] give a general equation for two layer laminar flow between wide parallel plates. Applying this to the oil-water system and using subscript o for the oil (upper) layer and subscript w for the water (lower) layer:

$$Q_o = \frac{\Delta P b g_c}{12\mu_o\,\Delta L}\left[\frac{M_1\mu_o + M_2\mu_w}{M_3\mu_o + M_4\mu_w}\right] \quad \ldots\ldots\ldots\ldots (1)$$

$$Q_w = \frac{\Delta P b g_c}{12\mu_w\,\Delta L}\left[\frac{N_1\mu_o + N_2\mu_w}{N_3\mu_o + N_4\mu_w}\right] \quad \ldots\ldots\ldots\ldots (2)$$

Eq. (1) and (2) can be expressed in terms of a Fanning type friction factor. Walket et al [19] have shown that if 4a is chosen as the equivalent diameter for a parallel plate system, the Reynolds number corresponding to the termination of laminar flow is the conventional figure 2,000. On this basis, a parallel plate friction factor can be defined using the superficial velocity of the water phase.

$$f_{pp} = \frac{\Delta P g_c\,(4a)}{2\,\Delta L V_w^2 \rho_w} \quad \ldots\ldots\ldots\ldots (3)$$

V_w is defined for the parallel plate system as $\frac{Q_w}{2ab}$, where 2ab is the cross-sectional area available for flow.

$$f_{pp} = \frac{8\,\Delta P g_c a^3 b^2}{\Delta L\, Q_w^2\, \rho_w} \quad \ldots\ldots\ldots\ldots (4)$$

For any two given liquids Eq. (2) becomes

$$\Delta P = \frac{Q_w\,\Delta L}{b\,K_w g_c} \quad \ldots\ldots\ldots\ldots (5)$$

where

$$K_w = \frac{1}{12\mu_w}\left[\frac{N_1\mu_o + N_2\mu_w}{N_3\mu_o + N_4\mu_w}\right]$$

where N_1, N_2, N_3 and N_4 are functions of the in situ oil-water ratio

Combining this with Eq. (4)

$$f_{pp} = \frac{8ba^3}{\rho_w K_w Q_w} \quad \ldots\ldots\ldots\ldots (6)$$

The values of the water flow-rate, Q_w, which will assure that flow is in the laminar region, can be calculated by using the criterion for laminar flow between parallel plates described by Walker et al [19].

Walker defined Reynolds number for parallel plates as follows:

$$Re = \frac{4aV\rho}{\mu} \quad \ldots\ldots\ldots\ldots\ldots\ldots\ldots\ldots (7)$$

For water, this becomes:

$$Re = 37.4\,(10)^4\,aV \quad \ldots\ldots\ldots\ldots\ldots\ldots\ldots\ldots (8)$$

Since Walker found, experimentally, that Reynolds number must be below 2,000 for laminar flow, the upper limit on 4aV for the laminar flow of water must be 0.0216 ft.²/sec.

Before a plot of the theoretically computed friction factor versus the superficial velocity can be made, the geometry of the system must be fixed. Accordingly, it was decided to consider a parallel plate system of width one foot and separation 0.05 ft. The equation for the parallel plate friction factor now becomes:

$$f_{pp} = \frac{8.(0.025)^3}{\rho_w K_w Q_w}$$

The parallel plate friction factor, f_{pp}, was calculated for seven input oil-water volume ratios and for two different flow rates of 0.216 ft./sec. and 0.100 ft./sec. These flow rates were in the laminar region as indicated by the evaluation of Eq. (8). Figure 1 was prepared from these data to show the relationship between the parallel plate friction factor, f_{pp}, and V_w, the superficial water velocity for a stratified flow of water and an 18cp. oil. The curves in Figure 1 are lines of constant input oil-water volume ratios, R_v, calculated from the assumed in situ ratios.

Another important aspect of this theoretical development is the information which it gives regarding hold-up, defined as the ratio of the input flowing mixture to the in situ flowing mixture. To obtain Q_o and Q_w, a series of in situ ratios of oil to water were selected and the flow rates were calculated. The input ratio was then obtained by dividing Q_o and Q_w. Figure 2 was constructed to show the relationship between the hold-up ratio H_R, and the input oil-water volume ratio, V_R. This curve shows that for the laminar, two-layer flow of oil and water between two parallel plates, the hold-up should be a function of only the viscosity and the input volume ratios of the two liquids, but not of the individual velocities.

This consideration of the laminar flow of two immiscible liquids between parallel plates indicates the general form of the friction factor–Reynolds number relationship for laminar flow and the effect on it of the input ratio. It also indicates that the hold-up ratio in laminar flow is a function of the input ratio and the viscosities. While the flow of two immiscible phases in a circular pipe presents a much different problem, it is reasonable to anticipate a similar general pattern in the laminar region.

Experimental Equipment

A schematic flow diagram of the equipment is shown in Figure 3. The main test section was about 35 ft. of transparent cellulose acetate butyrate pipe of one-inch inside diameter supported in a horizontal position by a frame-work made of light steel sections. The pipe was tapped six ft. from the inlet end, and about two ft. from the discharge end, providing a test section of 28.18 ft. and a calming section of about nine ft. A third tapping point was provided half way along the test section.

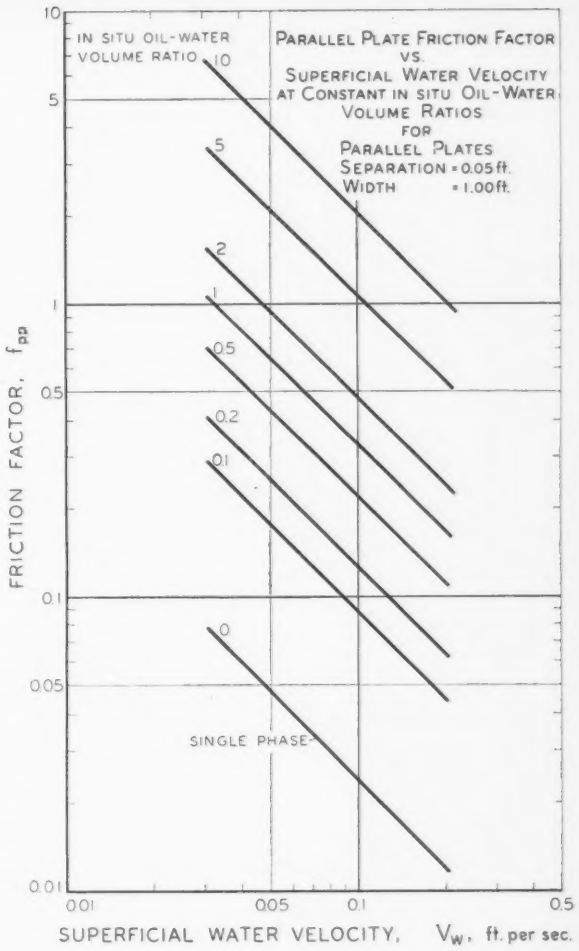

Figure 1—Calculated relations between friction factor and superficial water velocity for various input ratios of water and an 18-xp. oil flowing in a hypothetical parallel plate flow cell.

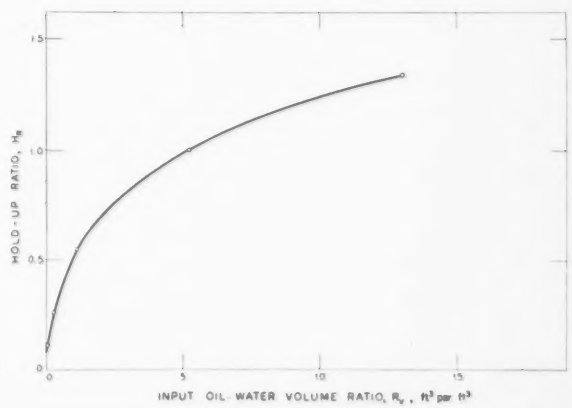

Figure 2—Calculated relation between hold-up ratio and input oil-water volume ratio for the flow of water and an 18-c.p. oil flowing in laminar motion in a hypothetical parallel plate flow cell.

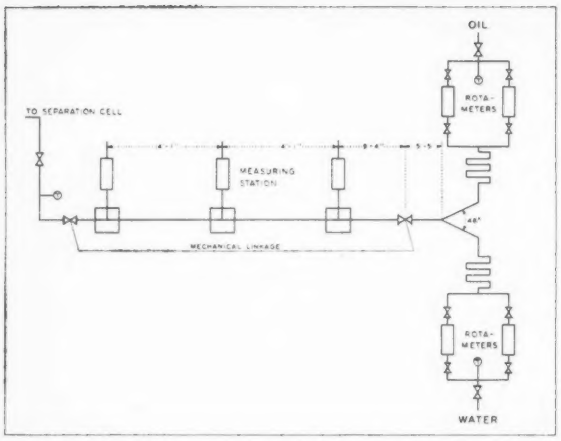

Figure 3—Schematic flow diagram of pipeline assembly for the study of the horizontal flow of mixtures of oil and water.

At the inlet end, the acetate butyrate pipe was joined to the input manifold by an 8-foot copper pipe terminating in a welded 48 degree Y. To prevent transmission of vibration from the pumps to the test section and to provide for flexible positioning of the Y. the copper was connected to the input manifold by rubber hose. The discharge end of the test section was attached to a separator by rubber hose. Two roundport quick-closing valves connected by a mechanical linkage were installed at both ends of the plastic pipe for measuring hold-up.

The metering of the oil and water was done with calibrated rotameters. To give a very wide range of flow rates, two rotameters (one large and one small) were mounted in parallel for each fluid, the small rotameters being equipped to operate with either a steel or plastic float. The small rotameters had a range from 0.152 to 4.52 Imp. gal./min. for the water and 0.0495 to 3.60 Imp. gal./min. for the oil. The large rotameters had a range of 3.54 to 17.3 Imp. gal./min. for water and 1.07 to 11.7 Imp. gal./min. for oil. The oil and water were pumped to the rotameters by two separate Moyno pumps taking suction from separate reservoirs.

A cooling coil was found to be necessary in the oil reservoir because of heat generated when the oil was recycled. The temperature in the water reservoir was controlled manually by the addition of hot or cold water.

The pressure measuring system consisted of pressure stations on the flow line with suitable lead lines and manometers. Special pressure measuring stations were designed to eliminate the entry of the oil-water mixture from the test line to the lead lines, and air was employed as the lead line transmitting fluid. The measuring station consisted of a block of lucite through which the test line passed. A hole ¼-inch in diameter was drilled into the top of the block and through the pipe wall. The hole in the block was enlarged and tapped to take a ¼-inch pipe nipple which supported the splash pot with its gauge, valve and tubing connections. A measuring scale was mounted on each splash pot and was adjusted to the same absolute elevation.

The pressure differentials were measured with three Meriam manometers: one 12-foot mercury manometer, one 12-foot water manometer, and one 30-inch inclined water manometer. These were connected to the three splash pots by ¼-inch polyethylene tubing.

The separator for recovering the oil from the flow line discharge was originally designed to operate continuously, but such severe emulsion problems were encountered that this was possible only at low flow-rates. The gravity cell, equipped with sight glasses, was constructed of sheet metal and was about 6 ft. high and 30 in. in diameter. The mixture flowing from the test pipe was introduced at the centre of this cell and allowed to separate by gravity. If the separation was incomplete the process was conducted batchwise and a steam coil used to break the water-in-oil emulsion. Water was allowed to flow from the bottom of the separator by gravity, and was either recycled back to the water reservoir or discharged into the sewer. The oil was decanted into a secondary drum where any additional suspended water tended to settle out. It was then pumped through a salt tower to take out final traces of water.

The oil used was a clear "white" mineral oil—Kremol 70 from the Sherwood Refining Company, Inglewood, New Jersey, U.S.A.—a paraffinic oil characterized by a viscosity of 18.0 cp. at 77°F. and a specific gravity of 0.834.

Experimental Procedure

1. Pressure differential measurements

Differential pressure measurements were made with various input ratios of oil to water in the range from 0.1 to 10 for 13 differential superficial water rates ranging from 0.116 ft./sec. to 3.55 ft./sec. The measurements were made as follows:

(a) All manometers were vented and balanced and the valves between the splash pots and the pipe test-section were closed. The pressure regulating valves on the lead line air supply were closed.

(b) All valves on the test section between the input manifold and the separator were opened. The discharge bypass valves on the pumps were opened, and the water and oil pumps started. The valves controlling the flow to the rotameters were then set to give the desired flow readings.

(c) After a sufficient time was allowed for the oil and water flow to reach a steady state—this was determined both visually and by pressure drop measurements to be less than about one minute for the rates under study—the valves on the measuring stations which spanned the test section under consideration were slowly opened. Care was taken to allow only oil to enter the splash pots. Fluid levels in both measuring stations were adjusted to the same absolute elevation by regulating the air pressure in the splash pot. The values connecting the pressure stations to the appropriate manometer were then opened, the splash pot levels readjusted and the pressure differential recorded.

(d) After the reading was recorded, all valves on the pressuring measuring system were closed and the manometer was rebalanced by venting. The oil flow-rate was then changed and the sequence of operations was repeated to obtain the new pressure reading for the new flow conditions.

2. Hold-up measurements

For measuring hold-up in the test section, the oil and water flow rates were adjusted to the desired values and the pipeline flow was allowed to reach a steady state. The quick-closing valves were closed and the pumps shut off simultaneously. The contents of the line were collected from the pipe in a four-liter measuring cylinder by injecting compressed air into the pipe and elevating it. It was generally found that 95% of the materal could be recovered for measurement. The oil and water separated on

TABLE 1

EXPERIMENTAL DATA FOR THE FLOW OF MIXTURES OF OIL AND WATER IN A CIRCULAR PIPE

Flowing Temperature = 77 ± 0.5°F. Oil Viscosity = 18.0 cp. Tube Diameter = 0.8057 in.
Water Viscosity = 0.894 cp. Oil Specific Gravity = 0.834 Length of Test Section = 28.18 ft.

(1)	(2)	(3)	(4)	(5)	(6)	(7)	(8)	(9)
Superficial Water Velocity, ft./sec.	Input Oil-Water Volume Ratio, $ft.^3/ft.^3$	Pressure Drop, in. of water		In Situ Oil-Water Volume Ratio, $ft.^3/ft.^3$		Hold-up Ratio**	Friction factor, f_a	
		First reading	Second reading	First reading	Second reading		First reading	Second reading
0.718	0.68	12.9	12.5	0.97	0.91	0.72	0.080	0.078
	1.28	17.7	17.2	1.48	1.47	0.87	0.110	0.107
	1.81	22.9	21.7	1.87	1.95	0.95	0.142	0.135
	2.26	28.5	28.1	2.28	2.28	1.00	0.177	0.175
	2.73	36.3	33.5	2.74	2.81	0.98	0.226	0.208
	3.17	41.4	38.9	3.15	3.38	1.05	0.256	0.242
	4.08	49.6	49.6	3.95	3.80	1.05	0.308	0.308
	4.54	54.4	55.0	4.48	4.43	1.02	0.336	0.342
	0.68	7.0*	7.1*				0.087*	0.088*
	1.28	9.5*	9.7*				0.117*	0.120*
	1.81	11.8*	11.7*				0.146*	0.146*
	1.26	14.5*	13.5*				0.180*	0.168*
	2.73	17.1*	16.2*				0.212*	0.201*
	3.17	19.6*	18.5*				0.243*	0.229*
	3.63	22.0*	20.6*				0.273*	0.258*
	4.08	25.2*	23.7*				0.312*	0.296*
	4.54	27.6*	26.2*				0.345*	0.325*
1.79	0.27	20.2	25.9	0.29	0.31	0.90	0.020	0.026
	0.51	26.3	31.6	0.45	0.43	1.16	0.026	0.031
	0.73	32.5	39.1	0.58	0.56	1.27	0.032	0.039
	0.91	38.7	35.8	0.69	0.70	1.31	0.038	0.035
	1.09	31.3	30.1	0.78	0.81	1.37	0.031	0.030
	1.27	35.8	34.1	0.96	0.93	1.34	0.035	0.034
	1.45	41.0	33.4	1.03	1.04	1.39	0.040	0.033
	1.64	39.5	37.5	1.22	1.21	1.35	0.039	0.037
	1.82	37.5	41.5	1.31	1.38	1.39	0.037	0.041
	0.27	20.2	25.9	0.29	0.31	0.90	0.026*	0.023*
	0.51	26.3	31.6	0.45	0.43	1.16	0.029*	0.029*
	0.73	32.5	39.1	0.58	0.56	1.27	0.036*	0.036*
	0.91	38.7	35.8	0.69	0.70	1.31	0.043*	0.043*
	1.09	31.3	30.1	0.78	0.81	1.37	0.049*	0.049*
	1.27	35.8	34.1	0.96	0.93	1.34	0.049*	0.053*
	1.45	41.0	33.4	1.03	1.04	1.39	0.044*	0.048*
	1.64	39.5	37.5	1.22	1.21	1.35	0.037*	0.039*
	1.82	37.5	41.5	1.31	1.38	1.39	0.042*	0.042*

*Friction factor calculated with data from the second-half of the test-section.

**Hold-up Ratio = $\dfrac{\text{input oil-water volume ratio}}{\text{in situ oil-water volume ratio}}$

standing and the volume of each was measured and the hold-up calculated.

3. Examination of flow pattern

A transparent material was chosen for the pipe test-section so that visual observations could be made of the flowing material. At low flow-rates a quiet interface existed between the oil and water streams, while at high flow-rates the interface tended to break up. A photographic record of typical flow patterns was made using a 4 x 5 inch Linhoff press camera with a 90 mm. lens and a 1/2,000 second electronic flash which effectively stopped the flow in the pipe at all the flow rates used in the investigation.

Experimental Results and Discussion

The key experimental and calculated results are presented in Table 1 (Partial) for the lowest and highest of the 13 superficial water velocities studied. (The complete tabular data have been deposited as Table 1 in Document No. 5772* with the American Documentation Institute Auxiliary Publications Project, Photo Duplication Service, Library of Congress, Washington 25, D.C. Pressure-drop data were obtained for thirteen different water rates at input oil-water volume ratios ranging from 0.1 to 10.0. Hold-up data were obtained for all water rates in the laminar region and for three rates in the turbulent region.

Column 1 in Table 1 was calculated by dividing the volumetric water discharge by the total cross-sectional area of the pipe. The input oil-water volume ratio—Column 2—was obtained by dividing the volumetric oil flow-rate by volumetric water flow-rate. The pressure drop over the 28.18 ft. of pipe is recorded in inches of

*A more detailed form of this paper has been deposited as Document No. 5772 with the ADI Auxiliary Publications Project, Photoduplication Service, Library of Congress, Washington 25, D.C. A copy may be secured by citing the Document No. and by remitting $1.25 for photoprints, or $1.25 for 35 mm. microfilm. Advance payment is required. Make cheques or money orders payable to: Chief, Photoduplication Service, Library of Congress.

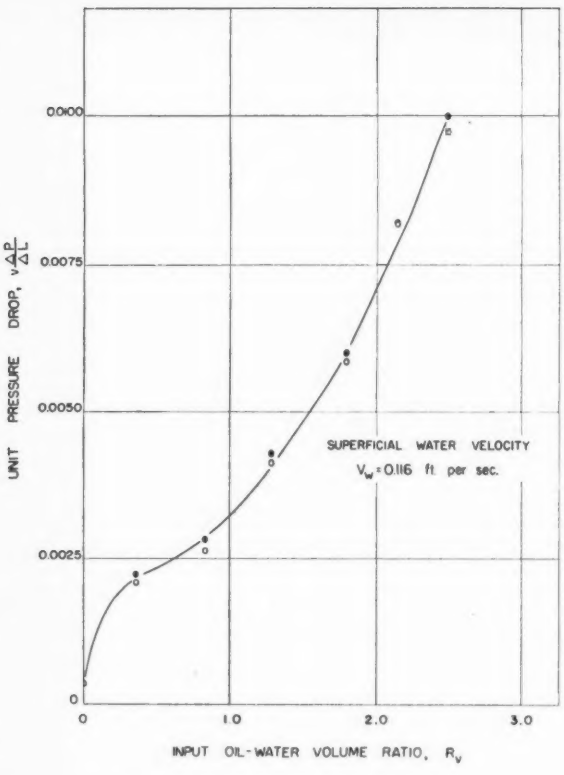

Figure 4 — Experimental pressure drop measurements related to oil-water input ratio for low water flow rates.

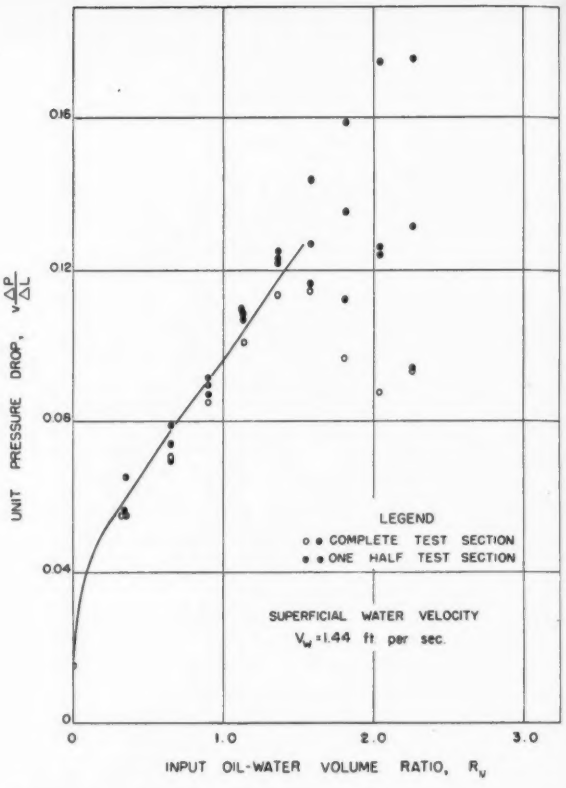

Figure 5 — Experimental pressure drop measurements related to oil-water input ratio for low water flow rates. showing scattering effect of mixed or emulsified flow at high input ratios.

water in Columns 3 and 4. The in situ oil-water volume ratio obtained by direct measurement of the test section contents is tabulated in Columns 5 and 6. Column 7 is obtained by dividing Column 2 by the average of Columns 5 and 6. The modified friction factor, defined as $f_w = \frac{\Delta P g_c D}{\rho \Delta L(2) V_w^2}$, is recorded for the tabulated rates in Columns 8 and 9.

In order to compare the results with similar results on gas-liquid systems, the pressure-drop data are presented as unit pressure drop in feet of water/ft. plotted against the input of oil-water volume ratio. Sample curves are shown in Figures 4 and 5 for superficial water velocities of 0.116 ft./sec. and 1.44 ft./sec. These rates were plotted to show the two inflections present. The inflection in the curve in Figure 4 corresponds to a similar one reported by Govier et al and used as a basis for defining the boundary conditions between bubble and slug flow. In this work the inflection corresponds to a boundary between bubble and stratified flow. The wide scattering of data points at R_v values above 1.5 shown in Figure 5 seems to correlate with the appearance of mixed flow.

The effect of input ratio on the flow pattern is shown in Figures 6, 7 and 8 for three different water velocities. The drawings of Figures 6, 7 and 8 were prepared directly from photographs to show how the liquid interface is affected by changes in the input ratio. By examining the pattern at any one velocity it may be seen that the interface becomes increasingly wavy as the mixed flow-pattern is approached.

Friction factors based on the water properties and flow rates are plotted in Figures 9 and 10 for two of the different water rates. The data plotted in Figures 9 and 10 are both for the complete test section and for the second-half of the test section. The purpose of plotting both sets of data was to detect any changes in the flowing material as it passed through the pipeline, and Figure 10 taken at higher water rates does show a divergence of the data for one half-test-section from that for the complete test section over a small range of input oil-water volume ratios. This is thought to be due to the increase in the emulsification of the system along the pipeline. Once the material becomes completely emulsified, the results begin to coincide again. The ordinates at the zero abscissa values on Figures 9 and 10 represent the friction factors when water is flowing alone. These experimental values checked well with the generally accepted values.

Thirteen plots similar to Figures 9 and 10 were constructed to enable interpolation for the construction of Figure 11 which relates the superficial friction factor to the superficial water velocity for input oil-water volume ratios ranging from 0.1 to 10.0. This plot shows that in the laminar region the lines have a slope of minus one, but that at higher water velocities they gradually curve down towards the single-phase line. Although data are not available at still higher rates, two factors can be expected to affect the relation. The viscosity will have little effect at high velocities and the phases will be well mixed due to turbulence. This indicates that at sufficiently high velocities the curves at all input ratios will reduce to the single-phase line.

The conditions under which the various flow patterns

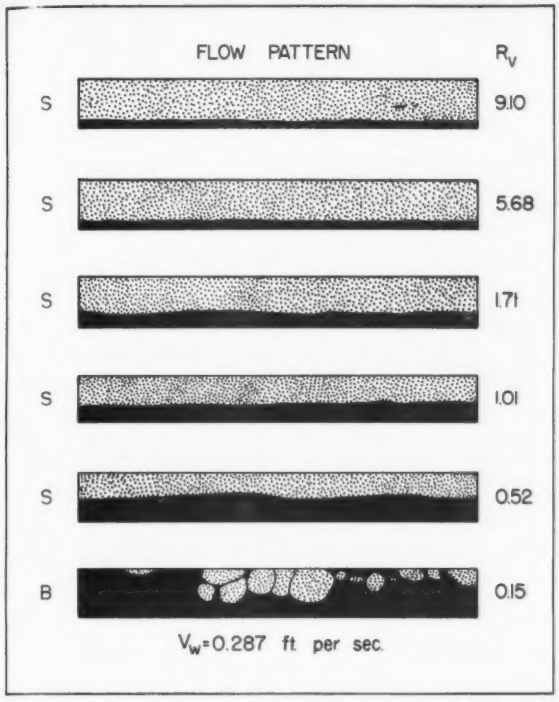

Figure 6—Drawings prepared from photographs showing the transition from stratified to bubble flow as the oil to water ratio is decreased for a relatively low, fixed water flow.

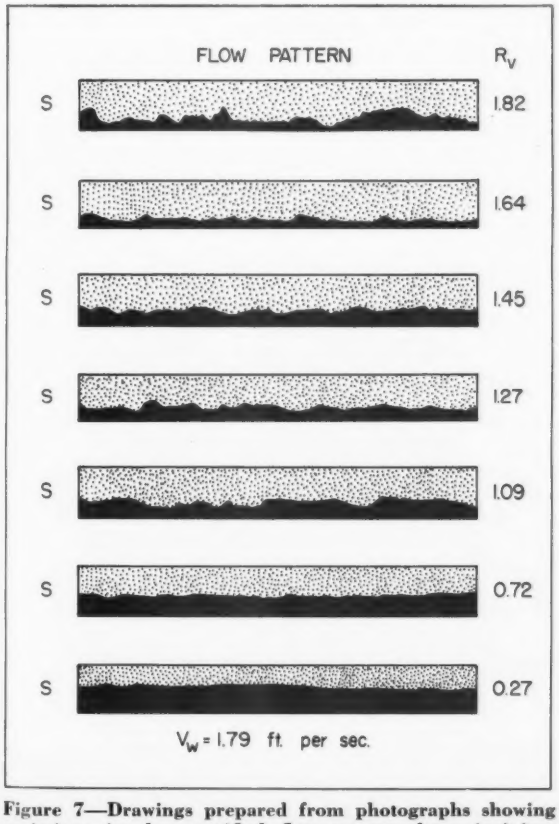

Figure 7—Drawings prepared from photographs showing variations in the stratified flow pattern from incipient mixed flow to quiet stratified flow.

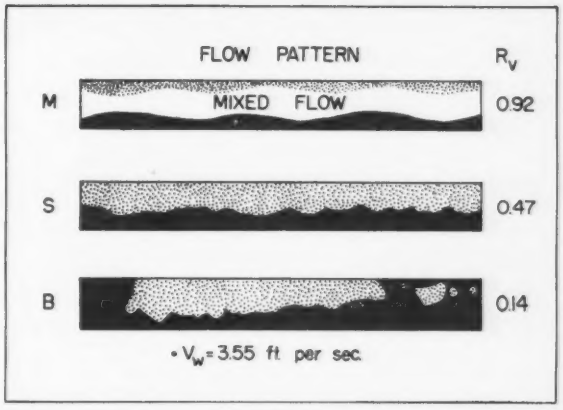

Figure 8—Drawings prepared from photographs showing transition from mixed flow, through stratified flow, to bubble flow for a relatively high fixed water flow.

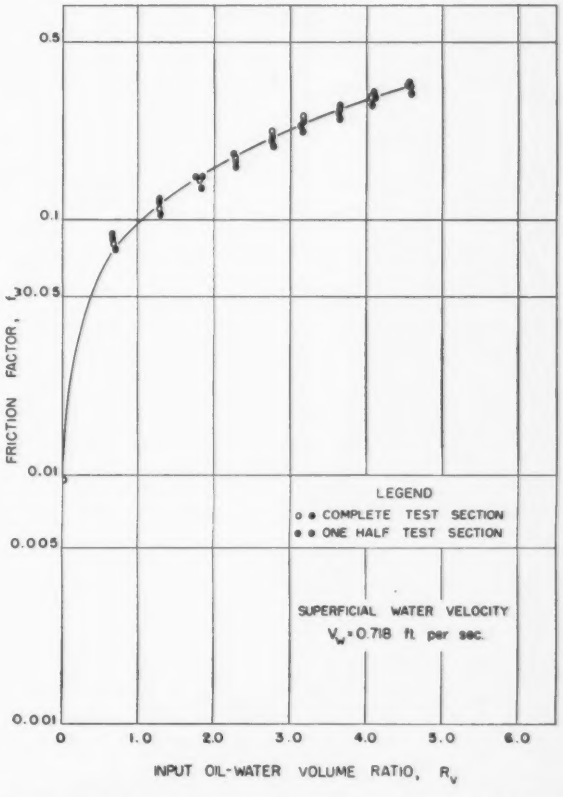

Figure 9—Observed friction factor as a function of input oil-water ratio for a relatively low rate of water flow.

were observed are also indicated in Figure 11 from the results of the photographic observations. From these observations, and the inflections in the friction factor curves, the area covered by the figure is divided into (a) regions where the overall flow may be considered laminar, transitional or turbulent, and (b) regions of the visually observed bubble, stratified and mixed flow-patterns. Martinelli [8] observed that when two phases are present, either can be laminar, transitional or turbulent. This can be seen from Figure 11. A visual observation may indicate the flow to be stratified, but it can be seen that the water

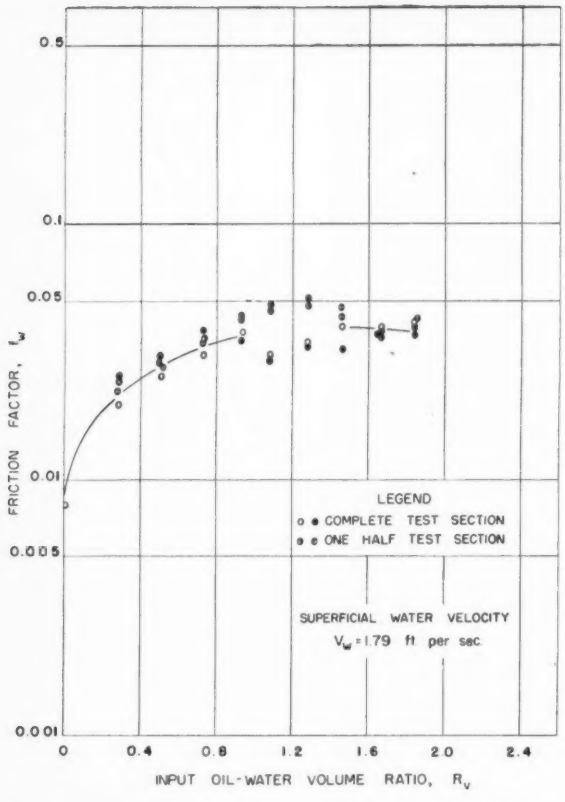

Figure 10—Observed friction factor as a function of input oil-water ratio for a relatively high rate of flow for the water showing an unsteady state of flow during the transition from stratified to emulsified flow.

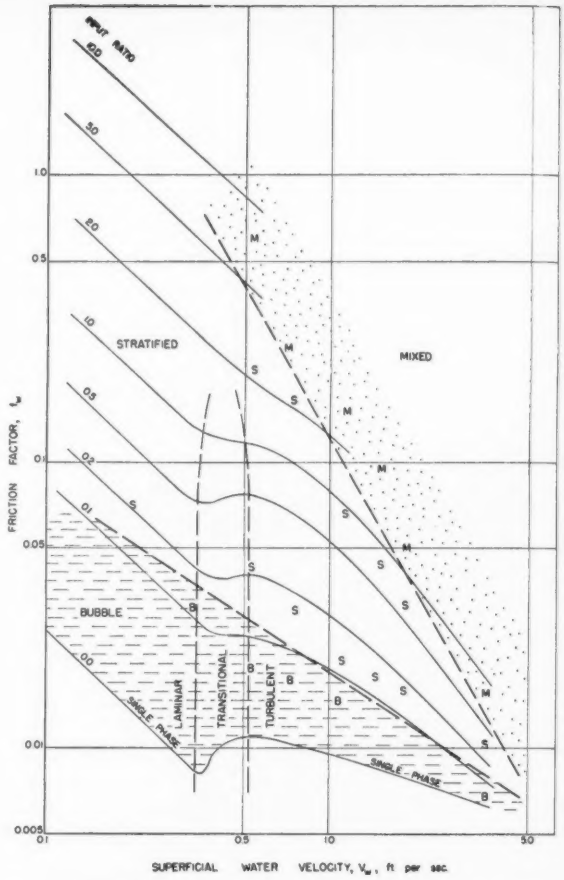

Figure 11—Plot of friction factor versus superficial water velocity for various oil-water ratios showing regions of mixed, stratified and bubble flow extending from the region of laminar flow through the transitional region to that of turbulent flow.

phase could be in a laminar, transitional or turbulent flow zone. As the superficial water velocity increases, the stratified pattern seems to disappear. This is what would be expected as the high turbulence developed tends to mix the two liquids.

Comparing the type of flow patterns encountered in this work with those reported for the horizontal and vertical flow of gas and liquid, it can be seen that some similarities exist. The stratified flow corresponds to what White and Huntington [12] report as stratified and ripple flow. Bubble flow is similar to that described by Govier et al, except for the position of the bubbles. In the vertical pipe the bubbles travelled inside the liquid, whereas in the horizontal pipe the bubbles travelled along the top of the liquid because of the density differential. Mixed flow is analagous here to froth flow in gas-liquid systems. With increasing flow rates in the oil-water system, once mixed flow has developed no other type of flow can be observed since the flowing material just becomes more and more fully emulsified due to shearing action in the pipe.

A comparison of Figure 11, representing the experimental work, with the theoretical results for wide parallel plates in Figure 1 indicates excellent agreement in general form. In the laminar region the friction factors are of the same order of magnitude, and the experimentally determined curves have the same slope and exactly the same spacing as the theoretical curves at low input oil-water volume ratios.

Figure 12 shows two curves of the hold-up ratio versus the input oil-water volume ratio. One represents the experimental results under laminar flow conditions and the other the calculated theoretical hold-up for the parallel plate system. The experimental data taken for five different water velocities show some scattering, but there is a strong indication that the hold-up is independent of the superficial water velocity in the laminar region. The general form of the two curves is in quite close agreement, especially if the differences in geometry of flow are taken into account.

The hold-up relationships in the turbulent region have the same form, but are dependent on the superficial water velocities as shown in Figure 13. Govier et al [14] found similar relationships for gas-liquid hold-up data.

Conclusions

(1) Pressure-drop data have been correlated by plotting a Fanning type friction factor based on the water properties versus a superficial water velocity. The relationship applies only to water and oil of 18.0 centipoise viscosity and 0.834 specific gravity flowing in a one-inch horizontal pipe at 77°F. The correlation shows good agreement in general form in the laminar region, with a similar plot obtained by defining a friction factor from equations developed for laminar flow of the same two liquids between wide parallel plates.

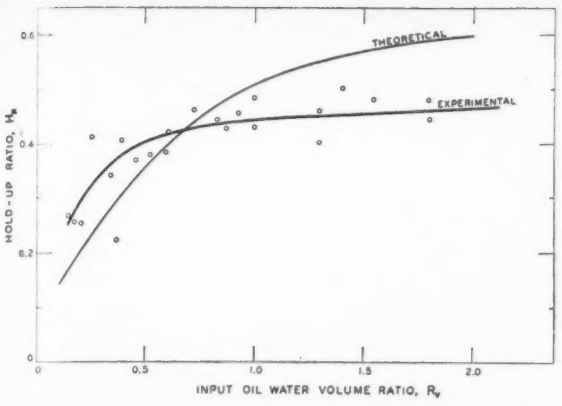

Figure 12—Comparison of the experimental hold-up data for the flow of oil with water with the calculated data for the flow in a parallel plate cell in the region of laminar flow.

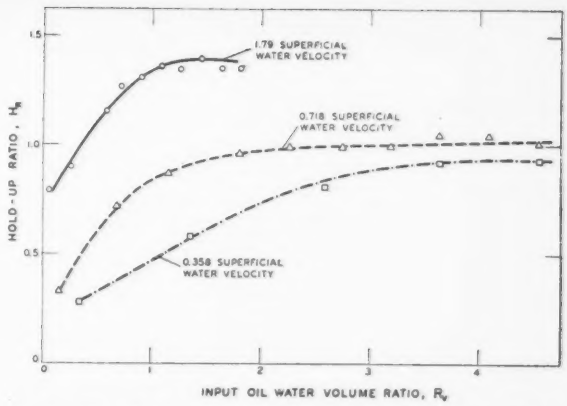

Figure 13—Hold-up input ratio relations for oil-water flow in the turbulent region showing the effect of superficial water velocity on the observed hold-up ratio.

(2) For the liquid ratios and water rates studied, three flow patterns have been visually observed: bubble, stratified, mixed. Any of these patterns could be in a condition of laminar, transitional or turbulent flow.

(3) Experimental hold-up measurements are in accord with those developed for flow between wide parallel plates. In the laminar region, hold-up is a function of liquid input ratio and viscosity. In the turbulent region, hold-up is also a function of superficial water velocity.

Nomenclature

$2a$ = distance between parallel plates, ft.
b = width of plates, ft.
D = diameter of pipe, ft.
f = friction factor, dimensionless.
g_c = dimensional conversion factor, lb_M. ft./$lb._F$ sec.^{2}
L = length, ft.
$M_1 = (-32a^3y + 36a^2y^2 - 12ay^3 + y^4$
$M^2 = (-16a^4 + 32a^3y - 24a^2y^2 + 8ay - y^4)$
$M_3 = (-y)$
$M_4 = (y - 2a)$
$N_1 = (-y^4)$
$N_2 = (4ay^3 - 12a^2y^2 + y^4)$
$N_3 = (-y)$
$N_4 = (y - 2a)$
ΔP = total pressure drop over length ΔL, $lb._F/ft.^2$
V = velocity, ft./sec.
y = distance from bottom plate to interface, ft.
μ = viscosity, $lb._M$/ft. sec.
ρ = density, ft.^{3}/$lb._M$
ϵ = relative roughness, ft.
μ_w = viscosity of water, $lb._M$/ft. sec.
μ_o = viscosity of oil, $lb._M$/ft. sec.
ρ_w = density of water, ft.^{3}/$lb._M$
ρ_o = density of oil, ft.^{3}/$lb._M$
f_w = superficial friction factor based on water properties, dimensionless.
f_{pp} = parallel plate friction factor based on water properties, dimensionless.
H_R = hold-up ratio: ratio of input to in situ oil-water volume ratio, dimensionless.

$$K_w = \frac{1}{12\mu_w}\left[\frac{N_1\mu_o + N_2\mu_w}{N_3\mu_o + N_4\mu_w}\right], \text{ ft. sec./lb.}_M$$

Q_w = volumetric water flow-rate, ft.^{3}/sec.
Q_o = volumetric oil flow-rate, ft.^{3}/sec.
R_v = input oil-water volume ratio, ft.^{3}/ft.^{3}
V_w = superficial water velocity, ft./sec.
V_G = average velocity of gas phase, ft./sec.
V_L = average velocity of liquid phase, ft./sec.

References

(1) Clark, K. A., private communication, (1948).
(2) Clark, A. F., and Shapiro, A., (to Socony Vacuum Oil Company, Inc.) U.S. Patent 2,533,878, May 31 (1949).
(3) Muskat, M., Physical Properties of Oil Production, First Edition, McGraw Hill Book Co. Inc., New York (1949).
(4) Bruce, W. R., Hodgson, G. W., and Clark, K. A., Trans. Can. Inst. Min. Met. 55, 422 (1952).
(5) Uren, L. C., Gregory, P. P., Hancock, R. A., and Feshov, G. V., Trans. A.I.M.E. 86, 208 (1930).
(6) Nowels, K. B., Trans A.I.M.E. 86, 200 (1932).
(7) Lockhart, R. W., and Martinelli, R. C., Chem. Eng. Prog. 45, 1, 45 (1949).
(8) Martinelli. R. C., Boelter, L. M. K., Thomson, E. C., Taylor, T. H. M., and Morrin, E. H., Trans. A.S.M.E. 66, 2, 139 (1944).
(9) Jenkins, R., M.Ch.E. Thesis, Two-Phase Two Component Flow of Water and Air, Univ. of Delaware (1947).
(10) Bergelin, O. P., Chem. Eng. 56, 104 (1949).
(11) Baker, O., "Design of Pipelines for the Simultaneous Flow of Oil and Gas". Paper presented at the fall meeting of the Petroleum Branch, A.I.M.E. Dallas, Texas, October (1953).
(12) White, P. P., and Huntington, R. L., Pet. Engineer, 27, D.40 (1955).
(13) Chenoweth, J. M., and Martin, M. W., Petroleum Refiner 34, 10, 151 (1955).
(14) Govier, G. W., Radford, B. A., and Dunn, J. S. C., Can. J. Ch. E., 35, 2, 58 (1957).
(15) Short, W. L., M.Sc. Thesis in Chem. Eng., Univ. of Alberta (1949).
(16) Sullivan, G. A., and Govier, G. W., private communication, Jan. (1958).
(17) Moore, T. W., and Wilde, H. C., Trans. A.I.M.E. 92, 296 (1931).
(18) Russell, T. W. F., and Charles, M. E., C.J.Ch.E., 37, 1, 18 (1959).
(19) Walker, J. E., Whan, G. A., and Rothfus, R., A.I.Ch.E. 3, 484 (1957).

★ ★ ★

The Effect of the Less Viscous Liquid in the Laminar Flow of Two Immiscible Liquids[1]

T. W. F. RUSSELL[2] and M. E. CHARLES[3]

Instances are cited in which the pressure gradient in an oil pipe line has been reduced by the injection of water into the pipeline. A general mathematical analysis is presented for two immiscible liquids flowing (1) in two layers between wide parallel plates, and (2) concentrically in a circular pipe. This will form a basis for the further study of oil-water systems. Equations are derived relating the volumetric flow rates and the viscosities of the liquids with the pressure gradient. The conditions for which minimum pressure gradients and minimum power requirements occur were determined and these minimum values have been compared with known values for a pipeline flowing full with only a single liquid. The factors by which the pressure gradient and power requirement can be reduced are very large. For example, for an oil of viscosity 1,000 cp. flowing concentrically with water, the reduction factor is approximately 500. The pressure gradient reduction factors reported in the literature are compared with those predicted by theory, and conclusions are drawn regarding the position of the water phase.

One of the problems facing producers of heavy viscous crude oils is the difficulty encountered in pipeline transportation. The main problem arises because a very viscous oil does not flow readily unless a very high differential pressure is applied to it, and this results in a need for pumping units that are large, and closely-spaced, along a pipeline. One approach to a solution of this problem is the introduction of water into the oil flowing in the pipeline to reduce the resistance to flow. It should be noted that the same volumetric flow rate of the oil is maintained when the water is introduced.

Clark [1] studied the heavy viscous crude oil from the McMurray oil sand of Alberta, and observed a pressure drop reduction when water was injected into this oil in a 0.375-inch pilot pipeline. The flow was laminar, with Reynolds numbers ranging from 10 to 20, and at the temperatures investigated the oil viscosity ranged from 800 to 1000 cp. Injection of 7-13% water reduced the pressure gradient, which is the pressure drop per unit length of pipe in the direction of flow, by factors from 6 to 12. The relative positions of the oil and water were not known, but it was suggested that the water wetted the inside of the pipe preferentially.

Clark and Shapiro [2] patented a process in 1950 for a method of pumping viscous petroleum by injection of water and demulsifying agents into a crude oil pipeline. The patent described results from investigations in a 6-inch commercial pipeline, 3 miles long, under laminar flow conditions. Oil viscosities were not reported, but an estimate based on similar types of crude oil from the same region indicates oil viscosities from 800 to 1000 cp. Injection of 7-24% water reduced the pressure gradient by factors from 7.8 to 10.5, and it was found that the optimum pressure reduction occurred when 8-10% water was injected with the crude oil.

Russell, Hodgson and Govier [3] observed the simultaneous flow of oil and water in a transparent horizontal pilot pipeline 28 ft. long and 0.806 in. in diameter. The oil used was a white mineral oil with a viscosity of 18 cp. In the laminar region of flow, stratification occurred with the oil flowing above the water. For a given oil flow-rate it was found that the pressure drop over the test section could be reduced by the addition of the water. The pressure gradient was reduced by a factor of 1.2 at a water content of about 10% with Reynolds numbers ranging from 10 to 400.

Water introduced into an oil pipeline can either form an emulsion or can flow as a separate phase. Tipman and Hodgson [4] and Pavlov [5] indicate that the viscosity of an oil-water emulsion is almost always greater than that of the pure oil and, therefore, if an emulsion is formed the pressure gradient would be greater than for the oil flowing alone. Since the pressure gradient for pumping a viscous oil has been shown to be reduced by the random injection of water, it must be concluded that the water is flowing as a separate phase.

The first flow system to be examined in the present paper deals with stratified flow of two immiscible liquids between parallel plates in which the stratification results from the density differential existing between the two liquids. Since the wide parallel plate system is the simplest geometrical conduit for stratified flow, equations relating pressure drop to geometry and liquid flow rates and viscosities will be developed for this case. Differentiation of the equations will give values of the position of the interface for minimum pressure gradient.

[1]*Manuscript received August 22, 1958.*
[2]*Present address: Carbide Chemicals Company, Division of Union Carbide Canada Limited, Montreal, Que.*
[3]*Research Council of Alberta, Edmonton, Alta.*
Contribution from the Research Council of Alberta, Edmonton, Alta.

The second flow system to be analysed will deal with the flow of the two immiscible liquids in a circular pipe. Since the majority of shear takes place near a pipe wall, it is reasonable to assume that a systematic injection of water around the inner periphery of a pipe should give greater power reduction than would a random injection into the flowing stream. For this reason equations relating flow rate and pressure gradient will be derived for the concentric flow of two liquids of equal density in a circular pipe. Differentiation of these equations will give values of the position of the interface for minimum pressure gradient and minimum power requirement.

The analyses of the flow of a single liquid between wide parallel plates and in a circular pipe are known—Streeter [6], Coulson and Richardson [7]. However, not much work has been done for the case of the simultaneous flow of two liquids. Coulson and Richardson [7] and Corcoran et al [8] touched on a special case of two liquids between parallel plates in student exercise, but no work has been reported on the concentric flow of two immiscible liquids in a circular pipe.

Theory

A theoretical discussion is presented for the simultaneous flow of two immiscible liquids in the following systems:

(I) Stratified flow between wide parallel plates;
(II) Concentric flow in a circular pipe.

Equations are derived which relate the volumetric flow-rate to the pressure gradient, the geometry of the system and the viscosities of the liquids. It will be shown how the maximum volumetric flow-rate per unit pressure gradient can be established, and the minimum power requirement will be calculated for concentric flow.

The theory applies only to incompressible Newtonian liquids in laminar motion. The velocity of liquid in contact with a stationary boundary is assumed to be zero, and the velocities of the two liquids at an interface are assumed to be equal. Derivations are presented separately for each system but as far as possible the development is similar in each case.

I Stratified liquid flow between wide horizontal parallel plates.

The system for stratified flow between wide horizontal parallel plates is illustrated in Figure 1. Liquid A forms the upper layer and is assumed to be more viscous than Liquid B. Edge effects are neglected because the width of the plates is considered to be very large compared with the distance between the plates.

(a) Nomenclature.

$2a$ = distance between plates, ft.
b = width, ft.
ΔL = length, ft.
y = distance from the bottom plate to the interface, ft.
x = distance from the bottom plate to a point in liquid A, ft.
z = distance from the bottom plate to a point in liquid B, ft.

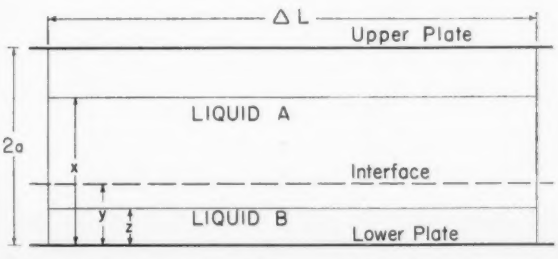

Figure 1—Two layer flow between wide horizontal parallel plates. Liquid A flows above liquid B.

U = velocity of liquid, ft./sec.
Q = volumetric flow rate of liquid, ft.³/sec.
μ = viscosity of liquid, lb.$_m$/ft. sec.
ΔP = total pressure drop over the length ΔL, lb.$_f$/ft.²
R_x = unit shear force in the liquid at distance x, lb.$_f$/ft.²
R_z = unit shear force in the liquid at distance z, lb.$_f$/ft.²
R_i = unit shear force at the interface of the two liquids, lb$_f$./ft.²
g_c = dimensional conversion factor, lb.$_m$ ft./lb.$_f$ sec.²
$\frac{\Delta P_{Full}}{\Delta P_{Min}}$ = pressure gradient reduction factor, dimensionless

Subscript A refers to liquid A, the upper fluid; subscript B to liquid B, the lower fluid.

(b) Evaluation of volumetric flow rates.

Consider the element of the upper liquid (liquid A) between x = y and x = x, length ΔL and width b, as shown in Figure 1. A force balance gives:

$$\Delta P(x - y)b - R_x \Delta L b + R_i \Delta L b = O \quad \ldots\ldots(1)$$

$$\text{But } R_x = -\frac{\mu_A}{g_c}\left(\frac{dU_A}{dx}\right) \quad \ldots\ldots(2)$$

Substituting (2) in (1), integrating using the boundary condition that $U_A = O$ when $x = 2a$ we obtain:

$$U_A = \frac{g_c}{\mu_A}\frac{\Delta P}{\Delta L}\left(2a^2 - 2ay - \frac{x^2}{2} + yx\right) + \frac{g_c}{\mu_A} R_i (2a - x) \quad \ldots(3)$$

Consider the element of the lower liquid (liquid B) between z = z and z = y and length ΔL (Figure 1). A force balance gives:

$$\Delta P(y - z)b - R_z \Delta L b - R_i \Delta L b = O \quad \ldots\ldots(4)$$

Substituting for R_z and integrating using the boundary condition that $U_B = O$ when $z = O$ we obtain:

$$U_B = \frac{g_c}{\mu_B}\left(\frac{\Delta P}{\Delta L}\right)\left(yz - \frac{z^2}{2}\right) - \frac{g_c}{\mu_B} R_i(z) \quad \ldots\ldots(5)$$

At the interface $U_A = U_B$, and by using equations (3) and (5) we have:

$$R_i = \left(\frac{\Delta P}{\Delta L}\right)\left(\frac{4\mu_B a^2 - 4\mu_B ay + (\mu_B - \mu_A)y^2}{2(\mu_B - \mu_A)y - 4\mu_B a}\right) \quad \ldots\ldots(6)$$

The volumetric flow rates are obtained by evaluating the integrals:

$$Q_A = b\int_{x=y}^{x=2a} U_A dx \text{ and}$$

$$Q_B = b\int_{z=O}^{z=y} U_B dz$$

giving

$$Q_A = \frac{bg_c}{12\mu_A}\left(\frac{\Delta P}{\Delta L}\right)\left(\frac{M_1\mu_A + M_2\mu_B}{M_3\mu_A + M_4\mu_B}\right) \quad \ldots\ldots(7)$$

$$Q_B = \frac{bg_c}{12\mu_B}\left(\frac{\Delta P}{\Delta L}\right)\left(\frac{N_1\mu_A + N_2\mu_B}{N_3\mu_A + N_4\mu_B}\right) \quad \ldots\ldots(8)$$

where

$M_1 = (-32a^3y + 36a^2y^2 - 12ay^3 + y^4)$
$M_2 = (-16a^4 + 32a^3y - 24a^2y^2 + 8ay - y^4)$
$M_3 = (-y)$
$M_4 = (y - 2a)$
$N_1 = (-y^4)$
$N_2 = (4ay^3 - 12a^2y^2 + y^4)$
$N_3 = (-y)$
$N_4 = (y - 2a)$

(c) **Position of interface for minimum pressure gradient.**

Rearrangement of Equation (7) gives:

$$Q_A' = \frac{bg_c}{12\mu_A}\left(\frac{M_1\mu_A + M_2\mu_B}{M_3\mu_A + M_4\mu_B}\right) \quad \ldots\ldots(9)$$

where $Q_A' = Q_A/\left(\frac{\Delta P}{\Delta L}\right)$ is the volumetric flow rate per unit pressure gradient.

The value of y for which Q_A' is a maximum is found by differentiating Equation (9) and equating to zero. This gives:

$$(\mu_A - \mu_B)^2y^4 - 8(\mu_A - \mu_B)^2a\,y^3 + (3\mu_A^2 + 6\mu_B + 11\mu_A\mu_B)a^2y^2 + 16\mu_B(3\mu_A - 2\mu_B)a^3y - 16\mu_B(\mu_A - \mu_B)a^4 = 0$$

Since one root of this equation is $y = 2a$ the following cubic is obtained:

$$y^3 - 6ay^2 + \frac{4\mu_B}{\mu_A - \mu_B}\left(\frac{3\mu_B - 5\mu_A}{\mu_A - \mu_B}\right)a^2y + \frac{8a^3\mu_B}{\mu_A - \mu_B} = 0 \quad \ldots(10)$$

A trigonometric method is available for solving Equation (10). However, it is felt that because of the complexity of the roots they are best obtained by trial and error solution after substitution of values for μ_A and μ_B for a specific system.

The maximum pressure gradient reduction factor is found for any two liquids by solving Equation (10) for y and using the value of y obtained to evaluate M_1, M_2, M_3 and M_4 in Equation (7). The ratio $\Delta P_{Full}/\Delta P_{Min}$ is obtained by dividing the expression for the pressure drop for a liquid of viscosity μ_A flowing between wide parallel plates (Streeter [6]) $Q_A\mu_A/(0.66)ba^3g_c$ by ΔP_{Min} calculated from Equation (7).

(d) **Position of interface for minimum power requirement.**

The power requirement per unit length of pipe is given by $\frac{\Delta P}{\Delta L}(Q_A + Q_B)$ and it is theoretically possible to differentiate this expression and obtain a value of y for which the power requirement is a minimum. However, the complexity of Equations (7) and (8) makes this unfeasible and the minimum power requirement is best left for a trial and error solution for a given specific system when values of the viscosities are known.

II Concentric flow in a circular horizontal pipe.

The system for concentric flow in a circular horizontal pipe is illustrated in Figure 2. The liquids are assumed to have equal densities. Liquid A is the more viscous and flows inside liquid B.

(a) **Nomenclature.**

r_o	= inside radius of pipe, in.
r_i	= radius of interface between liquids, in.
r	= radius of a particle of liquid, in.
ΔL	= length of pipe considered, ft.
ΔP	= pressure drop over length ΔL, $lb._f/ft.^2$
U	= velocity of liquid at radius r, ft./sec.
U_i	= velocity of liquids at interface, ft./sec.
C	= integration constant, ft./sec.
Q	= volumetric flow rate, $ft.^3/sec.$
μ	= viscosity, $lb._m/ft.$ sec.
R_r	= shear force per unit area at radius r, $lb._f/ft.^2$
R_i	= force acting on element at interface, $lb._f$
$\frac{\Delta P_{Full}}{\Delta P_{Min}}$	= pressure gradient reduction factor, dimensionless

(b) **Evaluation of volumetric flow rate.**

Consider the cylindrical element of liquid A having radius r and length ΔL, as shown in Figure 2. A force balance gives:

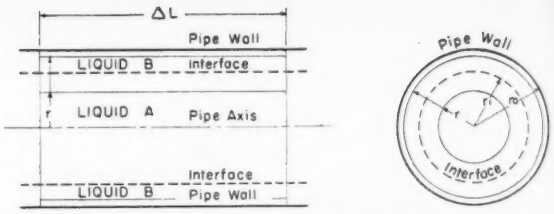

Figure 2—Concentric flow in a circular pipe. Liquid B flows between liquid A and the pipe wall.

$$\Delta P\pi r^2 + 2\pi r\Delta L R_{rA} = 0 \quad \ldots\ldots(11)$$

$$\text{But, } R_{rA} = -\frac{\mu_A}{g_c}\left(\frac{dU_A}{dr}\right) \quad \ldots\ldots(12)$$

Substituting (12) in (11), integrating using the boundary condition that $U_A = U_i$ when $r = r_i$ we have:

$$U_A = -\frac{g_c}{4\mu_A}\left(\frac{\Delta P}{\Delta L}\right)(r_i^2 - r^2) + U_i \quad \ldots\ldots(13)$$

Now consider the hollow cylindrical element of liquid B having inner radius r_i, outer radius r and length ΔL. (Figure 2). A force balance gives:

$$\Delta P\pi(r^2 - r_i^2) + 2\pi r\Delta L R_{rB} - R_i = 0 \quad \ldots\ldots(14)$$

where R_i is the force acting on the element at the interface.

Substituting for R_{rB} and integrating we have:

$$U_B = -\frac{g_c}{2\mu_B}\left(\frac{\Delta P}{\Delta L}\right)\left(r_i^2 \ln r - \frac{r^2}{2}\right) - \frac{g_c R_i \ln r}{2\pi\mu_B\Delta L} + C \quad \ldots(15)$$

where C is the constant of integration.

In equations (13) and (15) R_i, C and U_i are unknown.

A force balance on liquid A gives

$$R_i = -\Delta P\pi r_i^2 \quad \ldots\ldots(16)$$

Substituting Equation (16) in Equation (15) and using the boundary condition that $U_B = 0$ when $r = r_o$ we obtain:

$$C = -\frac{g_c}{4\mu_B}\left(\frac{\Delta P}{\Delta P}\right)r_o^2 \quad \ldots\ldots(17)$$

Substituting the boundary condition that $U_B = U_i$ when $r = r_i$ in Equation (15) and using Equation (16) and (17) we obtain:

$$U_i = -\frac{g_c}{4\mu_B}\left(\frac{\Delta P}{\Delta L}\right)(r_o^2 - r_i^2) \quad \ldots\ldots(18)$$

Hence from Equations (13) and (18)

$$U_A = -\frac{g_c}{4\mu_A\mu_B}\left(\frac{\Delta P}{\Delta L}\right)(\mu_A r_o^2 - (\mu_A - \mu_B)r_i^2 - \mu_B r^2) \quad \ldots(19)$$

and from Equations (15), (16) and (17)

$$U_B = -\frac{g_c}{4\mu_B}\left(\frac{\Delta P}{\Delta L}\right)(r_o^2 - r^2) \quad \ldots\ldots(20)$$

The volumetric flow rates are obtained by evaluating the integrals:

$$Q_A = 2\pi\int_{r=0}^{r=r_i} rU_A dr \text{ and}$$

$$Q_B = 2\pi\int_{r=r_i}^{r=r_o} rU_B dr$$

Taking ΔP as the pressure drop in the direction of flow integration gives:

$$Q_A = \frac{\pi r_i^4 g_c}{8}\left(\frac{\Delta P}{\Delta L}\right)\left[\frac{1}{\mu_A} + \frac{2}{\mu_B}\left(\frac{r_o^2}{r_i^2} - 1\right)\right] \quad \ldots\ldots(21)$$

$$Q_B = \frac{\pi g_c}{8\mu_B}\left(\frac{\Delta P}{\Delta L}\right)(r_o^2 - r_i^2)^2 \quad \ldots\ldots(22)$$

Equations (21) and (22) are similar to the equations developed by Yuster [6] in a theoretical analysis of multiphase flow in capillary systems.

(c) **Position of interface for minimum pressure gradient.**

Rearrangement of Equation (21) gives:

$$Q_A' = \frac{\pi r_i^4 g_c}{8}\left[\frac{1}{\mu_A} + \frac{2}{\mu_B}\left(\frac{r_o^2}{r_i^2} - 1\right)\right] \quad \ldots\ldots(23)$$

where $Q_A' = Q_A/\left(\frac{\Delta P}{\Delta L}\right)$ is the volumetric flow rate per unit pressure gradient.

The value of r_i for which Q_A' is a maximum is found by differentiating Equation (23) with respect to r_i^2 and equating to zero.

This gives:

$$r_i = \sqrt{\frac{\mu_A}{2\mu_A - \mu_B}} \cdot r_o \quad \ldots\ldots(24)$$

Substituting Equation (24) in Equation (23) we have:

$$Q_A'_{(Max)} = \frac{\pi r_o^4 g_c}{8}\left[\frac{\mu_A}{\mu_B(2\mu_A - \mu_B)}\right] \quad \ldots\ldots(25)$$

For a pipe of radius r_o flowing full of liquid A, Coulson and Richardson [7] developed the equation:

$$Q_A'_{(Full)} = \frac{\pi r_o^4 g_c}{8\mu_A} \quad \ldots\ldots(26)$$

The factor by which the pressure gradient can be reduced by the introduction of the less viscous liquid B into the pipe is obtained by dividing Equation (25) by Equation (26).

$$\frac{\Delta P_{Full}}{\Delta P_{Min}} = \frac{\mu_A^2}{(2\mu_A - \mu_B)\mu_B} \quad \ldots\ldots(27)$$

If μ_A is very much greater than μ_B Equation (27) becomes

$$\frac{\Delta P_{Full}}{\Delta P_{Min}} = \frac{\mu_A}{2\mu_B} \quad \ldots\ldots(28)$$

Combining Equation (26) and (28) we have:

$$\left(\frac{\Delta P}{\Delta L}\right)_{Min} = \frac{16\mu_B Q_A}{\pi r_o^4 g_c} \quad \ldots\ldots(29)$$

Equation (29) gives the minimum pressure gradient in terms of the volumetric flow rate of liquid A, the viscosity of liquid B and the pipe radius.

(d) **Position of interface for minimum power requirement.**

The power requirement per unit length of pipe to pump a given quantity of liquid A is given by:

$$\text{Power} = \frac{\Delta P}{\Delta L}(Q_A + Q_B) \quad \ldots\ldots(30)$$

For a given Q_A the pressure gradient can be evaluated from Equation (21), and substituting this pressure gradient in the expression for Q_B (Equation 22) we obtain:

$$Q_B = \frac{(r_o^2 - r_i^2)^2 Q_A}{\mu_B r_i^4\left[\frac{1}{\mu_A} + \frac{2}{\mu_B}\left(\frac{r_o^2}{r_i^2} - 1\right)\right]} \quad \ldots\ldots(31)$$

Substituting for Q_B and $\left(\frac{\Delta P}{\Delta L}\right)$ in Equation (30) and simplifying we have:

$$\text{Power} = \frac{8\mu_A\mu_B Q_A^2}{\pi g_c}\left[\frac{\mu_A r_o^4 - (\mu_A - \mu_B)r_i^4}{4\mu_A^2 r_o^4 r_i^4 + (2\mu_A - \mu_B)^2 r_i^8 - 4\mu_A(2\mu_A - \mu_B)r_o^2 r_i^6}\right] \quad \ldots\ldots(32)$$

The value for r_i for which the power is a minimum is found by differentiating Equation (32) with respect to r_i^2 and equating to zero. This gives:

$$r_i^{10} - \frac{2\mu_A}{(2\mu_A - \mu_B)} r_o^2 r_i^8 - \frac{2\mu_A}{\mu_A - \mu_B} r_o^4 r_i^6 + \frac{6\mu_A^2}{(2\mu_A - \mu_B)(\mu_A - \mu_B)} r_o^6 r_i^4 - \frac{4\mu_A^3}{(\mu_A - \mu_B)(2\mu_A - \mu_B)^2} r_o^8 r_i^2 = 0 \quad (33)$$

This is a 5th power equation in r_i^2. Assuming that μ_A is very large compared with μ_B then Equation (33) becomes on factorisation:

$$r_i^2(r_i^2 - r_o^2)^2(r_i^2 - 0.618r_o^2)(r_i^2 + 1.618r_o^2) = 0 \quad \ldots\ldots(34)$$

The required root is $r_i = 0.786r_o$. The minimum power requirement is obtained by substituting this value of r_i in Equation (32) after it has been modified for the case when μ_A is very large compared with μ_B. This gives:

$$\text{Power}_{Min} = \frac{22.2\mu_B Q_A^2}{\pi r_o^4 g_c} \quad \ldots\ldots(35)$$

The optimum factor by which the power requirement can be reduced by introducing the less viscous liquid B into the pipe is found by dividing the expression for the power requirement in a pipe flowing full of liquid A by the expression for minimum power (Equation 35):

$$\frac{\text{Power}_{Full}}{\text{Power}_{Min}} = \frac{\mu_A}{2.78\mu_B} \quad \ldots\ldots(36)$$

It is interesting to compare Equation (36) with Equation (28). The power requirement cannot be reduced to the same extent as the pressure gradient because of the increase in volumetric flow caused by the addition of liquid B.

Computation

The flow-rate Equations (7, 8, 21 and 22) were verified in the following way. The sum of Q_A and Q_B was obtained for $\mu_A = \mu_B = \mu$. For the parallel plate system this sum was found to be identical with the expression $\frac{2ba^3 g_c}{3\mu}\left(\frac{\Delta P}{\Delta L}\right)$ developed by Streeter [6] for a liquid of viscosity μ flowing between parallel plates. For the pipe system the sum was identical with $\frac{\pi r_o^4 g_c}{8\mu}\left(\frac{\Delta P}{\Delta L}\right)$ which is the Poiseuille equation and is developed by Coulson and Richardson [7] for a liquid of viscosity μ flowing in a pipe of radius r_o.

The flow rate/unit pressure gradient was computed for the parallel plate system for a range of five viscosities from 0.1 to 1000 cp. for each liquid at ten interface positions between O and 2a. The general form of the flow-rate curves for liquid A is illustrated in Figure 3.

For the concentric flow system the flow rate per unit pressure gradient was computed for an identical range of viscosities from 0.1 to 1000 cp. for each liquid, for nineteen in situ ratios and sixteen pipe diameters from 0.5 inches to 20 inches. The general form of the flow-rate curves for liquid A is illustrated in Figure 4. The detailed computed data for this system is on file at the Research Council of Alberta.

The general form of the variance of the pressure gradient and power requirement with position of the

interface when the viscosity of liquid A may be considered to be very much greater than the viscosity of liquid B is shown in Figure 5.

The forms of the velocity profiles calculated from Equations (3), (5), (19) and (20) are indicated for both systems in Figure 6.

Discussion

The simultaneous flow of two immiscible liquids stratified between parallel plates, and concentrically in a circular pipe, has been analysed, and final expressions evaluated for a wide range of conditions of flow. It should be emphasized again that the reduction in pressure gradient is obtained by introducing a less viscous liquid into the conduit without reducing the volumetric flow-rate of the more viscous liquid.

The magnitude of the reduction in pressure gradient is very much greater in the case of concentric flow than in the parallel plate system, and the reason for this is apparent from a consideration of the velocity profiles shown in Figure 6. In the circular pipe with the more viscous liquid in the core the majority of shear takes place in the less viscous liquid near the pipe wall. In a sense the inner liquid could be considered as flowing in a moving pipe. In the parallel plate system, however, one surface of the more viscous liquid is in contact with the stationary

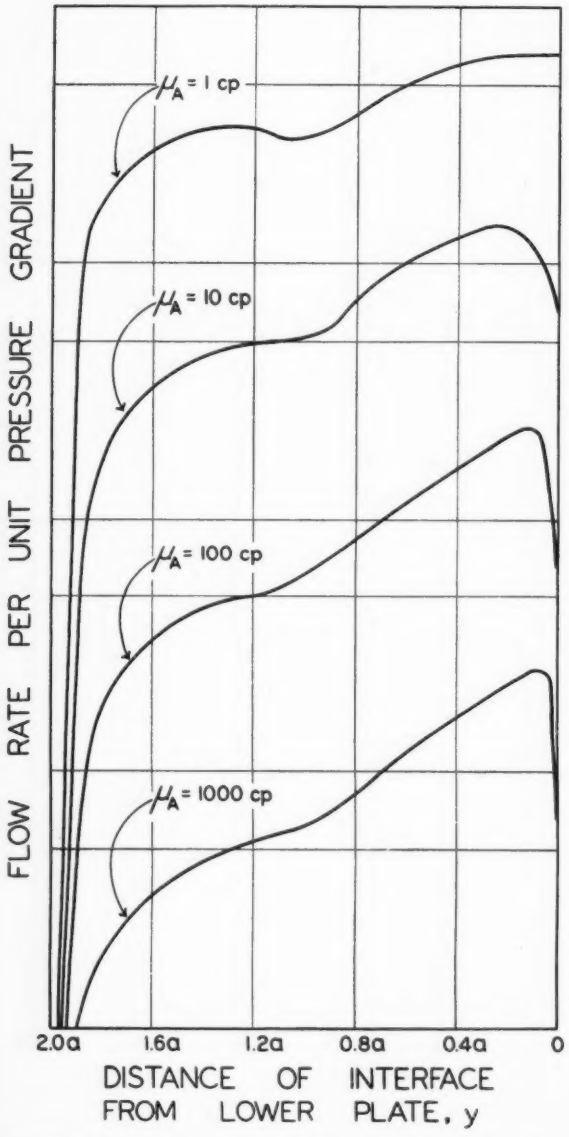

Figure 3—The general form of the variance of the flow rate of liquid A per unit pressure gradient with the position of the interface for the parallel plate system. The curves are drawn for a constant volumetric flow rate of liquid A, and liquid B is assumed to be water with a viscosity of 1 cp. The intersections of the curves with the line y = 0 give the flow rates per unit pressure gradient obtained when the plates are completely occupied by liquid A.

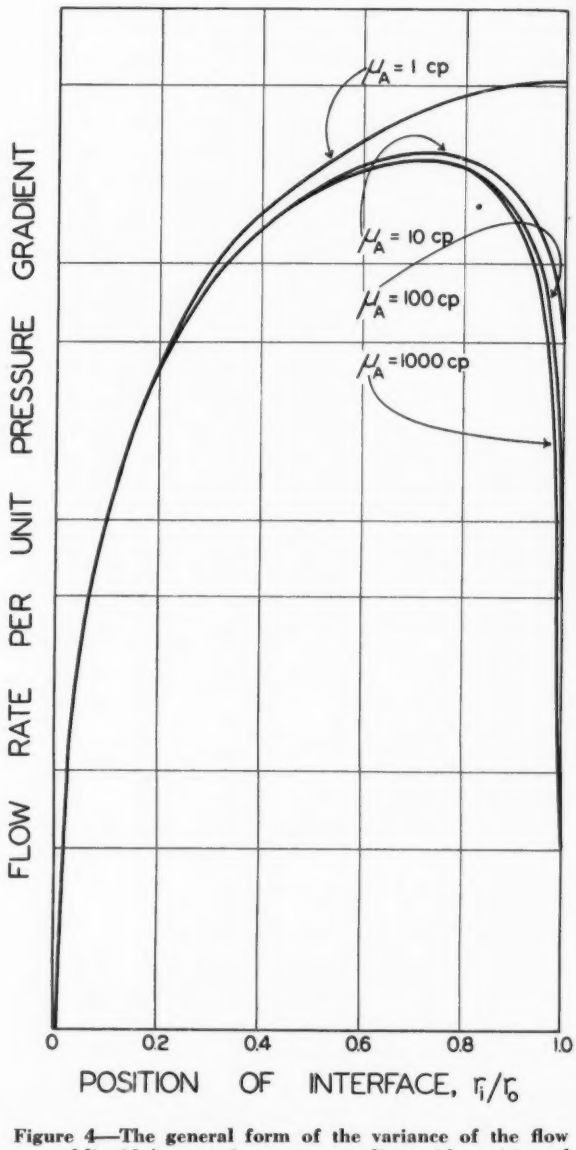

Figure 4—The general form of the variance of the flow rate of liquid A per unit pressure gradient with position of the interface for concentric flow in a circular pipe. The curves are drawn for a constant volumetric flow rate of liquid A, and liquid B is assumed to be water with a viscosity of 1 cp. The intersections of the curves with the line $r_i/r_o = 1$ gives the flow rates per unit pressure gradient obtained when the pipe is completely occupied by liquid A.

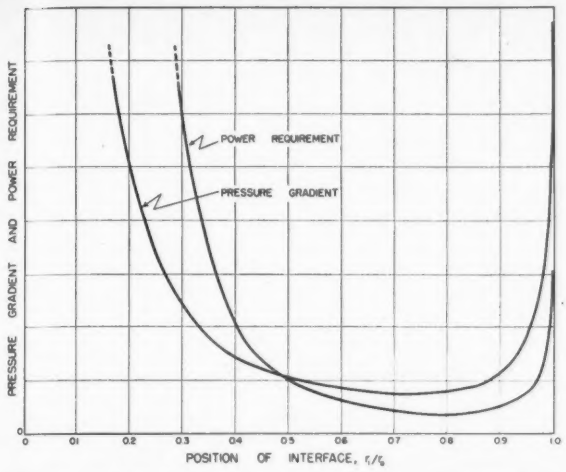

Figure 5—The general variance of the pressure gradient and power requirement with position of the interface for the concentric flow of oil (liquid A) and water (liquid B) in a horizontal pipeline. It is assumed that the flow rate of the oil is constant and that the viscosity of the oil is very much greater than the viscosity of the water. The minimum of the power curve is at $r_1/r_0 = 0.786$ and the minimum of the pressure gradient curve is at $r_1r/_0 = 0.717$.

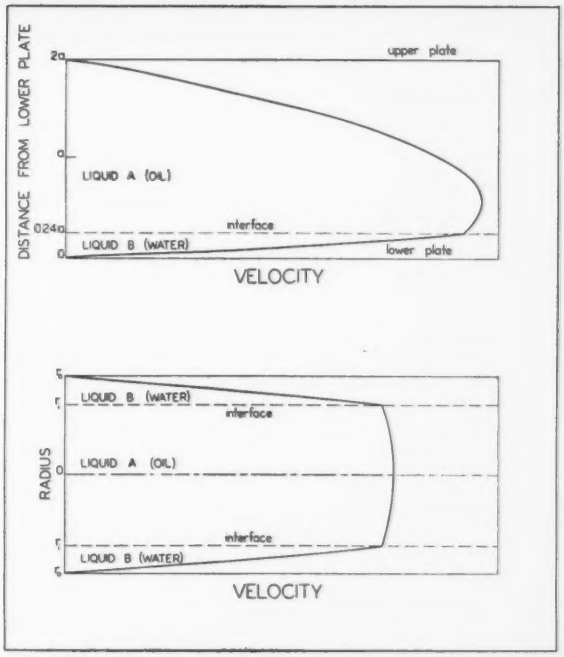

Figure 6—The form of the velocity profiles for two liquid layers flowing between parallel plates (upper) and for the concentric flow of two liquids in a circular pipe (lower). Both are drawn for conditions when the viscosity of liquid A is much greater than the viscosity of liquid B and the flow rate of liquid A per unit pressure gradient is a maximum.

conduit wall and considerably more shear takes place in the more viscous liquid than in the case of concentric flow.

With regard to the initial problem of flow of a viscous oil in the presence of water, it is pertinent to calculate the maximum pressure reduction factors to be expected for the three oils studied by Clark, Clark and Shapiro, and Russell et al. Table 1 shows the values of the reduction factors calculated for all three oils in both concentric and stratified flow and the observed pressure gradient reduction factors. There are two points to notice: firstly, the results for the low viscosity oil indicate that the maximum reduction factor observed for stratified flow in a circular pipe is less than the reduction factor predicted for stratified flow between parallel plates. This difference can be attributed to the difference in conduit geometry, including edge effects. Secondly, by analogy with the oil used by Russell et al, the pressure gradient reduction factor for the stratified flow in a circular pipe may be predicted as being less than the 3-4 for the more viscous oil. The observed values fall, then, between the values predicted for concentric flow and stratified flow in a circular pipe. Although Clark, and Clark and Shapiro, claimed a preferential water wetting of the pipe the water could not have wetted the complete inner periphery otherwise larger pressure gradient factors would have been observed. It is, therefore, reasonable to conclude that that flow was intermediate between the stratified and concentric types.

Conclusions

The following equations have been developed giving the flow rates of two immiscible incompressible Newtonian liquids flowing in laminar motion.

For two layers flowing between wide horizontal parallel plates:

$$Q_A = \frac{bg_c}{12\mu_A}\left(\frac{\Delta P}{\Delta L}\right)\left[\frac{M_1\mu_A + M_2\mu_B}{M_3\mu_A + M_4\mu_B}\right]$$

$$Q_B = \frac{bg_c}{12\mu_B}\left(\frac{\Delta P}{\Delta L}\right)\left[\frac{N_1\mu_A + N_2\mu_B}{N_3\mu_A + N_4\mu_B}\right]$$

TABLE 1

PREDICTED AND OBSERVED PRESSURE GRADIENT REDUCTION FACTORS FOR OIL-WATER FLOW

Reference	Oil type	Oil gravity, °API.	Oil viscosity, cp.	Maximum predicted pressure gradient reduction factor		Maximum observed pressure gradient reduction factor
				Concentric flow	Parallel plates	
Clark[1]	Crude	7.0	800–1000*	400–500	3–4	12
Clark and Shapiro[2]	Crude	13.4	800–1000**	400–500	3–4	10.5
Russell et al[3]	Refined	38	18	9	2.2	1.2

*Estimated viscosity of McMurray oil-sand oil at 70°C., the temperature at which the observations were made.
**Estimated from a general knowledge of the viscosity of heavy crude oils at normal pipeline temperatures.

For concentric flow in a horizontal circular pipe:

$$Q_A = \frac{\pi r_i^4 g_c}{8}\left(\frac{\Delta P}{\Delta L}\right)\left[\frac{1}{\mu_A} + \frac{2}{\mu_B}\left(\frac{r_o^2}{r_i^2} - 1\right)\right]$$

$$Q_B = \frac{\pi r_i^4 g_c}{8\mu_B}\left(\frac{\Delta P}{\Delta L}\right)\left[r_o^2 - r_i^2\right]^2$$

These equations lead to the theoretical prediction that reductions in pressure gradient, and therefore reductions in power requirement, can be obtained when a less viscous liquid B is introduced between the more viscous liquid A and the stationary boundaries of the flow area.

The maximum reduction obtained in the pipe system with concentric flow is considerably greater than in the parallel plate system. For the concentric flow system the pressure gradient can be reduced by a factor of $\frac{\mu_A^2}{(2\mu_A - \mu_B)\mu_B}$, and the power requirement can be reduced by a factor of $\frac{0.36\mu_A}{\mu_B}$ if μ_A is large compared with μ_B.

Acknowledgements

The authors wish to acknowledge the helpful advice given by G. W. Hodgson. Thanks are also due to the Physics Department of the University of Alberta for the use of their Royal McBee L.G.P. 30 computer.

References

(1) Clarke, K. A., private communication (1948).

(2) Clark, A. F., and Shapiro, A., U.S. Patent No. 2, 533, 878 (May 31, 1949).

(3) Russell, T. W. F., Hodgson, G. W., and Govier, G. W., C.J.Ch.E. 1, 9 (1959).

(4) Tipman, E., and Hodgson, G. W., J. Petrol. Tech. 8, No. 9, 91-3 (1956).

(5) Pavlov, P. P., Trudy Azerbaidzahn, Ind. Inst. im. M. Azizbekova, No. 9, 76-80 (1955).

(6) Streeter, V. L., Fluid Mechanics, First Edition, McGraw-Hill Book Co. Inc., New York (1951).

(7) Coulson, J. M., and Richardson, J. F., Chemical Engineering, Vol. I, Pergamon Press Ltd., London (1954).

(8) Corcoran, W. H., Opfell, J. B., and Sage, B. H., Momentum Transfer in Fluids, Academic Press Inc., New York (1956).

(9) Yuster, S. T., Proc. 3rd World Petroleum Congress, 2, 437 (1951).

★ ★ ★

Distribution of Residence Times in Continuous Series of Mixing Zones[1]

E. J. BUCKLER[2] and L. BREITMAN[2]

Tabulated numerical data, not hitherto available, are presented for the number fraction distribution of residence times of particles in fluid which passes through a series of 1, 2, 3, . . . up to 75 mixing zones in series. For the special case in which the weight of particles varies linearly with time, the weight fraction distributions of residence time are also tabulated. The theory is recapitulated and extended to include the effect of recycle.

When a fluid mixture of particles, defined below, passes at uniform rate through a series of zones, each of which is maintained perfectly mixed, the number fraction distribution of residence times of particles in the effluent mixture may be calculated in terms of the volume and number of mixing zones and the volume flow of the mixture. The component particles of the mixture are the largest elements which remain coherent during passage through the system; in a physical solution the component particles are molecules; in a suspension or colloidal dispersion, the particles are the molecules of the continuous phase and the entities of the disperse phase.

Several studies have been concerned with the space-time properties of flow systems. Engelbretsen [1] described an experimental study of short-circuiting in a series of continuous reactors; Danckwerts [2, 3] analyzed flow systems in terms of distribution functions of residence times; Denbigh [4] has presented the theory of distribution of residence times. MacMullin and Weber [5] have published numerical data relating to the distribution of residence times for systems comprising 1, 2, 3, 5, 10 and 20 mixing zones; Robinson and Roberts [6] have recently developed the theory in a form somewhat different from that of previous authors, and have presented numerical data for systems of up to 5 mixing zones. Determination of the distribution of residence times through term-by-term evaluation of previously published formulae becomes excessively laborious as the number of mixing zones becomes large.

In this paper it is shown how accurate values for the number fraction distribution of residence times can be obtained for systems comprising up to 75 mixing zones by use of tabulated values of the Poisson Exponential Binominal Limit. For the special case in which the weight or volume of the particles varies in a linear manner with residence time, it is also shown that the weight or volume fraction distribution of particles in the effluent according to residence time is readily derived from the number fraction distributon. Finally, the theory is extended to systems in which a portion of the effluent is recycled to the feed.

Theory

Frequency distribution of residence times.

Assume fluid material passes at volume flow rate w through N mixing zones, each of volume v, in series. At time t = 0, assume that particles are introduced into zone 1 to give ${}_0c_1$ per unit volume; at this time the concentration of these particles in all other zones is 0. At time t = T, assume that the concentrations in zones 1, 2, . . . i, . . . N, are ${}_Tc_1$, ${}_Tc_2$, . . . ${}_Tc_i$, . . . ${}_Tc_N$. The fraction of these particles which have completely left the system by time T is:

$$(v\,{}_0c_1 - v\sum_{i=1}^{i=N} T_i^e)/v{}_0c_1 = 1 - \sum_{i=1}^{i=N} T_i^e/{}_0c_1 = X \quad \ldots\ldots(1)$$

At time t the decrease in the number of particles in zone i, during a time interval dt is given by:

$$w\,({}_tc_i - {}_tc_{i-2})\,dt = -\,d\,(v\,{}_tc_i)$$

Hence:

$$d{}_tc_i/dt = -\,({}_tc_i - {}_tc_{i-1})/r \quad \ldots\ldots(2)$$

where r = v/w = average residence time in each zone. For i = 1, ${}_tc_1 - {}_1 = 0$. Integration of equation (2) between the limits t = 0 and t= T for i = 1 gives:

$${}_Tc_1 = {}_0c_1\,e^{-T/r} \quad \ldots\ldots(3)$$

Substitution of Equation (3) in Equation (2) for i = 2 followed by integration gives:

$${}_Tc_2 = {}_0c_1\,e^{-T/r}\,(T/r) \quad \ldots\ldots(4)$$

Proceeding stepwise in this manner, it will be found that:

$$T^e{}_i = {}_0c_1\,e^{-T/r}\,(T/r)^{i-1}/(i-1)! \quad \ldots\ldots(5)$$

Now R = Nr and T = ZR. Replacing T/r by ZN in Equation (5) and substituting in Equation (1) gives:

[1]*Manuscript received September 17, 1958.*
[2]*Research and Development Division, Polymer Corp. Limited, Sarnia, Ont.*
Contribution from the Research and Development Division, Polymer Corp., Limited, Sarnia, Ont.

$$X = 1 - e^{-ZN} \sum_{i=1}^{i=N} (ZN)^{i-1}/(i-1)! \quad \ldots\ldots(6)$$

This equation gives the cumulative number fraction X of particles with residence times up to ZR in a system of N zones. The frequency distribution may be described by an ordinate h at time T such that

$$dX = hdT = RhdZ \quad \ldots\ldots(7)$$

By differentiation of X with respect to Z in Equation (6) it will be found that:

$$Rh = N(ZN)^{N-1} e^{-ZN}/(N-1)! \quad \ldots\ldots(8)$$

Weight fraction distribution according to residence times.

If the mass y of each particle changes with time according to a relation of the form $y = a + bT$, then the mass dm of a fraction dX with residence times between T and T + dT is given by:

$$dm = k(a + bT)\, dX\, {}_0c_1 = k(a + bRZ)\, dX\, {}_0c_1$$
$$= k\, {}_0c_1 [a\, dX + bR(ZN)^N e^{-ZN}\, dZ/(N-1)!]$$

(see Equations (7) and (8))

By integration of this equation between the limits 0 and Z it will be found that:

$m_Z = k\, {}_0c_1 (aX + bRY)$ where

$$Y = 1 - e^{-ZN} \sum_{l=1}^{l=N+1} (ZN)^{l-1}/(l-1)! \quad \ldots\ldots(9)$$

When $Z \to \infty$ $X = Y = 1$ and $m_Z = M = k\, {}_0c_1 (a + bR)$

Hence the weight fraction of particles with residence times less than ZR is given by:

$$m_Z/M = X\, a/(a + bR) + YbR/(a + bR) \quad \ldots\ldots(10)$$

If $a = 0$, $m_Z/M = Y$. The frequency distribution corresponding to Y may be described by an ordinate j at the time T such that $dY = jdT = RjdZ$.

By differentiation of Y with respect to Z in Equation (9) it will be found that:

$$Rj = (NZ)^N e^{-NZ}/(N-1)! = ZRh \quad \ldots\ldots(11)$$
$$= N(NZ)^N e^{-NZ}/N!$$

Calculations

The expressions on the right hand sides of Equations (6) and (9) may be written in the form

$$1 - e^{-a}\left\{\sum_{x=0}^{\infty} a^x/x! - \sum_{x=c}^{\infty} a^x/x!\right\}, \text{ i.e., } e^{-a}\sum_{x=c}^{\infty} a^x/x!$$

This function will be recognized as the cumulative Poisson frequency distribution, usually written P(c,a), which has been tabulated [7] to six significant figures, for values of a from 0.001 to 100. Using the present notation, Equations (6) and (9) become

$$X = P(N, ZN)$$
$$Y = P([N+1], ZN)$$

The graphical forms of the functions X and Y plotted against Z are "S" shaped curves for each value of N. In order to present a complete family of curves in compact tabular form, the values of Z were calculated for each value of N corresponding to values of X and Y of 0.005, 0.010, . . . 0.990. These values of Z are given to three decimals for X and Y in Tables 1 and 2 respectively. Accurate graphs where required can be readily constructed for any value of N.

The expressions for Rh and Rj in Equations (8) and (11) may be written in the form $N\, e^{-a}\, a^x/x!$, where $a = ZN$, and $x = N-1$ for Rh, and $x = N$ for Rj. The function $e^{-a}\, a^x/x!$ will be recognized as an individual term of the Poisson distribution function. It has also been tabulated [8], for values of a from 0.001 to 100. The values of Rh and Rj are of little use for calculations and in general are required only for illustrative purposes. Values to three decimals of Rh and Rj for a few cases are listed in Table 3.

TABLE 1

CUMULATIVE DISTRIBUTION OF RESIDENCE TIMES

$$X = 1 - e^{-ZN} \sum_{i=1}^{i=N} (ZN)^{i-1}/(i-1)!$$

Number of Zones (N)	1	2	3	4	5	6	7	8	9	10	12	15	20	25	50	75
Cumulative Fraction of Effluent (X)	Fractions or Multiples of the Average Residence Time (Z_X) at Which the Cumulative Fraction, X, of Effluent has the Values Indicated															
0.005	0.005	0.051	0.111	0.167	0.215	0.256	0.291	0.321	0.348	0.372	0.412	0.460	0.518	0.560	0.672	0.727
0.010	0.010	0.074	0.144	0.205	0.255	0.297	0.333	0.363	0.390	0.413	0.452	0.498	0.554	0.594	0.701	0.751
0.050	0.051	0.176	0.272	0.341	0.394	0.435	0.469	0.498	0.522	0.542	0.577	0.616	0.663	0.693	0.779	0.818
0.100	0.105	0.265	0.367	0.436	0.486	0.525	0.557	0.582	0.604	0.622	0.652	0.687	0.726	0.753	0.823	0.855
0.200	0.213	0.412	0.512	0.574	0.618	0.651	0.676	0.697	0.714	0.729	0.753	0.779	0.808	0.828	0.879	0.902
0.300	0.358	0.548	0.638	0.691	0.727	0.753	0.773	0.789	0.802	0.813	0.831	0.850	0.871	0.886	0.921	0.936
0.400	0.511	0.688	0.762	0.803	0.830	0.848	0.863	0.874	0.883	0.891	0.902	0.915	0.928	0.929	0.958	0.967
0.500	0.693	0.840	0.891	0.918	0.934	0.945	0.953	0.959	0.963	0.967	0.972	0.978	0.984	0.987	0.993	0.996
0.600	0.917	1.011	1.035	1.044	1.047	1.049	1.049	1.048	1.048	1.048	1.046	1.045	1.041	1.038	1.030	1.025
0.700	1.204	1.220	1.205	1.191	1.178	1.168	1.159	1.151	1.145	1.139	1.129	1.119	1.104	1.095	1.069	1.057
0.800	1.609	1.497	1.427	1.379	1.344	1.318	1.297	1.279	1.264	1.252	1.231	1.209	1.183	1.164	1.117	1.096
0.900	2.303	1.945	1.775	1.670	1.599	1.546	1.505	1.471	1.444	1.421	1.387	1.343	1.296	1.264	1.185	1.151
0.950	2.996	2.372	2.098	1.938	1.831	1.753	1.692	1.644	1.604	1.575	1.520	1.460	1.395	1.351	1.244	1.197
0.990	4.605	3.319	2.802	2.512	2.321	2.185	2.083	2.000	1.941	1.883	1.796	1.700	1.594	1.524	1.358	1.288

CUMULATIVE FRACTION OF EFFLUENT (X) AT THE AVERAGE RESIDENCE TIME ($Z_X = 1$)

Number of Zones (N)	1	2	3	4	5	6	7	8	9	10	12	15	20	25	50	75
Cumulative Fraction (X)	0.632	0.594	0.577	0.567	0.560	0.554	0.550	0.547	0.544	0.542	0.538	0.534	0.530	0.527	0.519	0.515

TABLE 2

CUMULATIVE WEIGHT FRACTION DISTRIBUTION

$$Y = 1 - e^{-ZN} \sum_{1=1}^{1=N+1} (ZN)^{1-1}/(1-1)!$$

Number of Zones (N)	1	2	3	4	5	6	7	8	9	10	12	15	20	25	50	75
Cumulative Fraction of Product (Y)	Fractions or Multiples of the Average Residence Time (Z_Y) at Which the Cumulative Fraction (Y) has the Values Indicated															
0.005	0.103	0.166	0.223	0.269	0.307	0.339	0.367	0.391	0.413	0.432	0.465	0.504	0.553	0.590	0.689	0.738
0.010	0.148	0.216	0.274	0.319	0.357	0.388	0.415	0.438	0.459	0.477	0.508	0.545	0.591	0.622	0.717	0.762
0.050	0.353	0.408	0.455	0.492	0.522	0.547	0.569	0.587	0.603	0.617	0.641	0.669	0.704	0.728	0.797	0.830
0.100	0.531	0.551	0.581	0.608	0.630	0.649	0.665	0.679	0.691	0.702	0.720	0.742	0.767	0.788	0.842	0.867
0.200	0.824	0.767	0.766	0.772	0.781	0.789	0.797	0.803	0.810	0.816	0.826	0.838	0.854	0.865	0.898	0.914
0.300	1.097	0.957	0.921	0.903	0.903	0.902	0.902	0.902	0.904	0.905	0.908	0.912	0.918	0.922	0.941	0.949
0.400	1.377	1.142	1.070	1.037	1.018	1.006	0.999	0.993	0.989	0.986	0.981	0.979	0.977	0.976	0.978	0.980
0.500	1.680	1.337	1.224	1.168	1.134	1.112	1.096	1.084	1.074	1.067	1.056	1.045	1.034	1.027	1.013	1.009
0.600	2.023	1.553	1.392	1.309	1.258	1.224	1.198	1.179	1.164	1.152	1.132	1.113	1.092	1.079	1.050	1.039
0.700	2.440	1.808	1.588	1.473	1.401	1.352	1.316	1.288	1.265	1.247	1.219	1.190	1.158	1.137	1.090	1.071
0.800	2.995	2.139	1.838	1.681	1.581	1.513	1.462	1.422	1.391	1.365	1.326	1.284	1.238	1.207	1.138	1.110
0.900	3.890	2.661	2.227	1.998	1.855	1.756	1.681	1.624	1.578	1.545	1.484	1.422	1.353	1.309	1.207	1.165
0.950	4.745	3.148	2.585	2.288	2.103	1.974	1.878	1.804	1.750	1.697	1.624	1.541	1.454	1.397	1.266	1.212
0.990	6.639	4.203	3.349	2.901	2.622	2.428	2.286	2.187	2.092	2.018	1.904	1.786	1.656	1.576	1.382	1.303

CUMULATIVE FRACTION (Y) AT THE AVERAGE RESIDENCE TIME ($Z_Y = 1$)

Number of Zones (N)	1	2	3	4	5	6	7	8	9	10	12	15	20	25	50	75
Cumulative Fraction (Y)	0.264	0.323	0.353	0.371	0.384	0.394	0.401	0.407	0.413	0.417	0.424	0.432	0.441	0.447	0.462	0.469

The values for the cumulative distribution of residence times are of use in describing the time required for a change introduced in the composition of the incoming flow of material to become established in varying degrees in the effluent. The values of the cumulative distribution of weight fraction apply to reactions in which the mass or volume of particles changes in a linear fashion with time.

Frequency distribution of residence times with recycle.

The question may arise as to the effect on the distri-

TABLE 3

FREQUENCY DISTRIBUTION OF RESIDENCE TIMES

$Rh = N(ZN)^{N-1} e^{-ZN}/(N-1)!$; $Rj = (ZN)^N e^{-ZN}/(N-1)!$

Number of Zones (N)	1		2		4		10		25	
Fraction of Average Residence Time (Z)	Rh	Rj	Rh	Rj	Rh	Rj	Rh	Rj	Rh	Rj
0.05	0.956	0.048	0.181	0.009	–	–	–	–	–	–
0.1	0.905	0.091	0.327	0.032	0.008	–	–	–	–	–
0.2	0.819	0.164	0.536	0.107	0.077	0.015	0.002	–	–	–
0.3	0.741	0.222	0.659	0.197	0.236	0.071	0.027	0.008	–	–
0.4	0.670	0.268	0.719	0.287	0.451	0.180	0.132	0.053	0.002	–
0.5	0.607	0.303	0.736	0.368	0.668	0.334	0.363	0.182	0.032	0.016
0.6	0.549	0.329	0.723	0.433	0.840	0.504	0.688	0.413	0.208	0.125
0.7	0.497	0.348	0.690	0.483	0.944	0.661	1.014	0.710	–	–
0.8	0.449	0.359	0.646	0.517	0.977	0.782	1.241	0.993	1.393	1.115
0.9	0.407	0.366	0.595	0.535	0.949	0.854	1.318	1.186	–	–
1.0	0.368	0.368	0.541	0.541	0.878	0.878	1.251	1.251	1.988	1.988
1.1	0.333	0.366	0.488	0.536	0.794	0.873	1.085	1.194	–	–
1.2	0.301	0.361	0.435	0.522	0.694	0.833	0.874	1.049	1.065	1.278
1.4	0.247	0.345	0.341	0.477	0.456	0.638	0.473	0.662	0.290	0.406
1.6	0.202	0.323	0.261	0.417	0.287	0.458	0.213	0.341	0.048	0.077
1.8	0.165	0.298	0.197	0.354	0.169	0.303	0.083	0.149	0.005	0.010
2.0	0.135	0.271	0.147	0.293	0.095	0.189	0.029	0.058	–	–
2.4	0.091	0.218	0.079	0.189	0.027	0.064	0.003	0.007	–	–
2.8	0.061	0.170	0.041	0.161	0.007	0.019	–	–	–	–
3.2	0.041	0.131	0.021	0.068	0.002	0.005	–	–	–	–

bution of residence times of recycling a portion of the fluid mixture from the last zone to the inlet to the first zone. The required relationship between X, Z and N is as follows*

$$X = (1 - B)\cdot P(N,a) + B(1 - B)\cdot P(2N,a) + B^2(1 - B)\cdot P(3N,a) + \ldots\ldots + B^{s-1}(1 - B)\cdot P(Ns,a) + \ldots\ldots \quad (12)$$

where P(N,a), P(2N,a), P(3N,a) . . . etc. are tabulated values of the cumulative Poisson function in which

$a = NZ/(1\text{-}B)$

B = the ratio: recycle flow/(feed flow + recycle flow)

The infinite series in Equation (12) converges rapidly after s terms when s is greater than 1.2 Z/(1-B).

For given values of N and feed rate w, the effect of recycling is to broaden the distribution of residence times in a manner similar to that resulting from reduction in N without recycling. For very large recycle rates the compositions of all zones tend to become identical and the system behaves as a singe mixing zone.

Nomenclature

N = number of zones in which perfect mixing occurs.
Z = (residence time)/(average residence time).
R = average residence time in the N zones.
X = fraction of number of particles with residence times less than $Z_X R$.
Y = fraction of weight of particles with residence times less than $Z_Y R$.
w = volume flow rate of material.
v = volume of each mixing zone.
c_i = number of particles per unit volume at time t in zone i.
r = average residence time in each zone = v/w.
m_Z = weight or volume of particles for which the residence time is $\leq ZR$.
M = weight or volume of particles for which Z lies between 0 and ∞.
B = the ratio (recycle flow)/(feed flow + recycle flow).

*The derivation of Equation (12) was considered too long for inclusion in this paper but it may be obtained from the authors on request.

Acknowledgements

The authors are grateful to E. C. Molina and to the D. van Nostrand Company, Inc., for permission to use the numerical values tabulated in the copyrighted Poisson's Exponential Binomial Limit. Helpful discussions were held with P. F. Wade. Mrs. N. Fraser assisted with some of the numerical computations. Permission by Polymer Corp. Limited to publish this paper is appreciated.

References

(1) H. J. Engelbretsen, Private Communications to Reconstruction Finance Corporation, Sept. 24, 1945.
(2) P. V. Danckwerts, Chem. Eng. Sci. 2, 1-13 (1953).
(3) P. V. Danckwerts, Ind. Chemist 30, 102-106 (1954).
(4) K. G. Denbigh, Trans. Faraday Soc. 40, 352-73 (1944).
(5) R. B. MacMullin and M. Weber, Jr., Trans. Am. Inst. Chem. Engrs. 31, 409-58 (1935).
(6) J. N. Robinson and J. E. Roberts, C.J.Ch.E. 35, 105-12 (1958).
(7) E. C. Molina, Table II, p. 1 et seq., Poisson's Exponential Binomial Limit, D. van Nostrand Co., Inc., New York, 1942.
(8) E. C. Molina, ibid, Table I, p. 1 et seq.

★ ★ ★

Ultimate Velocity of Drops in Stationary Liquid Media[1]

M. WARSHAY[2], E. BOGUSZ[2], M. JOHNSON[2] and R. C. KINTNER[2]

The effects of high field viscosity and of low interfacial tension on the terminal velocity of single liquid drops falling through stationary liquid fields were investigated. Drops of tetrachloroethylene, ranging from 0.08 cm. to 1.4 cm. equivalent diameter, were allowed to fall through four different types of field fluids made by the addition of carboxy methyl cellulose, Lytron 890, corn syrup, and glycerine to water. Viscosities varied from 41.3 to 514 centipoises.

Low interfacial tension systems were ethylchloroacetate-water, furfural-water, and benzyl alcohol-water with interfacial tensions of 16.43, 5.70, and 4.25 dynes per cm. respectively.

For systems of high field viscosity, the usual drag curve appears to be more useful than the correlation proposed by Hu and Kintner. For systems of low interfacial tension (below 20 dynes/cm.) and low field viscosity (of the order of one centipoise) the latter serves to correlate accurately the data of 25 systems.

A comparison of the pour technique with the usual nozzle method for the introduction of drops resulted in a terminal velocity difference of less than three percent. Wall proximity corrections were made when necessary.

THE manufacture of many organic and of some inorganic products requires the contacting of one liquid phase with a second one. The objective of such an operation may be the transfer of heat or mass or both. Large momentum transfer is, in nearly all such cases, unavoidable. Most such operations use streams or clouds of the dispersed phase to attain the objective. It is believed by many that the best permanent foundation upon which to lay analysis, design, and operating calculations will come from a more complete knowledge of the phenomena involved in the movement of single drops. The results may then be modified to interpret the action of streams or clouds of them. The present report is concerned only with the gross terminal velocity of large liquid drops through a liquid field, the effects of net mass and heat transfer having been eliminated by a previously attained equilibrium between the two liquid phases.

A number of attempts to mathematically analyze and express the speed and motion of a liquid drop moving in a liquid field have been made. Unrealistic simplifying assumptions, necessary in setting up the model, have made most of the analyses comparatively useless. Without such simplifying assumptions, the mathematical situation appears to be quite hopeless. The problem of estimating the terminal velocity of a drop of specific size is presently an experimental matter, except in the region of very low Reynolds numbers where viscous forces are completely dominant.

Previous work

Several recent papers [1, 2, 3, 4, 12] dealing with the terminal velocity of liquid drops rising or falling through a liquid field have reviewed the existing pertinent literature on the subject. Water was, in nearly all cases, used as the continuous phase since the expense of filling the tanks with organic liquids is very high. Also, many such liquids present fire hazards which would require such extraordinary experimental precautions as to preclude their use. The containing tanks must be of several inches in diameter to avoid boundary effects and several feet high to avoid end effects.

Several efforts have been recently made to correlate the terminal velocities of drops with their size and the physical properties of the system. The terminal velocity is obtained by dividing a relatively long vertical height traversed by the drop by the time required for the drop to travel this distance. The distance must be long enough to insure that any periodic oscillations or other cylic phenomena will be repeated many times. Such a terminal velocity is attained when the forces of drag, buoyancy and weight are in a dynamic balance. The size of the drop is usually described by the convenient and easily determined equivalent diameter, defined as the diameter of a sphere having the same volume as that possessed by the drop.

Hu and Kintner [1] presented a correlation curve based on experiments with drops of eight organic liquids falling through a water phase contained in a tank of one square foot cross section and four feet in height. All of the systems exhibited high interfacial tensions in excess of 20 dynes/cm. The effects of elevated field phase viscosity and of low interfacial tension were not covered.

Licht and Narasimhamurty [2] presented drop velocity data and a correlation which permits a computation of the velocity in the region of large drops where the velocity is nearly constant. Excellent outline shapes and photographs of the falling drops were included. Their velocities for ethylchloroacetate drops falling through water are considerably in excess of those reported here. The rise of their curve above that for rigid spheres indicates that their drops began to circulate internally at

[1]*Manuscript received September 4, 1958.*
[2]*Department of Chemical Engineering, Illinois Institute of Technology, Chicago, Ill.*
Based on a paper presented at the Joint A.I.Ch.E.-C.I.C. Chemical Engineering Conference, Montreal, Que., June 20-23, 1958.
Contribution from the Department of Chemical Engineering, Illinois Institute of Technology, Chicago, Ill.

a smaller drop size than usual. This may well have been due to the high purity of their material as compared to others.

Keith and Hixon [3] investigated over a dozen liquid-liquid systems, six of them in the low interfacial tension range. In their experiments, the water phase was moving through the containing tube in a direction counter-current to that of the drop. Their use of a field velocity obtained by dividing the volumetric flow rate by the tube cross-section is questionable. A small wall effect is probably present in their work.

Klee and Treybal [4] presented two dimensional correlations for predicting drop velocity from drop diameter and the pertinent physical properties of the system. They divided the velocity vs. size curve into two regions and arrived at an equation for each. One of these applied to small drops for which velocity increased rapidly with increase in drop size and the other for the region in which velocity was nearly constant and independent of drop size. The peak velocity between the two regions were not accounted for. Many of their systems exhibited a low interfacial tension but none a high field viscosity. Their two equations were confirmed quite well by the data of Keith and Hixon and of Hu and Kintner but less closely by that of Licht and Narasimhamurty. Their materials were of commercial grade, and no attempt was made to purify them. Their equation for the largest drops predicted a velocity fully independent of drop size, while other data [1, 2] indicated that the velocity gradually decreases with increased drop size in this region.

Smirnov and Ruban [5] worked with tubes of such small diameter that the movement of the drops was affected by the container walls. Their field fluid was in continuous countercurrent motion in most of their runs. In order to compare their data with that of others obtained in large vessels a wall proximity correction must be made. For values of (d/D) less than 0.5, the following equation has been recommended by Strom and Kintner [6]

$$\frac{U}{U_\infty} = \frac{1}{K} = [1 - (d/D)^2]^{1.43} \quad \ldots\ldots\ldots\ldots (1)$$

This equation was recommended only for the region through and above the peak velocity. It does not apply to small drops at Reynolds numbers below twenty. The wall effect at lower Reynolds numbers is much larger but is believed to be less than for a rigid sphere.

Smirnov and Ruban used tap water of an uncertain nature, did not mutually saturate the two phases, and failed to measure and report the interfacial tensions at the somewhat low temperatures involved.

No suitable correlation seems to exist which adequately predicts the terminal velocity of a drop of specified equivalent diameter in systems of low interfacial tension below 20 dynes/cm.) or high field viscosity (above 50 centipoises).

Experimental

The drop liquid for all high viscosity field systems was tetrachloroethylene. Substances added to water to produce viscous solutions were carboxy methyl cellulose (Hercules Powder Company), Lytron 890 (Monsanto Chemical Company), glycerine (Armour and Company), and corn syrup (Corn Products Refining Company). Benzyl alcohol, furfural, and ethyl chloroacetate drops in a field phase of distilled water exhibited low interfacial tensions. These chemicals and the tetrachloroethylene were of reagent grade and purchased from laboratory supply companies. The phases were mutually saturated prior to all runs. This is especially necessary in the case of the benzyl alcohol system.

Physical properties pertinent to the work were the densities, viscosities, and interfacial tensions. Viscosities and interfacial tensions were determined for each system both before and after the terminal velocity measurements were taken to be certain that no appreciable change in these properties had taken place during the course of the runs. Densities were determined with a specific gravity bottle which had been calibrated with distilled water as the reference material. Ostwald-Cannon-Fenske viscometers in sizes No. 100 to No. 400 were used for viscosity determinations. Standards used were distilled water for the No. 100 tube highly purified cyclohexanol for the No. 300 tube and U. S. P. castor oil for the No. 400 tube. The carboxymethyl cellulose (hereafter referred to as CMC) solutions were sufficiently low in concentration that the 'apparent' or 'intrinsic' viscosities measured in this way could serve as real viscosities. No appreciable Bingham plastic effect and no hysteresis loop were found with a Brookfield viscometer. The Lytron 890 solution, on the other hand, was very thixotropic. Interfacial tensions were determined with a Cenco DuNouy tensiometer except in the case of the glycerine solutions. For these systems it was found necessary to resort to the more inconvenient capillary rise method. Representative physical properties of the systems are given in Table 1.*

Drops were formed in 25 ml. beakers containing the field liquid. Standard calibrated pipettes were used for the larger drops. Drops below 10^{-3} ml. were made with capillary tubes calibrated by calculating the volume that a cylinder of mercury occupied between the tip of the capillary and a specific point. The mercury was weighed on an analytical balance. The calibration procedure was repeated for several points along the capillary pipette. Drops were always formed with the tip of the pipette submerged in the field fluid contained in the beaker. The outside of the pipettes were wiped clean of any drop liquid and the tips of the pipettes examined to be certain that no air was trapped inside the pipette. Cleanliness of the beakers was extremely important to prevent the drops from adhering to the walls of the vessel. The beakers were transferred, one at a time, to the test tank and the drops carefully poured under the surface of the field fluid for the terminal velocity measurements.

The test tank consisted of a 3.75 inch I.D. glass cylinder, four feet high, mounted on a rigid framework of pipes. A thermometer was kept hanging halfway down the test tank to keep a close check on the water temperature which was maintained constant within one half degree Centigrade. Because of the quantity of water (three gallons) there was little variation in temperature during a series of runs. However, on the few occasions when the bath temperature needed adjustment, the field liquid was heated or cooled by water flowing on the outside of the tank and the field liquid then thoroughly mixed to bring it to a uniform temperature.

The terminal velocities of the drops were determined by timing, with hand-actuated electric timer, a distance of fall of 75 cm. The upper mark was sufficiently below the liquid level to insure that the terminal velocity was reached, and the lower mark was sufficiently above the tank bottom to eliminate end effects. Twenty measurements were made for each drop size, and the average of

*A more detailed form of this paper has been deposited as Document No. 5729 with the ADI Auxiliary Publications Project, Photoduplication Service, Library of Congress, Washington 25, D.C. A copy may be secured by citing the Document No. and by remitting $1.25 for photoprints, or $1.25 for 35 mm. microfilm. Advance payment is required. Make cheques or money orders payable to: Chief, Photoduplication Service, Library of Congress.

TABLE 1

PERTINENT PHYSICAL PROPERTIES OF THE SYSTEMS

System (Drop – Field)	Drop density ρ_D gm./cc	Field density ρ gm./cc	Density difference $\Delta\rho$ gm./cc	Drop Viscosity μ_D Centipoises	Field Viscosity μ Centipoises	Interfacial tension σ Dynes/cm.	Physical property group P Dimensionless	Temperature T °C
Furfural – Water	1.154	0.9966	0.1574	1.50	0.9075	5.9	1.96×10^8	26.50
Benzyl Alcohol – Water	1.040	0.9966	0.0434	5.15	0.8631	4.25	3.225×10^8	26.50
Ethylchloroacetate – Water	1.141	0.9966	0.1444	1.38	0.8585	16.43	57.5×10^8	26.75
Tetrachloroethylene – CMC–1	1.612	1.000	0.612	0.926	41.3	19.15	67×10^3	26.50
Tetrachloroethylene – CMC–2	1.612	1.00	0.612	0.926	128.7	11.99	162.3	26.00
Tetrachloroethylene – CMC–3	1.612	1.00	0.612	0.926	285.0	30.15	1.355	26.25
Tetrachloroethylene – Corn Syrup	1.614	1.395	0.219	0.926	514	35.2	5.26	26.50
Tetrachloroethylene – 96% Glycerine	1.615	1.243	0.372	0.926	287 to 386	9.71		28.2 to 30.2
Tetrachloroethylene – 90.75% Glycerine	1.615	1.231	0.384	0.926	141	13.35	4.30	27.0

these times was used for calculating the terminal velocity. Thus, each of the points on the curves in this report represents the average of 20 determinations. The percentage error was within 2%.

In order to compare the pour technique with the nozzle technique used by others, large 0.13 ml. drops of benzyl alcohol and 0.04 ml. drops of tetrachloroethylene were dropped through water, saturated with the particular drop liquid, using first the nozzle technique and then the pour technique. The equivalent diameters of the benzyl alcohol drops were 0.630 cm. and the tertachloroethylene drops were 0.425 cm. A comparison was then made between the terminal velocities obtained by the two techniques. With the benzyl alcohol drops, a velocity of 6.12 cm./sec. was obtained by the nozzle technique and 6.23 cm./sec. by the pour technique, a difference of 1.8%. In the tetrachloroethylene-water system, a velocity of 18.62 cm./sec. was obtained with the nozzle technique and 19.11 cm./sec. with the pour technique, a difference of 2.6%.

The nozzle technique of drop delivery employed a small metal tank with a nozzle attached to it. The tank was suspended above the glass tube, and a valve controlled the liquid flow through the nozzle. The nozzle itself was a piece of copper tubing filed on the end to form a smooth taper. The nozzle was then attached to a metal fitting so it could be screwed into the bottom of the tank. The nozzle was calibrated to determine the volume of the drops it delivered by submerging its tip below the surface of the field solution in the glass tube, and delivering 100 drops at a constant frequency. The drops were caught in a beaker, and the volume of drop liquid collected was determined. This volume was divided by 100 to get the average volume of one drop. After calibration the tank was again suspended above the glass tube and a number of drops delivered for the actual determination of terminal velocity. Special care was taken to see that the depth of the nozzle below the surface of the field solution, the height of drop liquid in the delivery tank, and the frequency of drop delivery were the same during terminal velocity determination as they were during the calibration. This helped to assure that the same drop volume was delivered in both cases.

Discussion

Low interfacial tension and low field viscosity systems

The benzyl alcohol-water and furfural-water low interfacial tension systems exhibited velocity vs. diameter curves with the characteristic rise to a maximum, followed by a gradual decrease in velocity with increasing diameter. The ethylchloroacetate-water system did not exhibit a peak velocity but merely leveled off at a constant maximum value. This type of velocity-diameter curve is typical of a large number of systems [2, 3].

It is believed that the best method of correlating data for systems of low field viscosity is as shown in Figures 1 to 4 inclusive, in which the data on 25 systems having interfacial tensions from 0.3 to 44.4 dynes/cm. were all accurately presented by the curve of Hu and Kintner [1]. They proposed correlating terminal velocity data by means of a dimensionless parameter, P, composed of the pertinent physical properties of a system combined as

$$P = \frac{\rho\sigma^3}{g\mu^4} \cdot \frac{\rho}{\Delta\rho} = \frac{4}{3} \cdot \frac{(Re)^4}{C_D\,(We)^3} \quad \ldots\ldots\ldots\ldots (2)$$

which is constant for each system at a specific temperature. They found that a plot of log $C_D We P^{0.15}$ vs. log $Re/P^{0.15}$ resulted in a single unique curve. Their curve was determined from data on eight high interfacial tension systems. It may now be concluded, on the basis of these recently available data, that the Hu-Kintner correlation also applies to systems having low interfacial tensions (below 20 dynes/cm.), provided the field viscosity be of the order of one centipoise.

The curve can be used to calculate directly the terminal velocity, drag coefficient, and Reynolds and Weber numbers for any given drop size. The break point on the curve can be used to predict the peak terminal velocity and its related quantities. Only the data of Licht and Narasimhamurty on ethylchloroacetate drops and that of Hu and Kintner on aniline drops in an aqueous continuous phase do not correlate well. The failure of the latter may

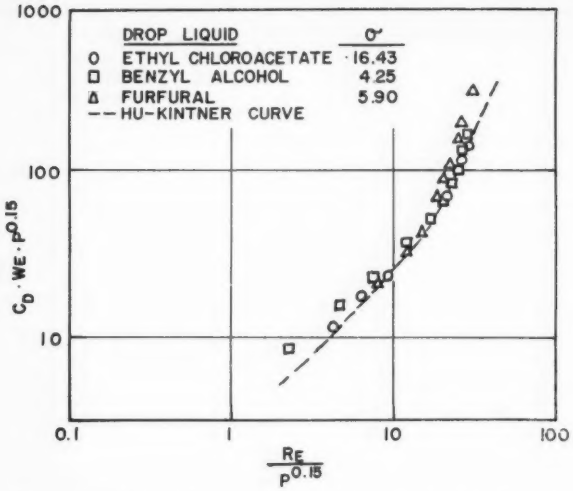

Figure 1—Comparison of data for organic liquid-water systems of low interfacial tension with Hu-Kintner correlation.

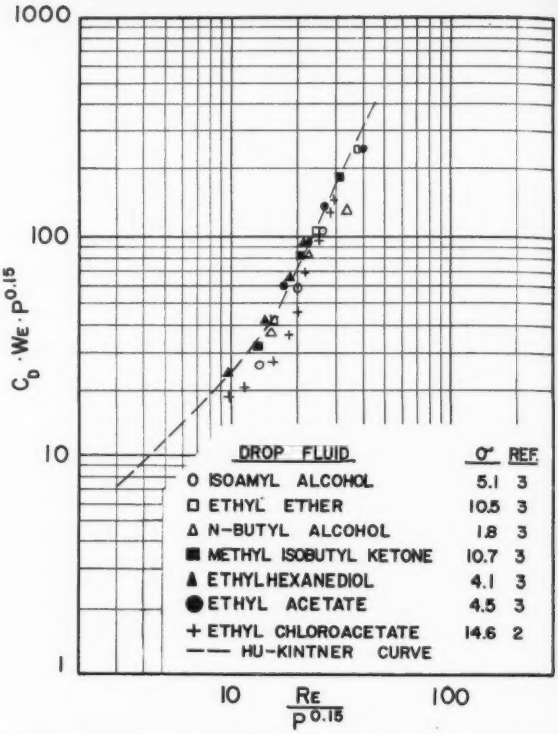

Figure 2—Comparison of literature data for low interfacial tension systems with Hu-Kintner correlation.

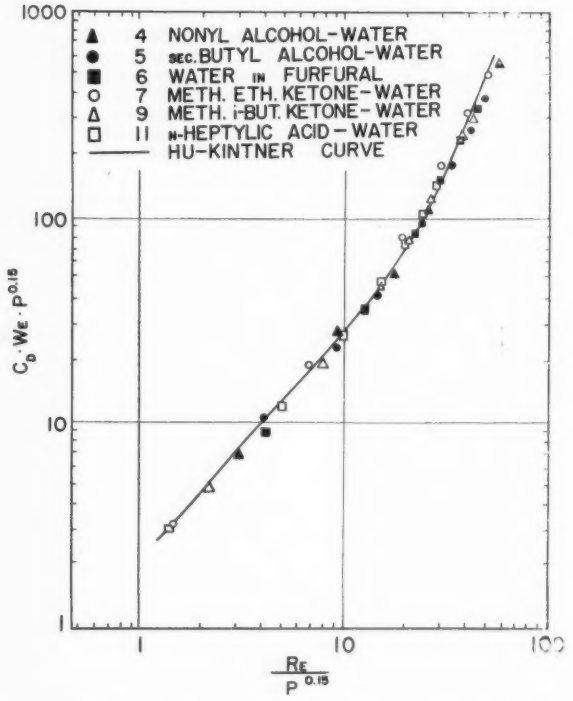

Figure 3—Comparison of data of Klee & Treybal with Hu-Kintner correlation.

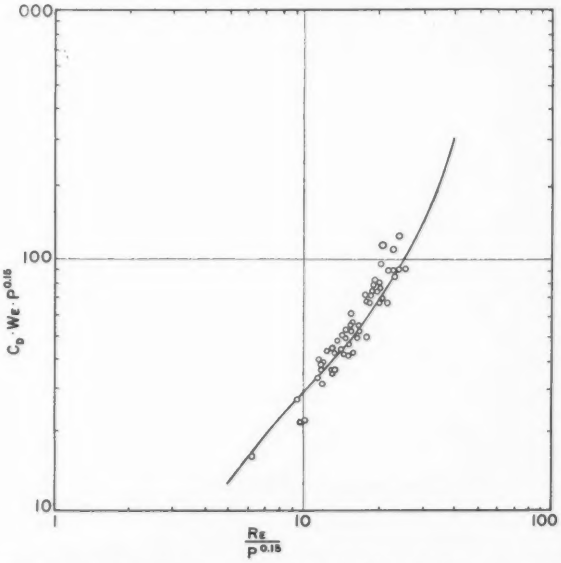

Figure 4—Comparison of corrected data of Smirnov and Ruban with Hu-Kintner correlation.

well be due to a faulty value of interfacial tension. Figure 1 is a plot of the data of the three low interfacial tension systems investigated in the present work. Figure 2 includes six systems by Keith and Hixon and one by Licht and Narasimhamurty. Figure 3 includes six systems by Klee and Treybal. Figure 4 shows the data of Smirnov and Ruban. As was previously mentioned, their experiments were conducted in small tubes so that a wall correction had to be made on their velocity data. Equation 1 was used for these corrections. No values of measured interfacial tensions were reported by them and it must be presumed that they made none. Data taken from the literature, with somewhat uncertain interpolations were used in calculating the Weber numbers needed in constructing Figure 4. Considering the experimental shortcomings of their work, their corrected data seem to be rather successfully correlated in this manner.

Over the portion of the curve corresponding to the

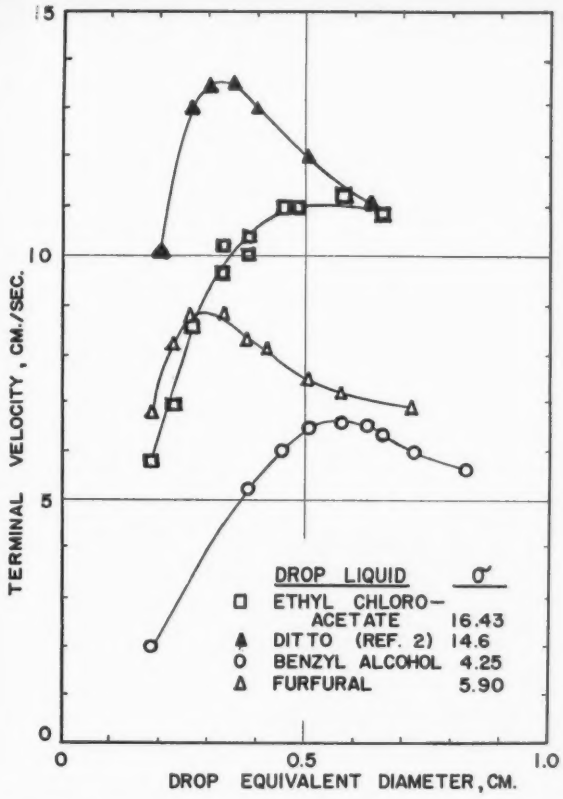

Figure 5—Variation of terminal velocity with drop size for low interfacial tension systems.

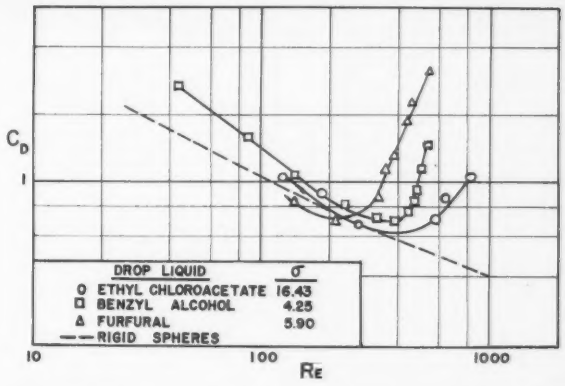

Figure 6—Drag curves for low interfacial tension systems.

smaller drops, the ethylchloroacetate-water system of Licht and Narasimhamurty deviates considerably from the recommended curve. The present experimental evidence for the same system obtained a much closer agreement between curve and data. As shown in Figure 5, the velocities of Licht and Narasimhamurty are as much as 50% above those of the present authors for drop sizes in the peak region. After the peak diameter is exceeded their velocity-diameter curve falls so rapidly that it actually coincides with the curve of the present authors at a diameter of 0.65 cm. A peakless curve is formed in systems which have a surface-active agent present. However, because a peakless curve is formed it does not necessarily follow that a surface-active agent is involved. Keith and Hixon, using pure organic drop materials, obtained both peaked and peakless velocity curves.

The effect of interfacial tension

When the velocity data are expressed in terms of drag coefficients, they give rise to the curves of Figure 6. At low Reynolds numbers the furfural-water curve falls below that for rigid spheres. The curves for the benzyl alcohol-water and ethylchloroacetate-water lie above the curve for rigid spheres. Others [2, 4] have also obtained results which lie both above and below the rigid sphere line at low Reynolds numbers. Since liquid drops are free to oscillate, vibrate, circulate, and deform from a spherical shape, the drag of the drops might well depart from that of a rigid sphere of the same volume. The increased velocity of ethylchloroacetate drops, as determined by Licht and Narasimhamurty, may well be due to the onset of internal circulation before the retarding effects of oscillation and deformation become operative. Klee and Treybal [4] point out that for nitrobenzene drops of various purities in water, Garner and Skelland [7] were able to develop drag coefficients varying by a factor of more than two at the same Reynolds number.

The density difference driving force of the ethylchloroacetate-water system was slightly lower than the density difference of the furfural-water system. Yet, for the same drop sizes, the velocities of ethylchloroacetate were higher than those of furfural. Since the respective interfacial tensions of ethylchloroacetate and furfural in water were 16.43 and 5.90 dynes per cm., we are led to the same conclusion as that made by Licht and Narasimhamurty, that lowering the interfacial tension lowers the terminal velocity. Drops with low interfacial tensions tend to be more easily deformed, and tend to oscillate and zig-zag more in their descent, processes which use up energy and result in reduced velocities.

High viscosity of continuous phase — the effect of increased field viscosity

In all seven high viscosity field fluid systems the velocity of tetrachloroethylene drops continuously increased with increasing drop diameter. None of the curves in Figures 7 and 8 exhibited a peak velocity typical of drops falling through low viscosity media. The largest stable drop size was not reached in CMC No. 1, and a peak velocity may occur at some higher value of drop diameter. In all other systems the drop size was increased to a value at which complete shearing occurred, the point where the drop broke up during its fall because the resistance force was great enough to overcome the interfacial force. The rate of increase of velocity varied with drop diameter, field viscosity, and with the difference in density between drop and continuous phase.

In Figures 9 and 10, it is readily apparent that the Hu-Kintner correlation is quite unsatisfactory for drops moving through a liquid field of viscosity well above that of water. Johnson and Braida [8], using viscous field fluids of viscosity up to about 30 centipoises, found that their data lay parallel to the correlation curve and that by applying a continuous phase viscosity correction resulting in a plot of log $C_D We P^{0.13} (\mu/\mu_D)^{0.14}$ vs. $Re/P^{0.15}$, the points would fall on the curve for drops falling through water. Such a correction did not suffice in the present work in still higher field viscosities. The curves of Figures 9 and 10 are not parallel to the Hu-Kintner correlation curve. Calderbank and Korchinsky [9], investigating heat transfer from drops of mercury falling through glycerine solutions, obtained curves similar to those presented in

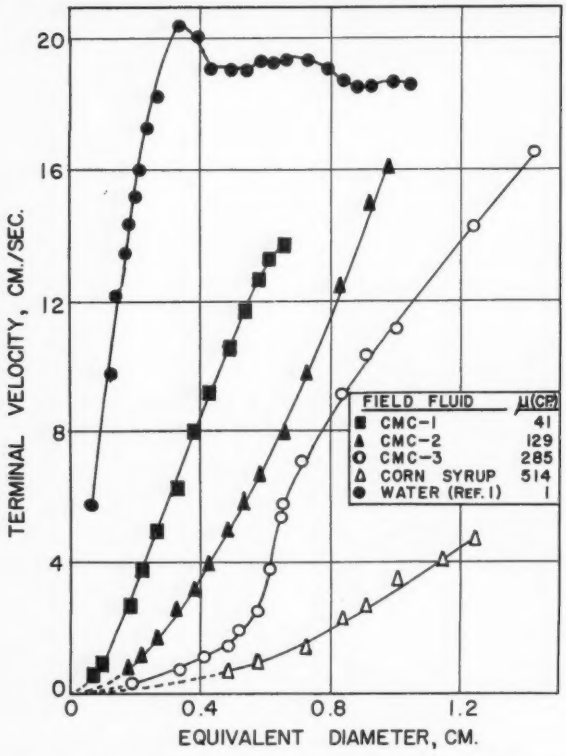

Figure 7—Variation of terminal velocity with drop size for C_2Cl_4 drops in various liquids.

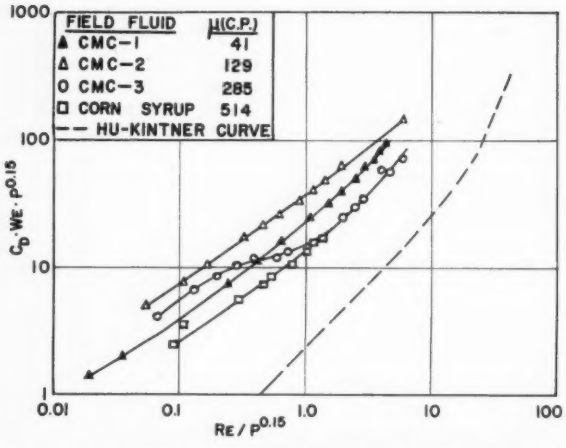

Figure 9—Comparison with Hu-Kintner curve of drops of C_2Cl_4 falling through various liquids.

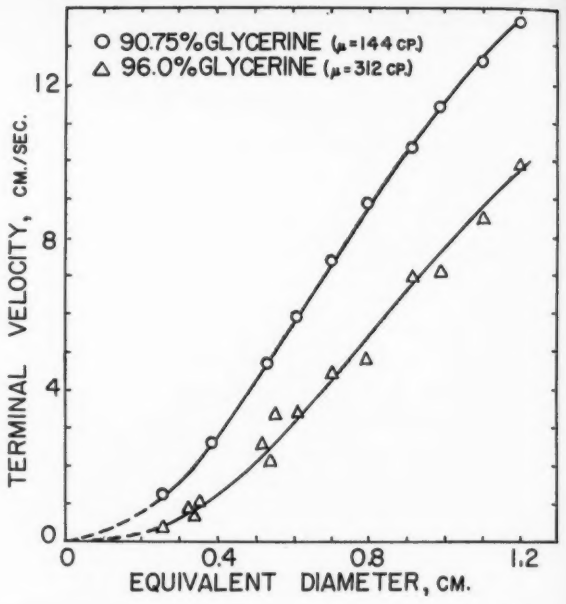

Figure 8—Terminal velocity of drops of C_2Cl_4 falling through glycerine solutions.

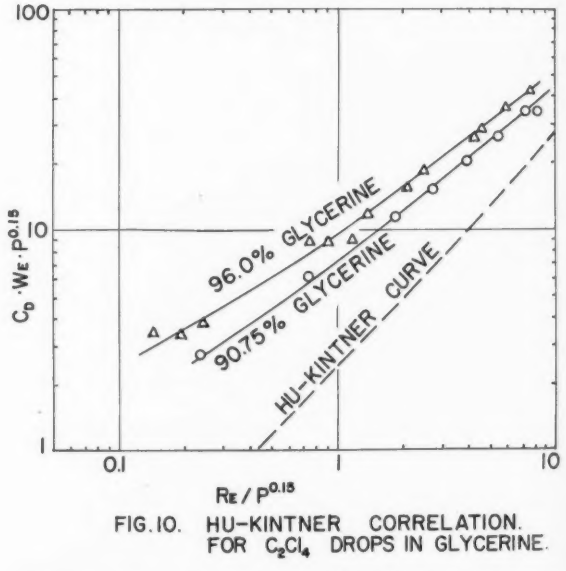

Figure 10—Hu-Kintner correlation for C_2Cl_4 drops in glycerine.

Figure 10. Their nozzles produced only a narrow range of drop size in any one medium, and the single curve drawn through all of their points is not considered correct. It does, however, show the same tendency as the present ones. It is also of interest to note that the data of Bryn [10] and of Haberman and Morton [11] on the rate of rise of air bubbles through liquids of a viscosity somewhat higher than that of water show a similar trend when plotted as in Figures 9 and 10. It may also be observed that the curves of Figure 9 do not deviate from the water line in order of increasing viscosity alone. It appears that $\Delta\rho$ is a factor. Corn syrup exhibited the highest viscosity but the lowest density difference. Its curve lies nearest to that for water. A shape, somewhat similar to the classical tear drop, was observed in CMC-3 solution and is shown in Figure 13. The curve for this solution crosses two of the others in the region where the change in shape occurs. This phenomenon is treated separately below.

Drag curve plots for the data are a more illuminating type of correlation to most readers. Figure 11 shows that drops falling through CMC-1 and CMC-2 follow the curve for rigid spheres up to Re of 10. The effect of internal circulation to increase velocity is just balanced

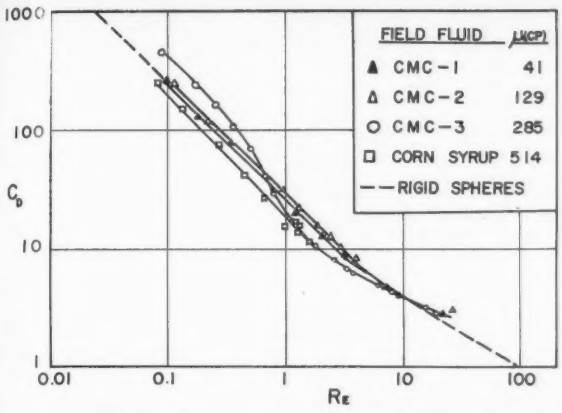

Figure 11—Drag curves for high field viscosity systems.

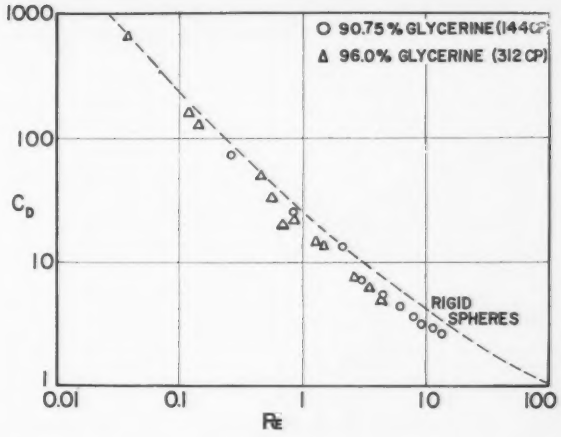

Figure 12—Drag curves for C_2Cl_4 drops in glycerine solutions.

by the increased drag due to larger projected frontal area and the increasing effect of inertial forces. The curve from CMC-3 crosses the others in the region where the tear drop shape appeared. Such a shape presents a smaller frontal area than would a sphere of equivalent volume. The combination of increasing internal circulation and decreased ratio of frontal area to equivalent spherical projected area should account for a decreased resistance and hence an increased velocity. Corn syrup, while of higher viscosity, possesses a higher density (smaller $\Delta\rho$), and therefore requires a larger drop to reach a specific value of Re. Internal circulation appears to be present at all values of Re covered by the data. Glycerine solutions (Figure 12) also show that internal circulation sets in at Re of less than 0.1 and that the spheroidal drops do not present a sufficient drag to match that of rigid spheres until Re exceeds ten. Any data for the rate of rise or fall of gas bubbles or liquid drops through a liquid field at this range of Re must be interpreted in the light of these opposing factors. A triggering mechanism, such as excessive nozzle velocity in the formation of drops or the presence of nearby container walls, may cause circulation to appear in smaller drops. The presence of impurities tends to inhibit circulation, and the drag curve of such solutions follows that for rigid spheres to still higher values of Re.

Tear drop shapes

The unusual shape of the drag curve for drops falling through CMC-3 solution is reflected in the terminal velocity curve of Figure 7. A rapid rate of increase of velocity with increased drop size occurs at a drop diameter of 0.6 cm. A pronounced change in drop shape accompanied this sudden increase in the slope of the curve. The change in form may be seen in four stages in Figure 13. Drops of 0.425 cm. equivalent diameter have changed very slightly from a spherical shape. Drops of 0.61 cm. diameter are elongated to a somewhat greater degree and present a slightly smaller frontal projected area. At 0.67 cm. diameter a tail is formed, and some evidence is visible of a filament extending upward from the rear of the falling drop. Drops of 0.83 cm. equivalent diameter exhibit a fully-developed tear drop shape and well-defined trail. Savic [12], studying circulation and distortion of liquid drops falling through a viscous medium, proposed the existence of a transition from non-circulating to circulating drops. He postulated a relatively incompressible surface layer in which the normal interfacial tension must be added to the integrated effect of the surface tractions to the outside fluid, with opposite sign. He reasoned that this would result in a distortion to the tear drop shape which he observed for water drops falling through castor oil. As drop speed increased, the surface layer became unstable and destroyed the rear stagnation point to result in a trailing filament. Arnold [13] also observed the same phenomenon. Savic's prediction of the streamline picture and the relation between size of the surface layer and drag were found to be in good agreement with experimental evidence for water drops falling through castor oil, but the critical drop radius for the beginning of circulation was in much less agreement.

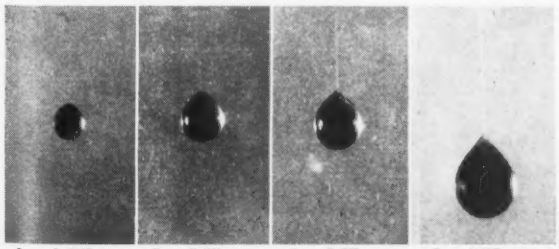

Figure 13—Tetrachloroethylene (C_2Cl_4) drops in a methyl cellulose solution. Viscosity = 463 c.p.

As may be expected from Savic's presentation, the appearance of the tear drop shape and the trailing filament was a function of drop-to-field density difference, field viscosity, and type of field. Additional qualitative experiments indicated that the phenomenon might only occur in non-Newtonian field fluids. All attempts to form such a shape in glycerine solutions of comparable viscosity were unsuccessful. In a highly thixotropic solution of Monsanto Chemical Company's Lytron 890, the shapes were easily formed. It is believed that further work is needed to check the theory that has been advanced by Savic.

Conclusions

Terminal velocity measurements are reported for single liquid drops falling through a stationary liquid field contained in 3.75 inch I.D. glass cylinder. Data for three systems of low interfacial tension, when combined with that of others reported in recently published papers, show that the correlation of Hu and Kintner [1] will serve to predict the terminal velocity of drops in systems of low field viscosity (of the order of one centipoise).

Terminal velocities of tetrachloroethylene drops falling through six different liquids of viscosities up to 500 centipoises indicated that no single correlation has been found to be applicable to all systems. None of the velocity-diameter curves for these systems exhibited a peak velocity. Velocity increased with increase in drop size until breaking up of the drop occurred. The drag curves for these systems deviated from the rigid sphere line but in an irregular manner.

A stable tear drop-shaped drop with a trailing filament, similar to those reported by Savic, was observed in a solution of carboxy methyl cellulose of a viscosity of 285 centipoises. All attempts to form such a shape in glycerine solutions of comparable viscosity were unsuccessful.

Acknowledgement

The authors wish to express their appreciation of the financial support of the National Science Foundation, Washington, D.C., in carrying out this work.

Nomenclature

C_D = Drag coefficient, or friction group ($1.33\Delta\rho dg/\rho U^2$)
d = Drop equivalent diameter
D = Inside diameter of tube or tank
g = Acceleration of gravity
K = Wall proximity correction factor (U_∞/U)
P = Physical property group ($\rho\sigma^3/g\mu^4$) ($\rho/\Delta\rho$)
Re = Reynolds number ($dU\rho/\mu$)
U = Gross terminal velocity of falling drop; in absence of wall proximity effect used as velocity in infinite medium
U_∞ = Terminal velocity in a medium of infinite extent; U_∞ = KU when considering velocities in small tubes
We = Weber number ($dU^2\rho/\sigma$)
σ = Interfacial Tension
μ = Viscosity of continuous phase
μ_D = Viscosity of drop phase
ρ = Density of continuous phase
$\Delta\rho$ = Difference of density between phases

References

(1) Hu, S., and Kintner, R. C., A.I.Ch.E. Journal, 1, 42 (1955).
(2) Licht, W., and Narasimhamurty, G. S. R., A.I.Ch.E. Journal, 1, 366 (1955).
(3) Keith, F. W., and Hixon, A. N., Ind. Eng. Chem., 47, 258 (1955).
(4) Klee, A. J., and Treybal, R. E., A.I.Ch.E. Journal, 2, 444 (1956).
(5) Smirnov, N. E., and Ruban, V. L., J. Appl. Chem. (USSR), 22, 1068 (1949).
(6) Strom, J. R., and Kintner, R. C., A.I.Ch.E. Journal, 4, 153 (1958).
(7) Garner, F. H., and Skelland, A. H. P., Chem. Eng. Sci., 4, 149 (1955).
(8) Johnson, A. I., and Braida, L., C.J.Ch.E., 35, No. 4 (1957).
(9) Calderbank, P. H., and Korchinski, I. J. O., Chem. Eng. Sci., 6, 65 (1957).
(10) Bryn, T., Forsch Geb. Ing., 4, 27 (1933).
(11) Haberman, W. L., and Morton, R. K., Rep. No. 802, D. W. Taylor Model Basin, Navy Department, Washington, D.C. (September 1953).
(12) Savic, P., Rep. No. MT-22, National Research Laboratories, Ottawa, Canada (July 1953).
(13) Arnold, H. D., Phil. Mag., 22, 755 (1911).

★ ★ ★

Methods of Noise Control[1]

T. F. W. EMBLETON[2]

The best method of noise control is elimination of the noise at its source by modification of the noise producer; in certain cases this may not be possible since the normal functioning of the noisy device would be impaired. Alternatively the source may be enclosed, either completely or partially so as to shield the observer from the source. A third method involves the treatment of surfaces in the room containing the observer and noise source to absorb the noise as it is propagated through the room. Finally the observer, or at least his ears, may be enclosed by a soundproof booth or the wearing of ear defenders.

Examples of the successful quietening of pieces of machinery will be discussed, including the couch roll of a paper making machine. A reduction of 15-20 decibels in sound pressure level has been achieved without interference with the paper making qualities of the roll.

THE need for reducing the levels of noise in industry is becoming more urgent with the passing of time and considerable attention and effort has been devoted to the problem in recent years. As productivity increases it is accompanied both by an increase in the output of individual machines and by an increase in the number of processes that are mechanized; these result in an increase in the intensity or loudness of the noises that are present in industry. Intense noises have a direct bearing upon the safety of individuals since they may be loud enough to mask the reception of warning signals and on prolonged exposure may be responsible for damage to a person's hearing [1]. Even noises of somewhat lower intensity levels may still have an important effect upon the well-being of the individual, whether he works in an industrial plant or in the office [2]. The effect is difficult to assess in quantitative terms but may vary from a nervous breakdown to reduced efficiency or lower morale. The matter of efficiency is perhaps most apparent in connection with an executive who needs "peace and quiet" in which to make his decisions. Most effort in noise control has been directed to the reduction of the more intense levels of noise which cause hearing damage and it is right that this should be so. These problems will continue to attract most of the attention but it is wise to consider also the less serious noise problems where noise control measures will pay for themselves through increased efficiency.

This paper aims to provide the plant engineer or safety engineer with enough basic material on the various methods of noise control to enable him to assess the applicability of the various methods to his own problem and to choose for himself the most suitable and economic way of achieving a satisfactory solution. It is assumed that he has assessed the existing noise situation by any necessary measurements that may be required and that he knows what are the acceptable noise criteria for the location in question – in short, that he has a problem and knows its magnitude [3, 4, 5]. However, there is a great variety of situations that call for noise control measures, many of which require the combination of several different methods of noise reduction and in some cases the plant engineer may wish to seek outside help from an acoustic engineer to obtain the best and most economical solution to his problem.

Four methods of noise control

The various methods of noise control may be grouped into four main classes. This classification is somewhat arbitrary but is convenient for the purposes of description. The use of each, and its effect upon the noise conditions throughout the plant will be illustrated with reference to the simplified, hypothetical situation shown in Figure 1. The lower part of the figure shows a cross-section of a plant containing one principal source of noise, here indicated as a piece of machinery on the lefthand side. The operator of this machine is situated perhaps two feet away and we shall assume initially that the noise level at the position of the operator is 95 decibels. There may be other men in the plant who are not situated close to any sources of noise, these are represented here by a man at a distance of 20 feet from the main source. Finally there are other areas devoted to office space, here represented at a distance of 200 feet from the noise source. It must be pointed out that in this illustration only broad classes of activity are considered and that these classes in practice require further subdivision. For example certain office personnel will be engaged in draughting and stenographic work whilst others will be working in an executive capacity. The criteria for acceptable noise levels are different in the two cases [2]. If it is assumed that the height of the building is 15 to 20 feet and that the floor and ceiling are completely non-absorbing then the sound level as a

Manuscript received August 24, 1958.
Division of Applied Physics, National Research Council, Ottawa, Ont.
Based on a paper presented at the Joint A.I.Ch.E.-C.I.C. Chemical Engineering Conference, Montreal, Que., April 20-23, 1958.

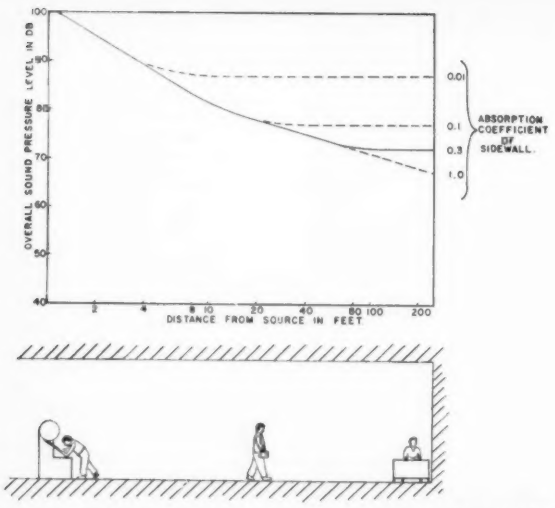

Figure 1—Overall noise level throughout a plant which contains one source of noise providing 95 db. at a distance of 2 ft., assuming a non-absorbing floor and ceiling.

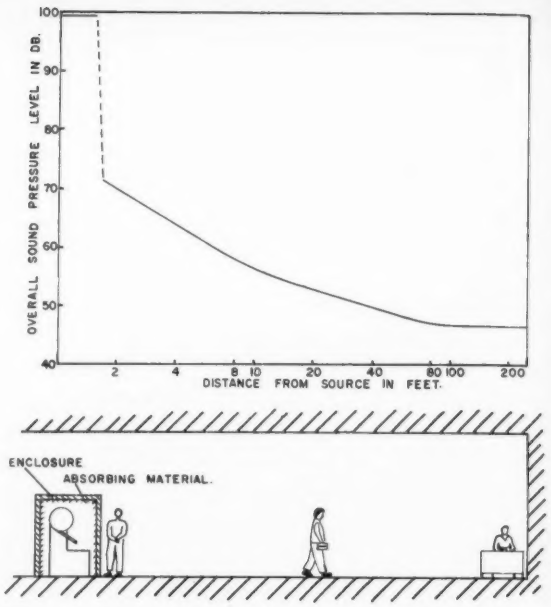

Figure 2—A typical overall noise level in the plant of Figure 1 when the source of the noise is surrounded by a complete enclosure.

function of distance from the source is roughly as shown in the upper part of Figure 1. At locations near the side walls of the building the sound level is determined partly by the absorption coefficient of the walls: for a low absorption coefficient of 0.01 the upper curve applies, if they are completely absorbing then the lower curve applies; any situation in practice usually lies between these two extremes. For the purposes of illustration in the later figures it will be assumed that an absorption coefficient of about 0.3 for the side walls.

Noise reduction at the source

So far the noise level is too high at all three locations; the operator of the machine is likely to suffer some hearing damage on prolonged exposure the man at 20 feet will find the noise annoying and in the office the noise level is high enough to interfere with efficient operation of the staff. The best method of reducing the noise is obviously to quieten the source of the noise. A factor to be considered here is the ease with which it is possible to modify the machine and any effect that there may be on its normal function. As an example of how a considerable reduction of noise was obtained in a particular case without in any way affecting the normal performance of the machine, the quietening of the couch roll on a paper making machine will be discussed below [5]. In the present case, if the source of the noise could be reduced by 25 db. the noise level at every point would be reduced by 25 db., see the upper part of Figure 2 for distances greater than 2 feet, and the various noise problems at each location would have been solved satisfactorily. Whilst this is the most elegant and in the long run often the cheapest method of noise control it is also frequently the most difficult since it may require some basic research on the machine itself to determine the source of the noise and suitable methods of reducing it.

Enclosure of the source

If quietening of the machine is not feasible other and more straight-forward methods may be employed. The machine may be enclosed completely as in Figure 2. It is important to understand the principles involved if the full potentialities of an enclosure are to be realized. The noise level inside the enclosure will always be higher than it would be at the same location in the absence of the enclosure since the sound energy is now prevented from propagating away from the machine. If the inside of the enclosure is essentially non-absorbing then the sound level inside will build up until it has risen sufficiently to overcome the transmission loss provided by the walls of the enclosure. Thus it is conceivable that an enclosure which has been built with walls sufficiently massive and impervious to air flow to provide say 28 db. attenuation might result in a noise reduction of only 8 db. in the plant because the level inside the enclosure had risen by 20 db. However, with an adequate amount of sound absorption inside the enclosure the noise level there may be prevented from rising by more than 2 or 3 db; with the same enclosure the noise reduction in the plant would now be 25 db. The graph of Figure 2 has been drawn for this case.

The necessary requirements then for the good performance of an enclosure are (a) adequate sound absorption inside, (b) sufficiently massive walls to provide the required transmission loss and (c) surfaces that are non-porous and well sealed at their edges so that sound may not escape by direct air passages out of the enclosure. In practice, cost is usually the most important factor in determining the relative contributions of sound absorption and transmission loss.

Complete enclosure of the noise source is impracticable if continuous or even frequent access to it is required. A suitable alternative is to enlarge the enclosure to the extent that it may surround both the machine and its operator – such is the situation when the machine is in a separate room. The above criteria for a good enclosure now apply to the machine room and the wall and door which separate it from the rest of the plant. In this case the noise reduction applies only to the remainder of the plant; the machine operator is subjected to the high noise level on the inside of the enclosure and derives no benefit from it at all – in fact he will probably be a few decibels worse off. It may be necessary to protect him in other ways as for example by the wearing of ear defenders.

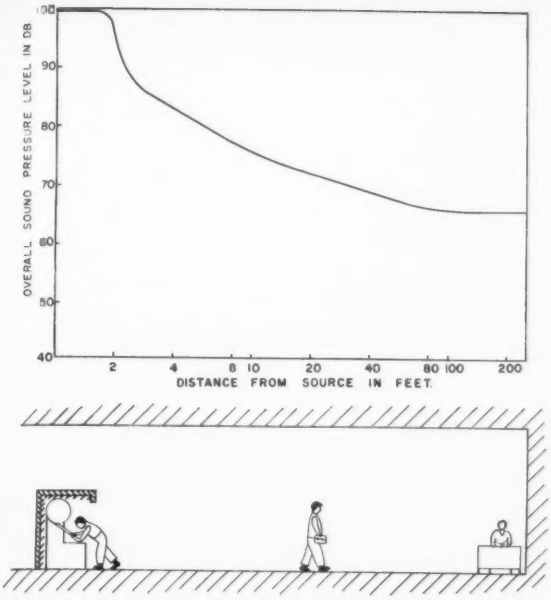

Figure 3—A typical overall noise level in the plant of Figure 1 when the source of the noise is covered by a partial enclosure.

Another alternative which is sometimes used is to surround the machine by a partial enclosure. In a partial enclosure the opening may be sufficiently large that the operator is essentially stationed inside and subject to the correspondingly high noise level, or the opening may be of the minimum size necessary to allow the entrance and exit of materials and the operator's hands. In this latter case the operator is essentially stationed outside and therefore derives at least some of the benefit of noise reduction afforded by the enclosure. Since with a partial enclosure there is a direct air passage to the outside through which sound may propagate it is not possible to obtain the same large transmission loss that is obtainable with a complete enclosure. However under favorable circumstances, as when the designer has freedom of choice over the orientation of the open portions of the enclosure, it can provide 15 to 20 db. of noise reduction. Figure 3 illustrates the use of a partial enclosure where the open area faces both the machine operator and the remainder of the plant. The graph shows the overall noise level when such an enclosure, providing 5 to 8 db. reduction, is used.

A special case of the partial enclosure is the baffle. Baffles are most commonly used to shield limited areas. If the surfaces of a baffle are completely non-absorbing then a noise reduction in one area is achieved only at the expense of increased levels in other areas. This may be unimportant if personnel are not normally in these other areas but otherwise baffles should be covered with sound absorbing material.

So far only the overall sound pressure level of a noise has been mentioned. However even the simplest noise cannot be fully defined by a single number. Other parameters are the distribution of its sound pressure level or intensity with time and with frequency, and it is well established that these quantities have an important bearing on the effect of noise upon the individual. For example, the low pitched rumble of a heavy truck on an uneven floor may have the same overall sound pressure level as the high pitched scream of an axial compressor and each

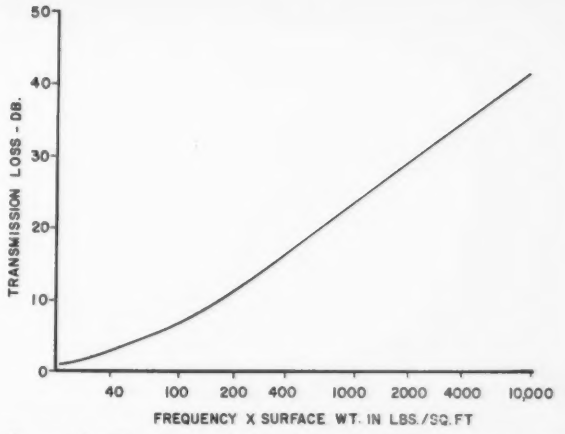

Figure 4—The transmission loss through a mass controlled wall as a function of its weight in lbs./sq.ft. and the frequency of the noise in c.p.s.

may be essentially continuous in time but there is little doubt that the high pitched noise has a much greater psychological effect upon a person. It is common practice to describe a noise by its sound pressure level in each of eight octave bands, these bands following the series: below 75 c.p.s., 75 to 150 c.p.s., 150 to 300, 300 to 600, 600 to 1200, 1200 to 2400, 2400 to 4800 and 4800 to 10,000 c.p.s. From such information one may readily determine such properties of the noise as its loudness [7], how it will interfere with speech intelligibilty [8] and to what extent it will prove annoying [9]. Non-continuous noises can be treated in terms of continuous noises of similar properties; an approximation is to take the time averaged sound pressure levels in each octave band and to consider these as the levels of the equivalent continuous noise. It is not intended to discuss these aspects of noise further here but it is necessary that the engineer concerned with noise control should be aware of the conventional methods of describing noise if he is to gain fruitful results from discussions with acoustical specialists.

The frequency characteristics of a noise will be altered by its transmission through the walls of an enclosure since a massive wall does not provide equal transmission loss at all frequencies. Figure 4 shows the relationship between transmission loss through a wall in decibels as a function of both the mass of the wall per unit surface area and the frequency of the sound field. For the complete analysis of a noise problem it follows that a different transmission loss must be used when considering each octave band, being greater the higher the frequency of the band. However, for a rough estimate one can in most cases think in terms of the overall noise level and the transmission loss for a frequency of 500 c.p.s.

Treatment of surfaces

In the above discussion concerning enclosures it was shown that an adequate amount of sound absorption is necessary if the noise reduction obtained in the plant is to approach the amount of transmission loss provided by the walls and it is generally true that whatever method of noise control may be used in any particular situation there must be provision made for the absorption of sound if the noise reduction capabilities of the other components in the system are to be realized. Sound absorption is most often obtained by the treatment of existing surfaces with absorbent material, a familiar example being perforated acoustic tile. A close examination of the graph of Figure 1 shows that the overall sound pressure

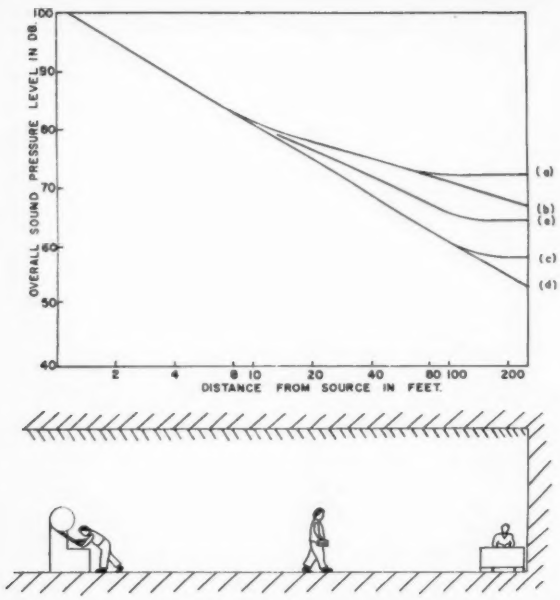

Figure 5—The overall noise level in the plant of Figure 1 for several different amounts and distributions of sound absorbing material on the ceiling and walls (see text for the applicability of the various curves.)

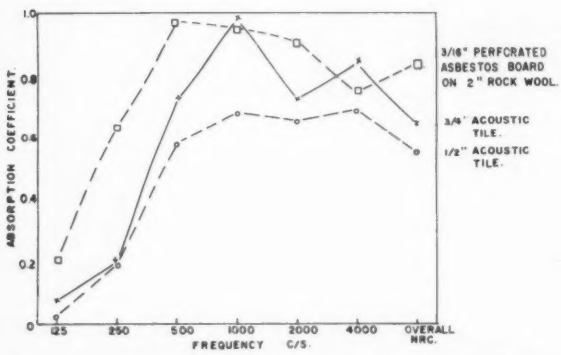

Figure 6—Absorption coefficients of three typical acoustical treatments for large flat surfaces as a function of the frequency of the noise in c.p.s.

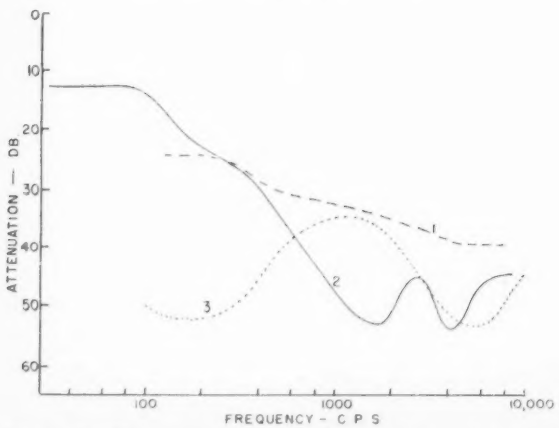

Figure 7—The attenuation that may be expected from well fitted ear plugs (curve 1) and ear covers (curve 2). Curve 3 shows the bone conduction limit.

level drops at the rate of 6 db. per doubling of distance from the source out to a distance roughly comparable with the height of the room – in this region the sound energy density is decreasing according to the inverse square law of distance as the wave fronts spread spherically. Beyond about eight feet from the source the non-absorbing surfaces of the floor and ceiling exert a gradually increasing effect until at distances beyond about 20 feet their effect predominates and the sound pressure level falls at the rate of 3 db. per doubling of distance. In this region there is no spreading of energy in the vertical direction, it is all reflected back into the space between floor and ceiling and hence the wave fronts may be thought of as spreading cylindrically. It is frequently not possible to treat the floor with any material having appreciable sound absorbing qualities; hence in Figure 5 it is considered that the whole of the ceiling is available for acoustic treatment whilst the floor remains essentially non-absorbing. Similarly certain areas of the walls, such as windows, will be unavailable for treatment; if for example half the wall area is treated with material having an absorption coefficient of unity then to a very rough approximation the average absorption may be taken as 0.5—this proportionality is not exact but it is good enough for most practical purposes. The various curves of Figure 5 relate to the following situations:–

(a) Zero absorption on the floor and ceiling, an average absorption coefficient of 0.3 on the side walls, the effective position of the noise source being at any height between the floor and ceiling.

(b) As (a) but with the absorption coefficient of the side walls increased to 1.0.

(c) An absorption coefficient of 1.0 over the whole ceiling, no absorption on the floor, an average absorption of 0.3 on the side walls and assuming that the noise source is at floor level.

(d) As (c) but assuming that the absorption coefficient of the side walls is 1.0.

(e) As (c) but with an absorption coefficient of 0.5 over the whole ceiling.

It will be noted that the application of sound absorbing material is capable of reducing the sound level only at points removed from the source and has no effect on the sound level in that region near to the source where the sound pressure level would fall at the rate of 6 db. per doubling of the distance even in the absence of the absorbing material.

Just as the transmission loss of a wall is not independent of frequency so the absorption coefficient of absorbing surfaces varies as a function of frequency. Figure 6 shows the absorption coefficient for random incidence as a function of frequency of three typical materials [10] used for the acoustic treatment of large flat surfaces–$\frac{3}{4}$" acoustic tile is probably the most widely used of all absorbing surfaces; it has good performance above 500 c.p.s. and whilst not as good as a perforated heavy surface with rock wool backing at low frequencies it is cheaper and easier to install. If one assumes a white noise spectrum for the sound field one may define an overall noise reduction coefficient for the surface and this is shown on the right hand side of Figure 6. For a rough estimate of the efficiency of such an absorbing surface in any particular situation one may apply the overall Noise Reduction Coefficient (NRC) to the overall sound pressure level.

It is important to realize that the sound absorbing properties of many surfaces depend upon the details of their mounting, etc. The curves of Figure 6 are drawn for acoustic tile backed directly by a rigid impervious

surface and painted on its front surface. The third construction is normally used only for ceiling treatment: the perforated asbestos board is 3/16 in. thick having 576 holes/sq. ft., the holes being 3/16 in. diameter on $\frac{1}{2}$ in. centres; the board is backed by a 2 in. blanket of rock wool which in turn is in contact with a rigid impervious surface; the asbestos panels are mounted at their edges to inverted T-brackets.

It was mentioned above that even when absorbing material is present the noise level inside an enclosure is higher than it would be in the absence of the enclosure. The amount of this rise, in decibels, is given by $-10 \log_{10}A$ where A is the average absorption coefficient of all the surfaces inside the enclosure. Thus for example if all inside surfaces were treated with $\frac{3}{4}$ in. acoustic tile the rise of 500 c.p.s. would be 1.3 db, if only half of the surfaces were so treated the rise would be roughly 4.3 db. We then have in general that N.R. = T.L. + $10 \log_{10}A$ where N.R. is the noise reduction on the outside of the enclosure and T.L. is the transmission loss through its walls.

Enclosure of the observer

In cases where it is necessary for personnel to be subjected to high noise levels it is still possible to provide protection by separate small enclosures for each individual –namely by the use of ear defenders. Ear plugs are perhaps the most widely used type of ear defender and there are a large number of different models on the market. A well fitted ear plug can be expected to give an attenuation curve as represented by curve 1, Figure 7. Its performance is determined by its mass and the compliance of the ear canal parallel to the axis of the canal. However, plugs are not usually well fitted unless molded to suit the individual. Even then changes in ear canal size may occur and spoil the fit or the individual may fail to adjust the plugs properly. Plugs are being designed to overcome this.

Cover type of ear defenders (often called ear muffs) enclose the whole outer ear and have the advantage of being more easily put on and removed. For most people they are also more comfortable than the insert type. However, they have the disadvantage of greater weight and bulk. The factors contributing to their performance are similar to ear plugs–the fit, mass and the stiffness (or spring constant) of the cushion. Most ear covers fail to provide for both the first and last factors at the same time. To achieve a proper fit they use sponge rubber cushions and thus provide inadequate stiffness. If a hard cushion is used then the fit is impaired unless undue pressures are used to force the ear cover to the head. A recently developed ear defender [6] makes use of a hollow cushion partly filled with a liquid. The hollow sheath is thin and hence is easily deformed and fitted to the head with comfort. Once it is fitted, however, further compression of the cushion is resisted by the high bulk modulus of the liquid filler and the high Youngs modulus of the sheath. A typical attenuation curve is shown by curve 2 of Figure 7. Its limit is set by the compliance of the skin and flesh around the ear.

Both ear plugs and ear covers have an ultimate effective limit beyond which they cannot give protection. This limit, curve 3 of Figure 7, is called the bone conduction limit and is set by the fact that sound can penetrate, with this degree of attenuation to the inner ear through the bones of the head.

Example of quietening of the source

The methods of noise control which have been discussed above are of general application and may be employed in any situation, either singly or in combination whichever may be the most economical and satisfactory way depending on the individual circumstances. However, if an attempt is made to reduce the noise at its source, by reducing the efficiency with which mechanical energy is converted into acoustical energy, then each different type of machinery presents a different problem. In order to illustrate the type of approach which may be required for this method of noise reduction consider, very briefly, one such mechanism by which the energy is converted into acoustical energy and how this conversion may be made less efficient.

The most serious sources of noise in a paper mill machine room are the suction rolls, i.e. press rolls and couch rolls, however the couch roll is usually the chief noise maker. The manner in which this noise is made is shown in Figure 8. The couch shell is perforated by an array of holes (usually about 5/16 in. diameter and about $3\frac{1}{2}$ holes p.s.i.) which permits the vacuum in the vacuum box to be communicated to the pulp sheet which lies on a fine mesh wire screen. The vacuum can thus suck water out of the sheet and the holes will be at the same pressure as the vacuum box until they leave the box and pass over the right-hand sealing strip when a sudden rush of air into each hole will bring it back to atmospheric pressure. Each circumferential row of holes is a siren which radiates at one point (viz. where the holes of that row leave the sealing strip) and has a fundamental frequency which is determined by the rate at which the air flow is chopped or pulsed. This of course is equal to the number of holes leaving the strip each second at that point. Such a row of holes usually occurs, on a conventional couch shell, each 9/32 in. distance measured along the axis and hence we have as an overall noise source, a linear array of stationary point sources.

A common drill pattern used on couch rolls in Canada is shown in Figure 9. If the axis of the roll is assumed to be across the page then the roman numerals refer to five of the circumferential rows of holes, and hence to five of the sirens. The holes numbered with arabic numerals belong to a row that would be parallel to the axis if all the sirens were in phase. It is evident, therefore, that adjacent sirens are one half cycle of the fundamental frequency out of phase and thus the phase parameter α for this pattern is designated as 0.5.

In general the air flow will be complicated and all possible harmonics of the fundamental frequency should be expected. Figure 10 shows such a spectrum, the frequency being plotted on the abscissa and the intensity, with respect to an arbitrary level, on the ordinate. Here the fundamental frequency is about 336 c.p.s.; most of the sound is radiated in the frequency range below 4,000 c.p.s. and in this range the even harmonics are the more important frequencies. The latter fact results from the particular value of the phase parameter α which was 0.5 in this case.

The energy goes through several stages in a couch roll, or siren before it finally reaches the ear of an observer, see Figure 11. In principle it is possible to effect some noise control at each one of these stages. In earlier sections of this paper noise reduction by the enclosure of the machine control of the propagation conditions through the plant and protection of the observer was discussed. This section will be limited to that part of Figure 11 labelled "Transformation Efficiency". For common sizes and speeds of paper machines, whose vacuum boxes normally have a pressure of 24 in. Hg below atmospheric pressure, the amount of energy available in the evacuated holes of the couch shell is around 20,000 watts. If this energy should flow uniformly away from the machine in all directions then at a distance of 12 ft. the intensity of

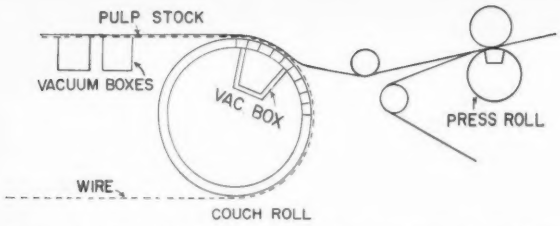

Figure 8—The chief source of noise on a paper machine. The couch produces its noise by chopping the flow of air from the atmosphere to fill the vacuum in the holes of the couch shell as they leave the vacuum box.

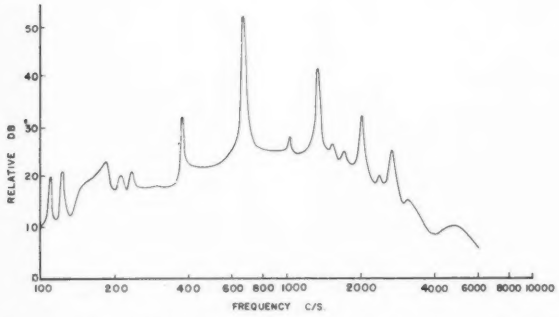

Figure 10—A frequency spectrum of the noise produced by a couch shell having the common drill pattern of Figure 9.

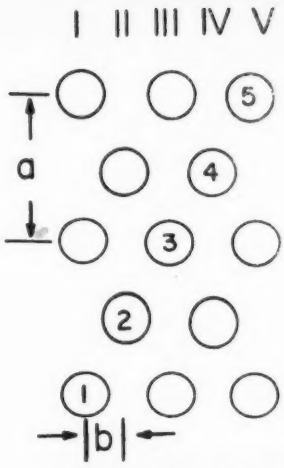

Figure 9—A common couch roll drilling pattern.

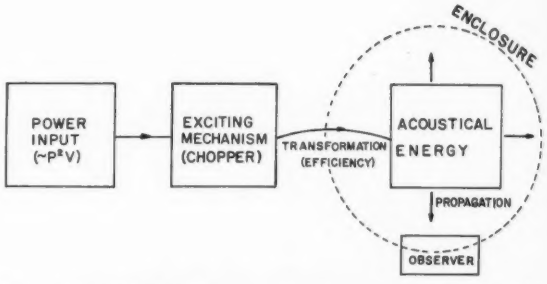

Figure 11—Block diagram of the energy flow at the couch from mechanical energy at the vacuum pumps to acoustic energy at the ear of an observer.

the noise would be 140 db., assuming a transformation efficiency of 100%. Fortunately the efficiency of this process is usually quite low, unless great pains are taken in the design of a particular acoustic instrument, and therefore it is not surprising that the efficiency in this case is only about 1% or less when the conventional drill pattern shown in Figure 9 is used. This low efficiency provides a drop of 23 db. in sound level and so the level near the machine is about 117 db. or lower. This sound level is too high, but by careful design of the drill pattern it is possible to reduce the transformation efficiency still further with a resulting reduction of sound level by an extra 20 or 25 db. down to an overall level of 90 to 95 db.

If a source has a given excitation (volume current of air) the efficiency with which it will radiate sound energy will be determined by the characteristics of the air into which it radiates, the dimensions of the source, the frequency and the relative phase between different parts of the source. There is little control of the first two factors in this case, nor of the frequencies which will depend on the speed of the machine and will include several harmonics. The last factor, however, is one that may be appreciably modified without affecting the performance of the machine and fortunately the radiation efficiency is strongly dependent on the relative phases of neighbouring small sources.

The value of the phase parameter α will always lie between zero and one, because at one it effectively repeats the pattern defined by $\alpha = 0$. The efficiency will depend on frequency but for present purposes it may be defined as relative to that which would exist under similar circumstances if the phase parameter α were zero. That is to say the interest here is not so much in the absolute value of the efficiency as in knowing how much it can be reduced. To design a quiet drill pattern or to evaluate a given pattern the chart shown in Figure 12 is used. The centre point of each of the lines marks the value of α (on the abscissa) for which the harmonic shown on the ordinate has maximum efficiency. How this chart is constructed can easily be seen since for n^{th} harmonic the maximum efficiency points lie at values of α which are at intervals of $\delta\alpha = \frac{1}{n}$ starting at $\alpha = 0$. These maximum efficiency points are marked in Figure 12 for the first 20 harmonics. The range of α covered is only $\alpha = 0$ to $\alpha = 0.5$ since the chart is symmetrical about the latter value. The width of the lines shows over what range of α near each maximum efficiency point the individual harmonics are suppressed less than 20 db. This width is a complicated function of the dimensions of the source and the frequency of the first harmonic; it is of considerable importance to the detailed design of quiet drill patterns but need not be considered further here.

It is now easy to see what the principal harmonics will be for a pattern whose value of α is known. For $\alpha = 0.5$ it is evident that only the even harmonics will have their normal efficiencies and the odd harmonics will be suppressed (see Figure 10). Since some harmonics will always remain unattenuated it is necessary to take into account their normal relative excitation if a realistic assessment is to be achieved of noise output. It was noted before that the frequencies above 4000 c.p.s. are not appreciably excited; hence for the standard drill pattern used in

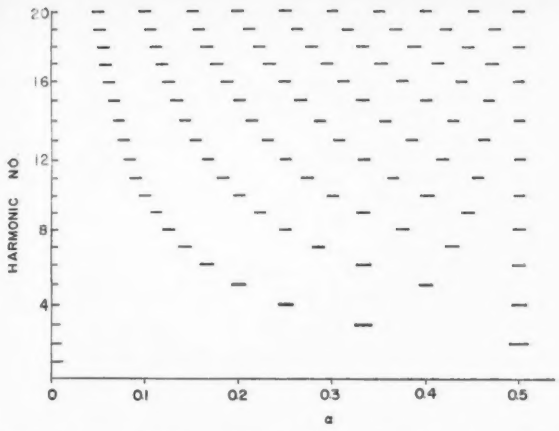

Figure 12—Drilling pattern design chart. The short horizontal lines indicate the range of the parameter α for which each individual harmonic is attenuated less than 20 db. relative to its maximum efficiency.

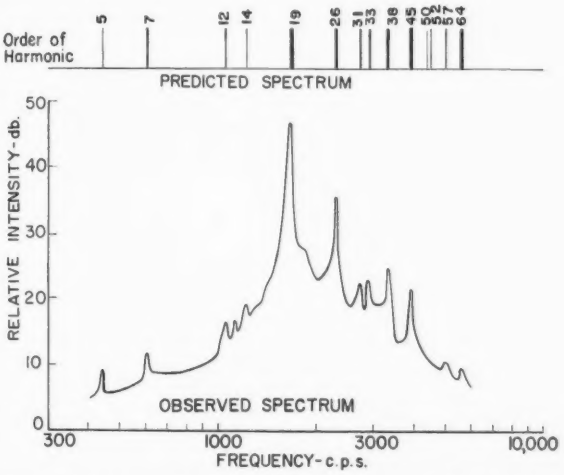

Figure 13—A comparison between the theoretical and experimental noise spectra for an unusual drill pattern used on a 9 in. model.

Canada if we eliminate all frequencies up to the tenth harmonic there will not be much left.

To what extent Figure 12 can be used to predict a spectrum is shown in Figure 13. Here is shown a frequency analysis of the noise from an unusual type of drill pattern used on a 9 in. model. The fundamental frequency is about 86 c.p.s. At the top, in the form of a line spectrum, is shown the predicted spectrum using Figure 12 with the numbers at the lines indicating the order of the harmonic while the widths of the lines are qualitative indications of intensity. All lines that were expected to be suppressed 30 db. or more are omitted altogether. It is seen that the agreement is quite good.

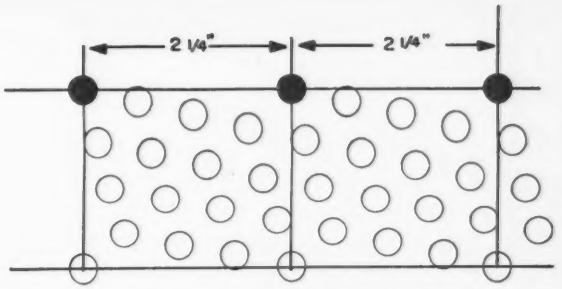

Figure 14—An early example of a quiet drilling pattern which provided 12 db. attenuation.

In practice the choice of a drilling pattern does not depend on its noise reduction qualities alone but also upon the ease and cost of drilling the roll and so a compromise must be found. These rolls are drilled with multiple spindle drilling machines which normally have a spacing between drills of 2¼ in. and it is generally true that the greater the noise reduction of the drilling pattern the greater is the spacing between the holes that can be drilled together. Thus a very quiet pattern, giving perhaps 25 db. reduction, may require every other drill (or even two out of every three drills) to be removed with a consequent increase in the cost of drilling. One of the first couch rolls designed to be quiet had the drilling pattern shown in Figure 14. For various reasons the compromise in this case was weighted entirely in favor of ease of drilling and no intermediate drills were removed from the drilling machinery (the shaded holes were drilled together); nevertheless in actual paper mill use it provided 12 db. of noise reduction. At the present time rolls are being drilled with every second drill removed and these give 15 to 20 db. of noise reduction.

References

(1) "The Relations of Hearing Loss to Noise Exposure", report by subcommittee Z24-X-2 of the American Standards Association.
(2) Beranek, L. L., Noise Control, 3, 19 (1957).
(3) Bonvallet, G. L., Amer. Indus. Hyg. Assn. Quarterly, 13, 136 (1952).
(4) Bonvallet, G. L., Paper read at the Canada-U.S. Engineering Conference, Montreal, April 1958.
(5) Beranek, L. L., Acoustic Measurements, John Wiley and Sons, New York.
(6) Thiessen, G. J., and Embleton, T. F. W., Pulp and Paper Mag. Canada, July 1957.
(7) Stevens, S. S., J. Acoust. Soc. Amer., 28, 807 (1956).
(8) Rosenblith, W. A., and Stevens, K. N., Handbook of Acoustic Noise Control, Vol. 2, "Noise and Man", Tech. Report 52-204, Wright Air Development Centre, Wright-Patterson Air Force Base, Ohio (1953).
(9) Speith, W., J. Acoust. Soc. Am. 28, 872 (1956).
(10) Bulletin 17 of Acoustical Materials Assn. "Sound Absorption Coefficients of Architectural Acoustical Materials".

★ ★ ★

The Canadian Journal of Chemical Engineering

formerly

Canadian Journal of Technology

INSTRUCTIONS TO AUTHORS

Manuscript Requirements

1. The manuscript should be in English or French.
2. The original and two copies of the manuscript should be supplied. These are to be on 8½ x 11 inch sheets, typewritten, and double spaced. Each page should be numbered.
3. Symbols should conform to American Standards Association. An abridged set of acceptable symbols is found in the third edition of Perry's Chemical Engineers' Handbook. Greek letters and subscripts and superscripts should be carefully made.
4. Abstracts of not more than 200 words in English indicating the scope of the work and the principal findings should accompany all technical papers.
5. References should be listed in the order in which they occur in the paper, after the text, using the form shown here: "Othmer, D. F., Jacobs, Jr., J. J., and Levy, J. F., Ind. Eng. Chem. 34, 286 (1942). Abbreviations of journal names should conform to the "List of Periodicals Abstracted by Chemical Abstracts". Abbreviations of the common journals are to be found in Perry's Handbook also. All references should be carefully checked with the original article.
6. Tables should be numbered in Arabic numerals. They should have brief descriptive titles and should be appended to the paper. Column headings should be brief. Tables should contain a minimum of descriptive material.
7. All figures should be numbered from 1 up, in Arabic numerals. Drawings should be carefully made with India ink on white drawing paper or tracing linen. All lines should be of sufficient thickness to reproduce well, especially if the figure is to be reduced. Letters and numerals should be carefully and neatly made, preferably with a stencil. Generally speaking, originals should not be more than twice the size of the desired reproduction; final engravings being 3¼ in. or 7 in. wide depending on whether one column or two is used.
8. Photographs should be made on glossy paper with strong contrasts. Photographs or groups of photographs should not be larger than three times the size of the desired reproduction.
9. All tables and figures should be referred to in the text.

Submission of Manuscripts

1. The three copies of the manuscript, including figures and tables, should be sent directly to:

   D. W. Emmerson, publishing editor,
   The Canadian Journal of Chemical Engineering,
   18 Rideau Street,
   Ottawa 2, Ont.
2. The authors addresses and titles should be submitted with the manuscript.
3. The author may suggest names of reviewers for his article, but the selection of the reviewers will be the responsibility of the editor. Each paper or article is to be reviewed by two chemical engineers familiar with the topic. Reviewers may request that they remain anonymous.
4. All correspondence regarding reviews should be directed to the editor.

Reprints

1. At least 50 free "tear sheets" of each paper will be supplied.
2. Additional reprints may be purchased at cost. An estimated cost of reprints, with an attached order form, will be sent to the author with the galley proofs.
3. Orders for reprints must be made before the paper has appeared in the Journal.

* * *